UNIVERSITE DE NEUCHATEL

FACULTE DES SCIENCES

Ferrocene- and Ferrocenium-containing Thermotropic Liquid Crystals: Design, Synthesis and Characterization of Redox-Active Anisotropic Materials

Thèse présentée à la Faculté des Sciences de l'Université de Neuchâtel pour l'obtention du titre de docteur ès sciences

par

Martin Schweissguth

Chimiste diplômé de la Technische Hochschule Darmstadt (Allemagne)

Juillet 1997

IMPRIMATUR POUR LA THÈSE

Ferrocene- and Ferrocenium-Containing Thermotropic LiquidCrystals: Design, Synthesis and Characterization of Redox-Active Anisotropic Materials

de M. Martin Schweissguth

UNIVERSITÉ DE NEUCHÂTEL

FACULTÉ DES SCIENCES

La Faculté des sciences de l'Université de Neuchâtel sur le rapport des membres du jury,

MM. R. Deschenaux (directeur de thèse), R. Neier, et J. Malthête, Paris

autorise l'impression de la présente thèse.

Neuchâtel, le 14 octobre 1997

Le doyen:

R. Dändliker

R. Dändliker

Ce travail a été effectuée sous la direction du Prof. Dr. Robert Deschenaux entre novembre 1993 et août 1996 à l'Institut de Chimie de l'Université de Neuchâtel.

Je tiens à remercier mon directeur de thèse Monsieur le Professeur Robert Deschenaux pour m'avoir offert l'opportunité de travailler sur un sujet très intéressant. Je le remercie pour ses nombreux encouragements et pour sa grande confiance qu'il ma témoigné.

J'aimerais aussi remercier Monsieur le Professeur Reinhard Neier (Université de Neuchâtel) et Monsieur le Dr. Jacques Malthête (Institut Curie, Paris) pour avoir accepté d'être membres du jury de cette thèse.

J'adresse mes remerciements au Dr. Anne-Marie Levelut (Université de Paris-Sud) pour les analyses rayons-X et au Dr. Raymond Ziessel (École de Chimie des Polymères et Matériaux Strasbourg) pour les mesures électrochimiques.

Mes remerciements s'adressent également au Drs. David Dunmur (Université de Sheffield) et Chris Frommen (Université de Marburg) pour les mesures magnétiques.

Je remercie Maria-Teresa Vilches qui a contribué à cette recherche dans le cadre de son travail de diplôme.

Enfin, j'exprime mes remerciements à mes collègues Bertrand Donnio, Blaise Nicolet, Claudio Masoni, Cornelia Zumbrunn, Eduardo Campillos, Elisabeth Serrano, Florence Monnet, François Turpin, Isabelle Jauslin, Jérôme Pellaud, Julio Santiago, Karine N'djoko, Maria Fernandez Ciurleo, Michaël Even, Phuong Tran, Sébastien Vaucher, Séverine Meyer, Sonia Megert, Thierry Chuard, Ulrich Scholten et Vladislav Izvolenski pour leur sympathique accueil et les bons moments passés ensemble.

Abbreviations:

acac	Acetylacetonato
Bn	Benzyl
cp	Cyclopentadienyl
cp^*	Pentamethylcyclopentadienyl
DCC	N,N'-Dicyclohexylcarbodiimide
DDQ	2,3-Dichloro-5,6-dicyano-1,4-bezoquinone
Col_h	Hexagonal Columnar Phase
DME	Dimethoxyethane
DMF	Dimethylformamide
DMSO	Dimethylsulfoxide
Col_r	Hexagonal Rectangular Phase
DSC	Differential Scanning Calorimetry
FAB	Fast Atom Bombardment
Fc	Ferrocenyl
MS	Mass Spectroscopy
N	Nematic Phase
N^*	Chiral Nematic (Cholesteric) Phase
N_D	Nematic Discotic Phase
NMR	Nuclear Magnetic Resonance
OTf	Trifluoromethanosulphonate
OTs	*p*-Toluenosulfonate
Ppy	4-Pyrrolidino pyridine
S_A	Smectic A Phase
S_C	Smectic C Phase
S_X	Smectic X Phase (not identified smectic phase)
TCNE	Tetracyanoethylene
TCNQ	7,7,8,8-Tetracyanoquinodimethane
TG	Thermal Gravimetry
TLC	Thin Layer Chromatography
TMEDA	N,N,N',N'-Tetramethyl ethylendiamine

Notice:

Numbers which include a letter (example: **27a**) generally describe ferrocenium derivatives.

Structures of ferrocene precursors:

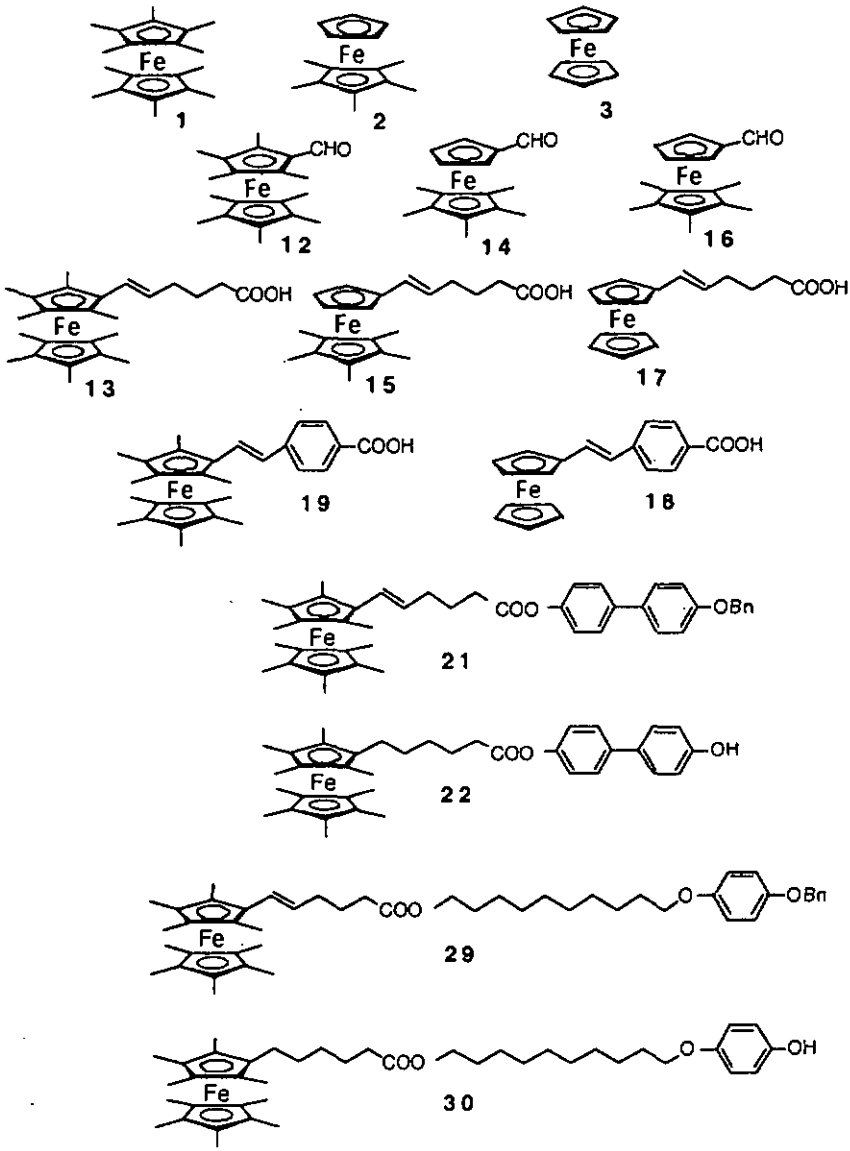

Structures of mesogenic permethylated ferrocene-derivatives:

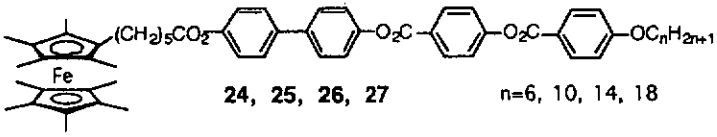

24, 25, 26, 27 n=6, 10, 14, 18

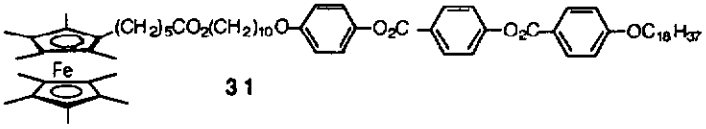

31

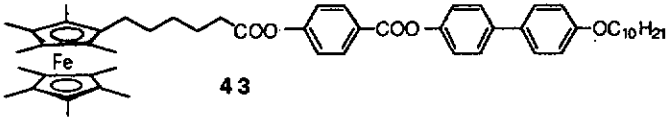

43

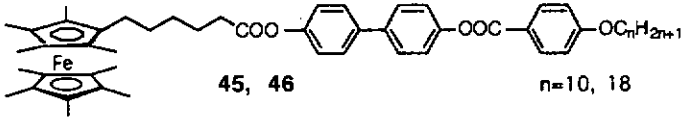

45, 46 n=10, 18

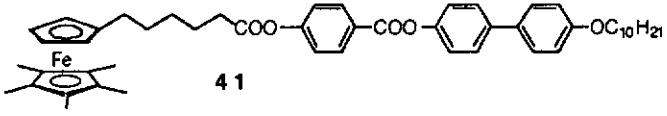

41

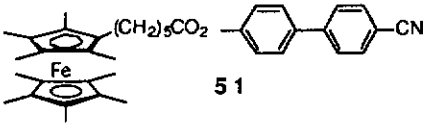

51

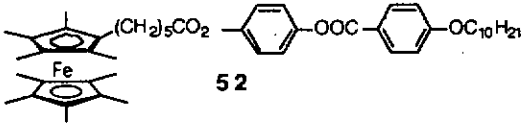

52

Structures of mesogenic ferrocenium-derivatives:

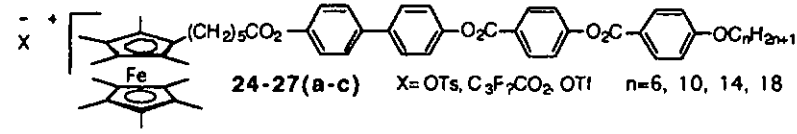

24-27(a-c) X= OTs, $C_3F_7CO_2$, OTf n=6, 10, 14, 18

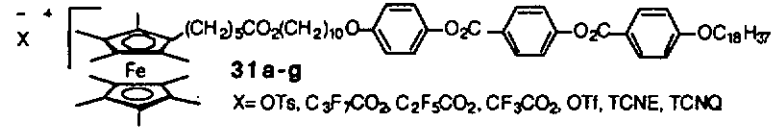

31a-g

X= OTs, $C_3F_7CO_2$, $C_2F_5CO_2$, CF_3CO_2, OTf, TCNE, TCNQ

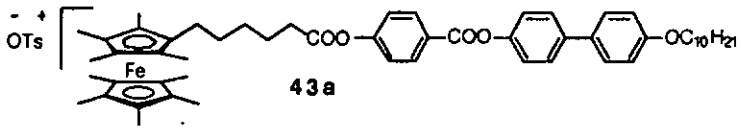

43a

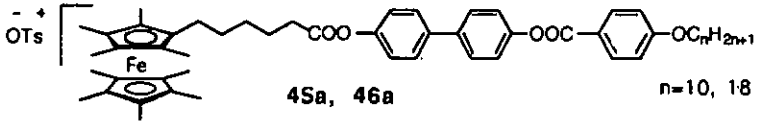

45a, 46a n=10, 18

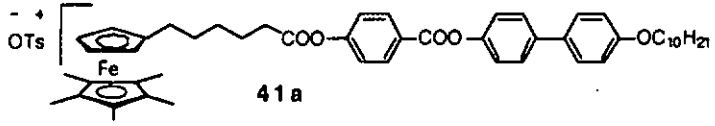

41a

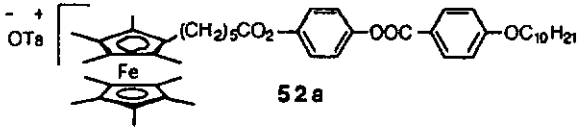

52a

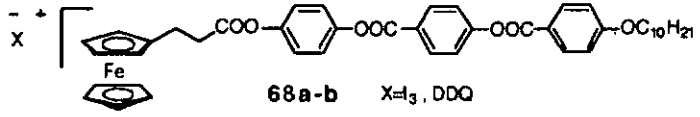

68a-b $X=I_3$, DDQ

Structures of mesogenic ferrocene-derivatives (1):

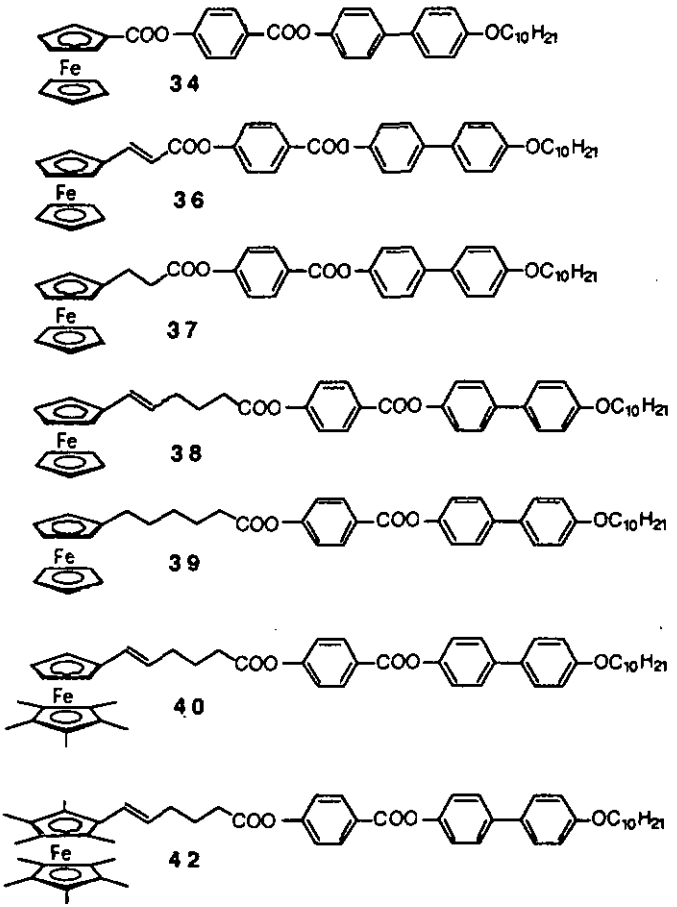

Structures of mesogenic ferrocene-derivatives (2):

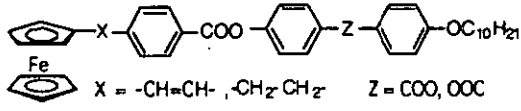

X = -CH=CH- , $-CH_2-CH_2-$ Z = COO, OOC

59-62

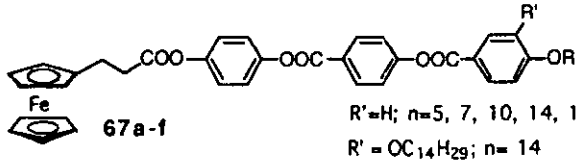

67a-f

R'=H; n=5, 7, 10, 14, 1

R' = $OC_{14}H_{29}$; n= 14

Structures of chiral ferrocene- and ferrocenium-derivatives:

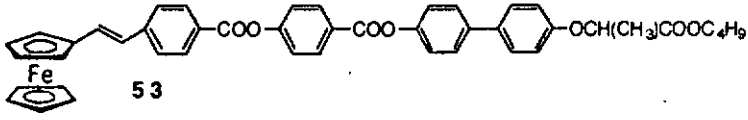

53

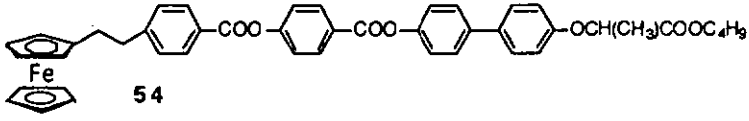

54

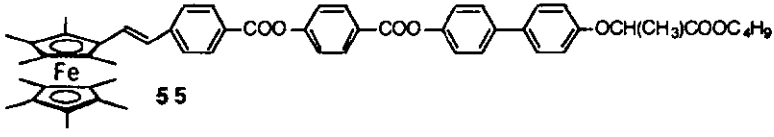

55

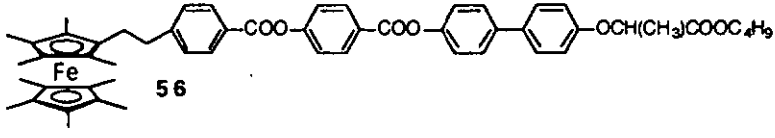

56

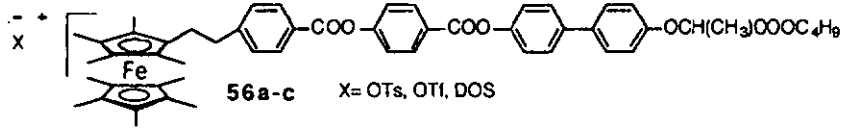

56a-c X= OTs, OTf, DOS

Contents

Chapter

1

Summary

Recent studies have shown that ferrocene can be a suitable building block for incorporation in liquid crystals [1]. Although ferrocene has been widely used as an electron-donor in redox-active systems [2-4]. Nevertheless, its capability to be oxidised in connection with liquid-crystalline systems has only received little attention [5-8] and the role of the oxidation process on the mesophase behaviour has not been investigated. Therefore, in the major part of this thesis the oxidation of ferrocene containing mesogens to ferrocenium-salts (Fig. 1.1.) and its influence on the mesomorphic properties has been investigated. The latter species can be used to understand electrostatic effects on the mesophase behaviour in thermotropic liquid crystals. Although the influence of size and shape of the counterion on the formation of mesophases has been studied.

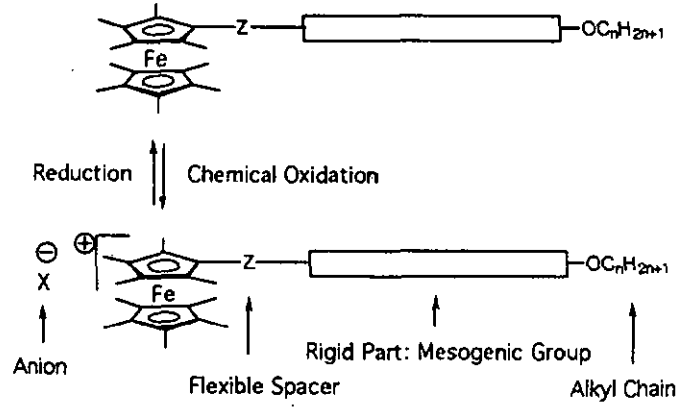

Figure 1.1. *Major structural parameters of ferrocenium containing liquid crystals to be examined in this thesis*

A peralkylated ferrocene derivative was selected as an electron donor because of the ease of oxidation of such a species (and related peralkylated compounds) in comparison with less substituted structures (Figure 1.2.). Therefore the main idea behind the use of decamethylferrocene (1) or pentamethylferrocene (2) as key-intermediates in the synthesis was to obtain a molecule bearing an easy oxidisable ferrocene unit. Silver salts were found to oxidise these persubstituted ferrocene derivatives without affecting the mesogenic core and delivering at the same moment a counter-anion. Ferrocenium derivatives containing several counterions such as tosylate,

triflate, heptafluorobutyrate, pentafluoropropionate, trifluoroacetate or organic radical anions (TCNE, TCNQ) have been synthesised.

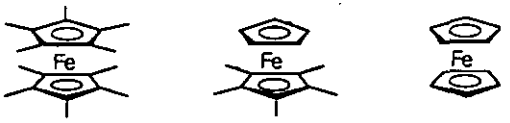

1 2 3

Figure 1.2. *Decamethylferrocene (1), pentamethylferrocene (2) and ferrocene (3)*

In conclusion, the occurrence and stability range of the thermotropic liquid-crystalline phases in ferrocenium derivatives depended strongly on the structure of the promesogenic core and the type of counter-anion.

Upon the oxidation process of ferrocene derivatives (mesomorphic or non-mesomorphic) the thermal behaviour changes. Liquid-crystalline phases of the related oxidised species are either induced, stabilised or transformed. The mesophases found in oxidised species were smectic A, smectic C and/or columnar. Organic counterions such as *p*-toluenesulphonate or heptafluorobutyrate were found to be favourable to the development of mesophases. Small counterions, however, such as hexafluorophosphate or triflate did not favour the formation of mesophases because of high crystallinity and consequently high transition temperatures. A large supercooling and/or strong dependence on the thermal history were observed as typical features for all oxidised substances. Figure 1.3. summarises the relationship between structural parameters and mesophase behaviour obtained for oxidised species.

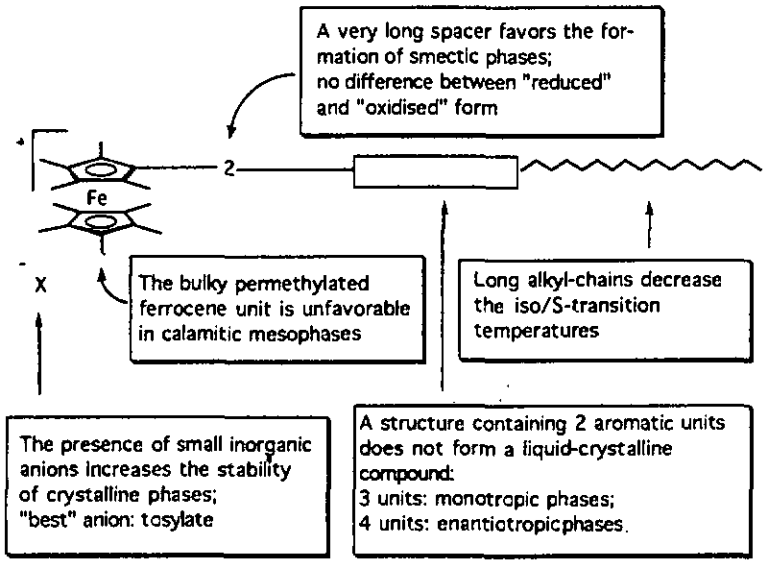

Figure 1.3. *Structural parameters and their influences on the liquid-crystalline properties*

The second part of this thesis deals with monosubstituted ferrocene derivatives and a more close look of mesophase behaviour of such compounds. In this part, the structural parameters of the rigid core such as the number of aromatic rings or the length of the terminal alkyl chain were varied and their influence on the liquid-crystalline properties was examined.

Different experimental techniques have been used in this thesis, in order to study the type and the formation of various liquid-crystalline phases:

- optical polarising microscopy;
- differential scanning calorimetry (DSC);
- X-ray investigations;
- cyclovoltametric measurements and
- magnetic susceptibility measurements.

Chapter

2

Introduction

In the first part of the general considerations a brief introduction of structures of liquid crystalline phases is given. The second part will focus on ferrocene with special regard to chemical, structural and electronic features of the ferrocene/ferrocenium-system. The third part gives a short overview of experimental techniques used for the investigation of synthesised compounds. Finally, in the fourth part a literature overview is given on related mesogenic compounds.

2.1. Classification of Liquid Crystals

When heated most substances undergo a single transition from the solid phase to the isotropic liquid phase. In contrast, some compounds pass through one or more phases in going from the crystalline solid to the isotropic liquid state (and or vice/versa). The intermediate phases are known as mesophases or liquid-crystalline phases and the compounds which exhibit this behaviour are known as mesomorphic compounds or liquid crystals or mesogens. Two main classes of thermotropic liquid crystals are usually distinguished: calamitic and columnar.

Lyotropic phases are formed by molecules in a solvent and the appearance of the phase is controlled by the temperature as well as the concentration.

Nematic phases

The less ordered mesophase is the nematic phase (N). In this phase the rodlike molecules align approximately parallel to each other, along a direction defined by the director, n. The transition enthalpy from the crystalline to the nematic phase (cryst→N) is normally high, which is a reflection of the fact that nematic phases are fluid, whereas the enthalpies of the nematic to isotropic (N→iso) transition usually is small (some kJ mol^{-1}). Introduction of a chiral centre into a nematic molecule leads to chiral nematic (N^*, cholesteric) phase behaviour, where the director n is helical. Figure 2.1. shows the structure of the nematic and the discotic nematic phases.

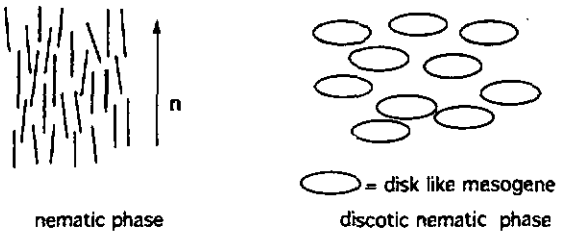

Figure 2.1. *Schematic representation of the structure of the nematic phase (N) and of the discotic nematic phase (N_D)*

Smectic phases

In the smectic phases the rodlike molecules order their main axis parallel to the director n and form layers. These layers can be perpendicular to the director [example smectic A (S_A) phase] or not [example smectic C (S_C) phase]. Both phases are the less ordered smectic phases. A high molecular mobility and a low viscosity are associated with these mesophases, whereas there are other types of smectic phases that show tri-dimensional order. These phases are associated with restricted molecular mobility and greater viscosity. Therefore they are known as crystalline mesophases. Figure 2.2. shows the structure of the smectic A and smectic C phases.

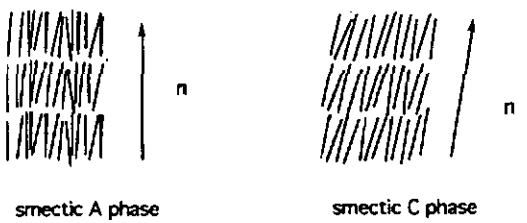

Figure 2.2. *Schematic representation of the structure of the smectic A (S_A) and smectic C (S_C) phases*

Columnar Liquid-Crystalline Phases

Disc-like molecules can arrange themselves in parallel columns, which form a periodic two-dimensional array. As significant examples the hexagonal columnar (Col_h) and the rectangular columnar (Col_r) phases are shown in Figure 2.3.

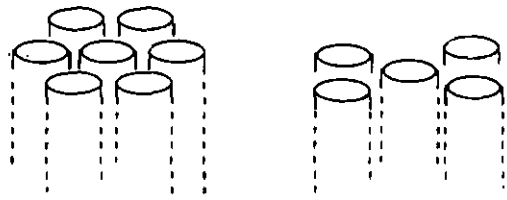

Figure 2.3. *Schematic representation of the hexagonal columnar (Col_h) and rectangular columnar (Col_r) phases*

2.2. Physical and Chemical Properties of Ferrocene and the Ferrocenium-Ion

2.2.1. Synthesis of Substituted Ferrocenes

There are two main routes for the synthesis of substituted ferrocenes (Fig. 2.4.). Generally the formation of substituted ferrocenes from the corresponding substituted cyclopentadienes is difficult, especially for the preparation of ferrocenes bearing two different ligands (bileptic compounds)[9,10].

This synthetic route, however, is related to the formation of ferrocene itself. For example decamethylferrocene is formed on treating $FeCl_2$ with lithiumpentamethyl cyclopentadienide ($LiCp^*$). The second route to substituted ferrocenes uses electrophilic substitution or metallated intermediates and is related to organic chemistry. Ferrocene undergoes facile electrophilic substitution, but often a common side reaction is the oxidation to the ion $[Fe(C_5R_5)_2]^+$ (R=H, alkyl).

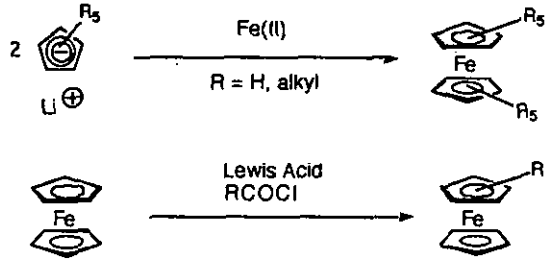

Figure 2.4. *Two principal synthetic pathways for the synthesis of substituted ferrocenes*

2.2.2. Ionic Dicyclopentadienyl-Iron Compounds

Many inorganic oxidising agents such as Ag^+, I_2, $FeCl_3$ or NO^+ can be used for oxidation of ferrocene [4] (Fig. 2.5.). The use of organic electron acceptors like TCNQ, TCNE or DDQ leads to deeply coloured ferrocenium charge-transfer complexes [7,11-16]. These compounds contain organic radical counter-anions and they are predominantly synthesised in order to investigate their magnetic properties, *e.g.* cooperative magnetic properties like bulk meta- and ferromagnetism. The reversible nature of the ferrocene-ferrocenium interconversion has been established electrochemically [17,18].

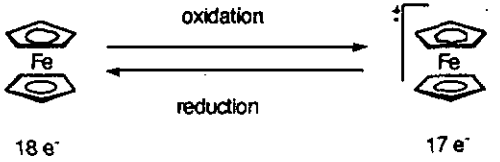

Figure 2.5. *Oxidation and reduction of ferrocene*

The presence of electrophiles catalyses readily the oxidation of dicyclopentadienyl iron(II) to dicyclopentadienyl iron(III), which is of blue or green colour. Strong non-oxidising acids lead to the protonation of ferrocene. Therefore, in terms of oxidation, ferrocene is stable to hot concentrated hydrochloric acid. Recently, protonation, and more generally, the electrophilic substitution mechanism has been studied by Mueller-Westerhoff [19] using H/D-exchange experiments. As a result the authors found that substitution should occur by *exo*-attack on the ring, followed by transfer of the proton to the metal (Fig. 2.6.). In the back-reaction the proton is transferred back to either one of the two rings.

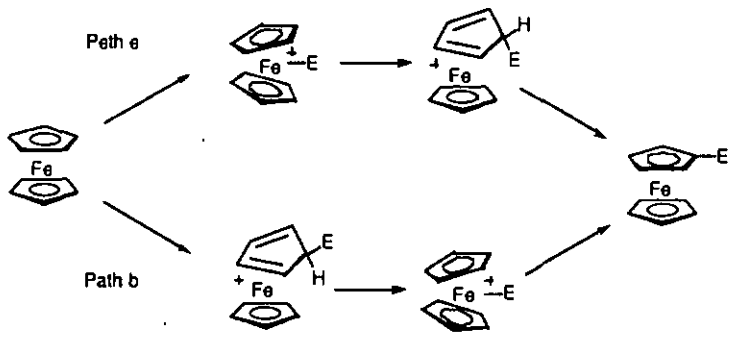

Figure 2.6. *Endo (path a) and Exo (path b) attack pathways for the electrophilic substitution of ferrocene discussed by Mueller-Westerhoff* [19]

For protonated ferrocene, a rapid equilibrium between ring- and metal-protonated species exists and the use of deuterated acids leads to rapid and complete H/D-exchange. When bound to the metal the proton transfers almost all of its charge to the ferrocene. This species is best described as having an almost neutral hydrogen atom attached to a ferrocenium system.

2.2.3. Substituent Effects on the Redox-Potential of Ferrocene

Substitution plays a significant role on the electrochemical behaviour of ferrocene derivatives. Aromatic substituents attached to the cyclopentadienyl rings can increase the redox-potential of ferrocene due to the mesomeric stabilisation of the negative charge of the cyclopentydienyl ring. Other electron-withdrawing groups attached to the Cp-ring are also known to increase the oxidation-potential.

In contrast, the introduction of electron-donating functions to ferrocene leads to a decrease of its redox-potential. For example, each alkyl group decreases the half-wave potential $E_{1/2}$ by 47 mV. This decrease occurs whether or not the alkyl groups are introduced successively at the same or different rings. Furthermore, the positions within the ring have no influence either. While alkyl, *e.g.* methyl groups favour oxidation, electron withdrawing groups stabilise ferrocene with respect to the ferrocenium ion. For example carboxy or ester groups increase the oxidation potential. Table 2.1. shows the redox-

potentials of some substituted ferrocenes depending on the type and number of substituents.

Table 2.1. *Polarographic half wave potentials ($E_{1/2}$) of various ferrocene derivatives versus a Saturated Calomel Electrode (SCE)* [16-18,20]

Compound	$E_{1/2}$ *(mV)*	*Compound*	$E_{1/2}$ *(mV)*
$[Cp_2Fe]$	+0.44	$[(CpCO_2H)(CpC_2Me)Fe)]$	+0.85
$[Cp^*CpFe]$	+0.13	$[(MeCp)_2Fe]$	+0.24
$[Cp_2^*Fe]$	-0.12	$[(CpCO_2H)CpFe]$	+0.62

2.2.4. Nature of Bonding in Ferrocene and Ferrocenium-Ion

Ferrocene is an 18-e⁻-system, whereas upon mono-oxidation results a 17-e⁻-system. In ferrocene eight electrons occupy four strongly bonding orbitals that are largely π-ring-orbitals in character. Four electrons reside in two bonding orbitals, which provide the d-π interactions between the ring e_{1g} and the metal d_{xz} and d_{yz} orbitals. The remaining six electrons fill the nonbonding molecular orbitals, which are the d_{z^2} (a_{1g}), and the d_{xy} and $d_{x^2-y^2}$ (e_{2g}) orbitals of the metal centre.

For ferrocene it was found that the bond energy to eclipsed ferrocene (D_{5h}-symmetry) or any other rotamer (D_5-symmetry) is equal and consequently nearly invariant to rotation. The presence of specific conformations is therefore not governed by electronic effects but packing forces or by repulsive effects of peripheral substituents.

The highest occupied orbitals are a_{1g} and e_{2g}, with the lowest unoccupied being e_{1g}. The electronic ground state of diamagnetic ferrocene is a singlet, $^1A_{1g}$ (e_{2g}^4, a_{1g}^2) and the electronic ground state of the paramagnetic ferrocenium-ion is a doublet, $^2E_{2g}$ (a_{1g}^2, e_{2g}^3). The three highest filled and the two lowest empty orbitals in both ferrocene and ferrocenium-ion are localised for the greater part on the metal atom (see Table 2.2.).

Table 2.2. *Electron configurations and energetic order of orbitals in ferrocene and the ferrocenium-ion*

compound	*electron-configuration* $(a_{1g})^2$, $(a_{2u})^2$, $(e_{1g})^4$, $(e_{1u})^4$	*energetic order of frontier orbitals*
$Fe(cp)_2$	$(e_{2g})^4$, $(a_{1g})^2$	$e_{1g} > a_{1g} > e_{2g}$
$[Fe(cp)_2]^+$	$(a_{1g})^2$, $(e_{2g})^3$	$e_{1g} > e_{2g} > a_{1g}$

Upon ionisation the sequence of certain MO orbitals in ferrocene invert. This means that the MO scheme is not static and modified with the charge of the cyclopentadienyliron-complex.

The lowest two ionisation potentials at 6.85 and 7.20 eV in the photoelectron spectrum of ferrocene are due to the removal of electrons from the e_{2g} and a1g orbitals. These orbitals are assumed to be localised on the iron atom. One would thus expect that the sequence of orbitals in ferrocene is $a_{1g} < e_{2g}$, which means that the energy associated with the a_{1g} orbital is larger. The reason is found in the different extent of the electronic rearrangement which occurs upon ionisation, depending on the nature of the orbital involved in the ionisation process. For a ligand orbital (e_{1u} or e_{1g} or a_{2u}) there is little electronic rearrangement upon ionisation. For a metal orbital (a_{1g} or e_{2g}) there is a remarkable rearrangement upon ionisation: while these orbitals include a small amount of ligand orbitals for the neutral molecule, they become nearly pure metal orbitals for the ion.

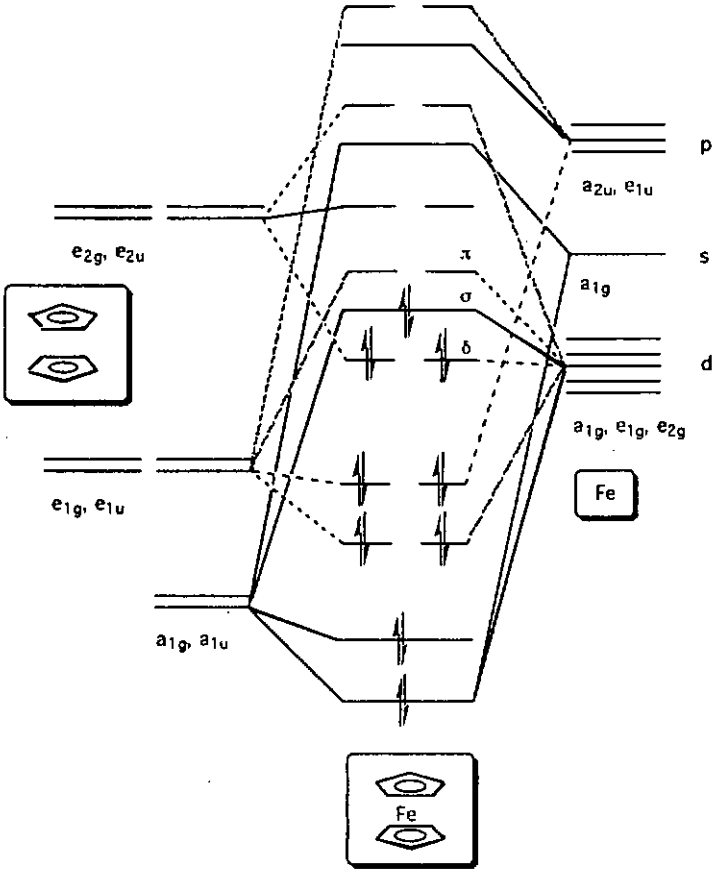

Figure 2.7. *Qualitative MO diagram for ferrocene in its staggered conformation* [21]

2.2.5. Molecular Geometry of Ferrocene and Ferrocenium-Ion

The cyclopentadienyl ligands in ferrocene are flat and arrange themselves co-planar to each other. The distance of 3.3 Å between them is comparable to the vertical van-der-Waals radius in an aromatic ring system. For example, the interplanar distance of crystalline arenes was determined to be ca. 3.4 Å. Therefore, the ferrocene structure is best described as a dimer of two aromatic ring systems incorporating an iron(II) atom.

The two cyclopentadienyl rings can nearly rotate freely and consequently a very low rotation barrier is found. It is about 4-8 kJ mol^{-1} depending on the

substitution pattern of the ligands. The adoption of either staggered (D_{5d}) or eclipsed (D_{5h}) conformations seems to be possible, whereas the eclipsed conformation is a marginally preferred against the staggered conformation [22,23].

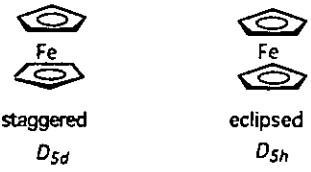

Figure 2.8. *The two principle conformations of ferrocene*

With such a small barrier there are various factors which can make the staggered form more stable. For example decamethylferrocene (1) both in the gas phase and the crystal phase adopts the staggered conformation. In this case repulsions of the methyl groups could be responsible for the difference. Apart from the different conformations both ferrocene (3) and decamethylferrocene (1) are very similar in their structural parameters. Table 2.3. lists some significant structural parameters of various ferrocenes and ferrocenium compounds.

Table 2.3. *Structural Data for some Ferrocene and Ferrocenium Compounds*

	Fe-C [Å]	*C-C in ring [Å]*	*Exocyclic C-C or C-H [Å]*	*Θ [°]*
$[Fe(C_5H_5)_2]$	2.064	1.440	1.104	+3.7
$[Fe(C_5Me_5)_2]$	2.064	1.439	1.503	-3.4
$[Fe(C_5H_5)_2][TCNQ]$	2.090	1.400	1.515	-
$[Fe(C_5H_4Me)_2][I_3]$	2.073	1.401	-	-

Upon oxidation the cyclopentadienyl rings remain eclipsed in $[Fe(C_5H_5)_2]^+$ as in ferrocene, whereas $[Fe(C_5Me_5)_2]$ undergoes an internal rotation from the staggered to the eclipsed form upon oxidation. The Fe-C bond increases small but significantly in going from ferrocene to ferrocenium. This is a reflection of the fact that the e_{2g} orbitals are only weakly bonding but there is also a small increase in the inter-ring distances on oxidation as expected for the removal of an electron.

The influence of the counterion on the electronic structure and the conformation of the two cyclopentadienyl rings in ferrocenium-cations has been studied using Raman, Infrared, Low-Temperature Electronic Absorption, and EPR-measurements [20,24]. X-ray investigations of various ferrocenium-salts have been determined and show an average Fe-C-distance of 2.07 Å for different counterions. The authors conclude, that such electron removal does not defragment the original ferrocene framework and that the constancy of the Fe-C-distance means that there is only little change due to the counterion.

2.3. Experimental Methods

2.3.1. Differential Scanning Calorimetry

Differential Scanning Calorimetry is an experimental method for the investigation of phase transition processes in chemical compounds and especially in liquid-crystalline substances. The main objective is to determine the transition temperature and the transition enthalpy associated with a process. The latter is measured by recording a heat flow, which is the result of a constant heating rate. A small sample is heated or cooled such that the temperature is a linear function of time. As the reference an empty sample pan is heated or cooled at the same rate, that there is no temperature difference between the sample and the reference pan. In the DSC experiment the difference of heat flow ΔQ is measured, which means the difference between Q_{Sample}, the power to the sample, and $Q_{Reference}$, the power to the reference. ($\Delta Q = Q_{Sample} - Q_{Sample}$). ΔQ is determined as a function of temperature. Any endothermic process (example: melting, phase transition on heating from a higher ordered LC state to a lower ordered LC state) will give rise to a peak in one direction and any exothermic process (example: crystallisation, exotherme reaction) will give rise to a peak in the opposite direction. The onset temperature is the characteristic temperature of the transition process and it is determined by the intersection of the baseline prior to the thermal event and the tangent of the peak. The parameters to consider in a DSC experiment are the size of the sample, the heating rate and the temperature range in the case of strong dependence of the thermal history. Usually the experiment is driven under protection gas such as nitrogen. Normally heating rates of a few °C min^{-1} are chosen.

2.3.2. Thermal Gravimetry

Thermal gravimetry is a experimental method for the determination of the mass of a sample as a function of temperature. A mass loss can indicate a chemical process, for example the loss of a portion of the sample like a volatile compound. Another example of a mass loss can be a chemical decomposition. The parameters to consider in a thermogravimetric analyses are the size of the sample, the heating rate and the composition of the pure gas. The variation of the heating rate can lead to superior resolution. Normally heating rates between 10 and 20°C min^{-1} are chosen.

2.4. Literature Survey

In 1910 Vorländer [25] reported the first thermotropic metal-containing liquid crystals. The synthesised alkali carboxylates of type $R\text{-}CO_2Na$ (R=aliphatic or aromatic) displayed lamellar phases, which are typical for amphiphilic molecules. In the meantime various different compounds were synthesised and investigated. These efforts are focused in reviews by Giroud-Godquin and Maitlis (1991)[26,27], Espinet et al. (1992) [28], Polishchuk and Timofeeva (1993) [29], Hudson and Maitlis (1993) [30] and recently by Neve (1996) [31] dealing with transition metal based ionic mesogens.

In this Chapter a literature overview will be presented concerning two subjects. Firstly, various ferrocene- or ferrocenium-containing compounds will be described. Especially, the influence of the substitution pattern on the thermal stability of the ferrocene will be discussed. Attention will be also paid to the mesomorphic properties.

Secondly, attention will be paid to compounds, being similar in their molecular architecture or shape to those molecules, to be presented in this thesis. This overview concentrates on a discussion of the liquid-crystalline properties of alkylpyridinium compounds. Silverstilbazole complexes will also be discussed.

2.4.1. Ferrocene and Ferrocenium Containing Liquid-Crystalline Polymers

In 1995 Zentel and coworkers [5] reported redox-active liquid crystalline side group copolymers containing a ferrocene unit. The corresponding ionomers were synthesised by oxidation of the ferrocene core with benzoquinone in the

presence of $Cu(ClO_4)_2$ or H_2SO_4 (Fig. 2.9). However, only a small amount (up to 10%) of redox active monomer (ferrocene monomer) was copolymerised with a mesogenic monomer.

Due to this reason, a main result observed by Zentel was that the presence of ferrocene units had only minor influence on the liquid crystalline properties of the side group polymers. Even the oxidation of ferrocene to ferrocenium does not strongly influence the mesophase behaviour. A comparison of the neutral copolymer and the oxidised copolymer shows that the phase transition temperatures of the oxidised copolymers containing the monoalkylated ferrocenes are only a few degrees higher. A smectic A and a nematic phase are therefore observed for the oxidised polymers (X=OCH_3). When heated into the S_A-phase, the ClO_4^- salt decomposes. For X=CN nematic phases are observed (anion=ClO_4^- and SO_4^-).

In this study copolymers with different content of ferrocene were synthesised. The mesophase width decreased with increasing ferrocene content and the glass transition temperatures of the oxidised polymers were shifted by a few degrees to higher values compared to the corresponding reduced form.

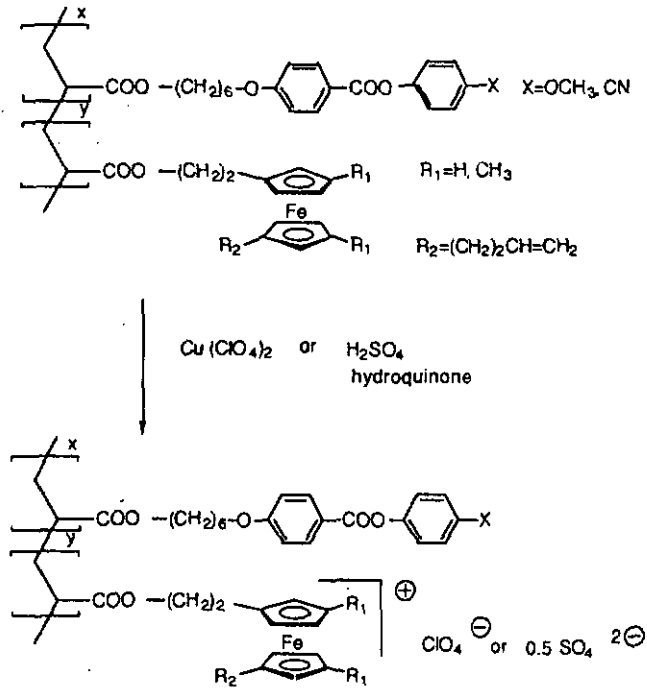

Figure 2.9. *Synthesis of ionomers according to Zentel* [5]

The relation of redox potential and different degrees of ring alkylation in precursors for potentially liquid-crystalline compounds was also investigated by Zentel et al. [8] who synthesised the ferrocene derivatives shown in Figure 2.10. The redox behaviour of the diols was determined and the authors found that alkylation leads to a strong decrease of the redox potential. A decrease of 45 mV per alkyl chain was calculated for a comparison between the precursors shown in Figure 2.10. (R=H, $E_{1/2}$= 0.23 V; R=CH_3, $E_{1/2}$= 0.14 V). For the peralkylated ferrocene derivative ($E_{1/2}$ = 0.0 V) the reduction of the redox potential per alkyl group was found to be smaller.

Figure 2.10. *Ferrocene precursors for the synthesis of ferrocene-containing copolyesters* [8]

Condensation of the diols yielded the polyesters shown in Figure 2.11. The redox potential increases by about 40 to 50 mV in going from the monomer to the polymer. The authors proposed that this increase in the redox potential by polymerisation is presumably due to a charge transfer interaction through the space between the electron poor ester groups and the ferrocene unit.

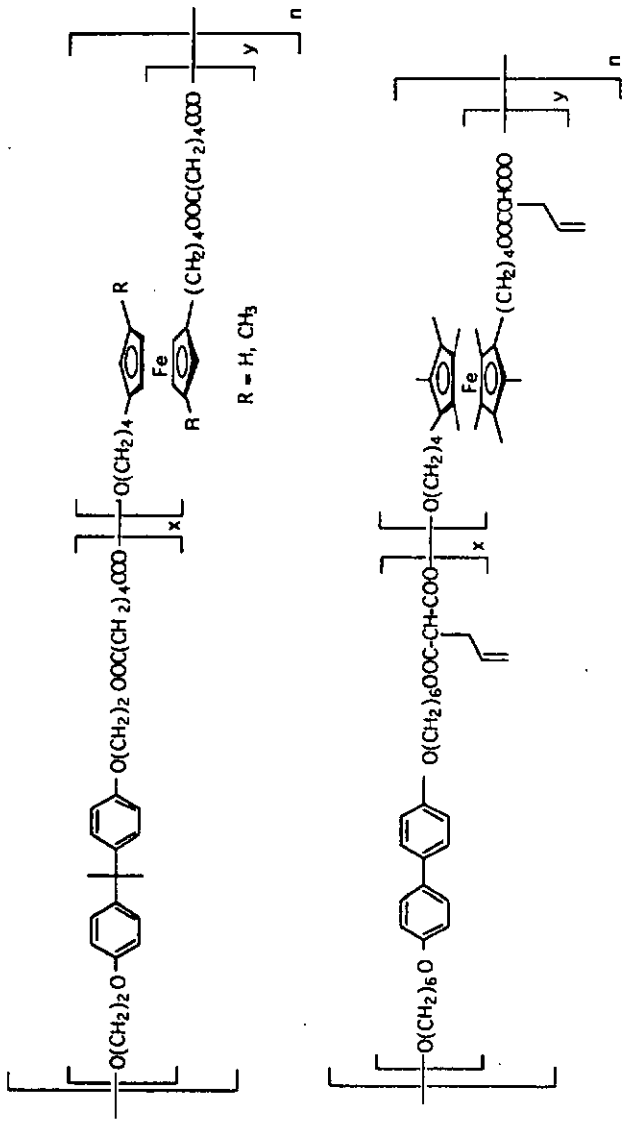

Figure 2.11. *Polymers synthesised by Zentel* [8]

The polycondensation of the peralkylated ferrocene diol (Fig. 2.10.) with allylmalonate and 4,4'-Bis(6-hydroxyhexyloxy)biphenyl resulted in the formation of a liquid-crystalline main chain polymer, peralkylated at the ferrocene unit (Fig. 2.11.). This polymer exhibited enantiotropic S_B and S_A phases. The authors note that these results show that the ferrocene unit is compatible with liquid-crystalline phases. However, the degree of incorporated ferrocene containing monomer is only about 9%. In this study no attempt to oxidise the ferrocene unit was undertaken.

Tanaka et al. [32] synthesised some monosubstituted ferrocenyl acrylates and the corresponding polymers. Thermal properties were investigated, both for monomers and polymers (Fig. 2.12.).

The resulting polymers were mixed with TCNE in the solid state at room temperature to demonstrate the formation of a charge-transfer complex. Indeed an ESR spectrum of the resulting compound showed the formation of unpaired electrons, as indicated by a broad singlet. No further investigations of the oxidised species such as the investigation of the liquid-crystalline properties were undertaken.

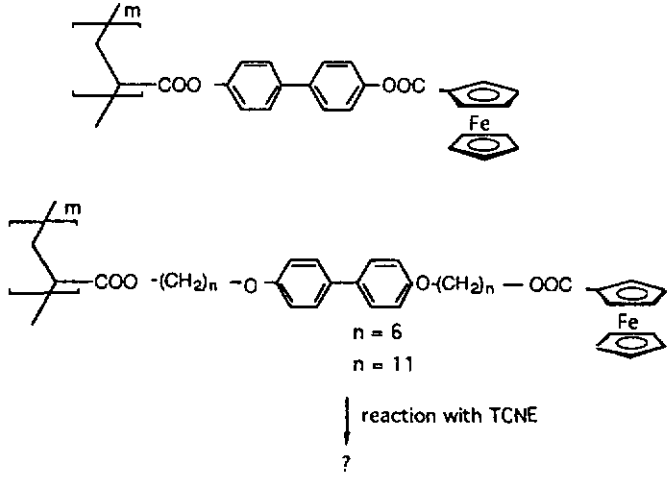

Figure 2.12. *Side chain ferrocene containing polymers synthesised by Tanaka et al.* [32]

In 1995 Cook [33] et al. presented an octasubstituted phthalocyanine containing a monosubstituted ferrocenyl core in one side-chain (Fig. 2.13.). This derivative is presented as the first example of a liquid crystalline ferrocenyl phthalocyanine. It exhibits a single mesophase which was characterised as a discotic columnar mesophase of hexagonal symmetry (Col_h).

A thin film was produced by spin coating techniques. Upon treatment of this film with iodine vapours the colour of the film changed from green to brown, indicating the oxidation of the ferrocene core. A visible region spectrum of this film also showed typical absorption maxima of a iron(III)cyclopentadienyl complex. However, after 40 min no more oxidised substance was detected. Probably due to the increased redox potential of this compound, bearing an electron-withdrawing CO_2-function at the ferrocene unit, the obtained oxidised compound was thermodynamically not stable. No further investigations of the oxidised species such as the investigation of the liquid-crystalline properties were undertaken.

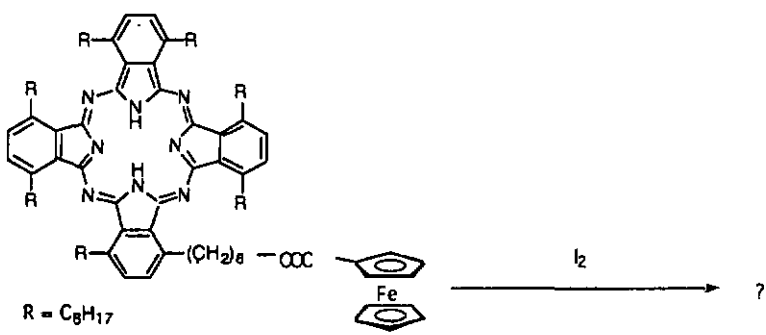

Figure 2.13. *Ferrocene derivative showing a columnar mesophase synthesised by Cook et al.* [33]

2.4.2. Liquid-Crystalline Ferrocenes

The first ferrocene containing liquid-crystals were prepared by Malthête in 1976 [34]. Since 1988 different groups have started to investigate the liquid-crystalline properties of ferrocene-derivatives [35-37]. In the meantime, mainly disubstituted ferrocenes (either 1,1', 1,2 or 1,3-position) have been studied. Recently these results were summarised in a review by Deschenaux and Goodby [1]. Mesogenic side groups are predominantly connected via ester

groups to the ferrocene unit, which makes it difficult to oxidise the iron-centre due to the increased oxidation potential of such ferrocene derivatives.

2.4.3. Liquid-Crystalline Pyridinium-Salts

The pyridinium complexes , shown in Figure 2.14. can be easily obtained by N-alkylation of pyridine with the appropriate alkylhalogenide [38]. The final molecules contain three distinct parts: a flexible aliphatic chain, a rigid polarisable aromatic core and a pyridinium ring. The latter is charged positively and associated with a negatively charged counterion like chloride, bromide or iodide. The authors report layered mesophases for all molecules, namely smectic in nature and A,B and/or E in type.

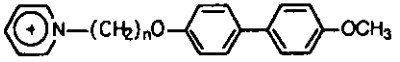

X^- n = 6, 8, 10, 12
X = Cl, Br, I

Figure 2.14. *Molecular structure of N-alkylpyridinium derivatives* [38]

These substances show always a marked hysteresis upon cooling when undergoing the transition from the liquid-crystalline state to the crystalline state. This phenomena of large supercooling periods is explained with the increased viscosity of such ionic species in comparison with non-ionic molecules. The present compounds are thermally stable up to 180°C. The structure of the smectic phase is ascribed as a head to tail arrangement. It seems plausible that the anions arrange themselves close to the positively charged ring. A schematic representation of the head to tail arrangement within the smectic layer is shown in Figure 2.15.

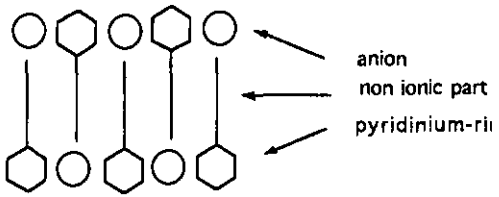

Figure 2.15. *Schematic representation of the head to tail arrangement within the smectic layers* [38]

As a result, the amphiphilic character of the molecules is associated with the segregation phenomena which is more complex than in layered phases formed by "usual smectogenic molecules". The electric interactions between the ionic parts overbalance the van-der-Waals effective repulsions. In case of these alkylpyridinium compounds two sublayers are formed: one containing the ionic part of the molecules and the other with the non-ionic parts, regardless of whether these are aromatic or aliphatic in nature.

Recently Guillon and co-workers [39] investigated the influence of the substitution pattern on the pyridinium ring in pyridinium bromides (Fig. 2.16.). An ethyl group was therefore positioned at each of the three available positions (2-, 3- or 4-position) at the pyridinium ring. 3-substituted derivatives do not show mesomorphism, whereas the 2- and 4-substituted derivatives form smectic phases (A, B or E in type) in case of a spacer length of 9 or 11 carbon atoms. The compounds with shorter spacer length such as 5 or 7 carbon atoms do not show mesomorphic behaviour. It is suggested that the 3-substituted derivatives pack more efficiently than their 2- or 4-substituted isomers. Figure 2.17. demonstrates the proposed arrangement of synthesised salts in the liquid-crystalline phase.

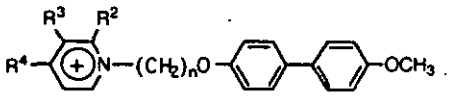

n = 5, 7, 9, 11
R = Et (monosubstituted either in 2-, 3- or 4-positi

Figure 2.16. *N-Alkyl(ethylpyridinium)bromides o-substituted with a methoxybiphenyl group* [39]

The molecular arrangement of these compounds in the smectic phase is similar to the non-alkylated derivatives (Fig. 2.14). The anions are sandwiched between the positively charged pyridinium rings in an up and down distribution. In such an arrangement the molecules are laterally positioned head to tail, having their long-axis perpendicular to the smectic planes. X-ray investigations and the calculated length for the rod-like ionic part of the molecules in their most extended configurations indicated the single layered arrangement as shown in Figure 2.17. In general, the authors conclude that ethyl substitution of the pyridinium rings lowered the thermal stability of the mesophases observed, but left the anisotropic domain unaffected.

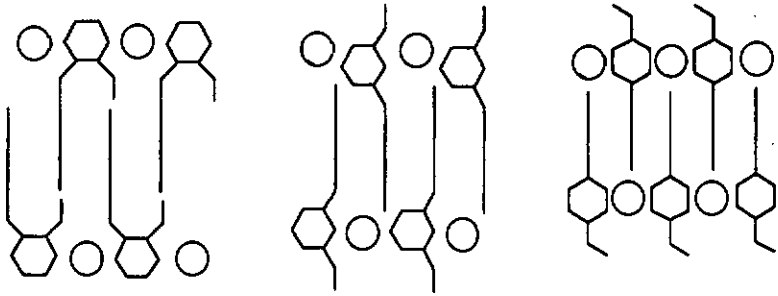

Figure 2.17. *Schematic representation of the head to tail arrangement of the (a) 2-ethylpyridinium, (b) 3-ethylpyridinium and (c) 4-ethylpyridinium salts* [39]

Jegal and Blumstein [40] studied the thermotropic mesophases of two polymers containing pyridinium-salts in the main chain (Fig. 2.18.). The counterions were bromide or tosylate. The polymers containing a bromide counterion are characterised by high melting points probably due to a high level of ionic interaction. They decompose on melting and do not display mesomorphic behaviour. The polymer containing a tosylate anion displayed a broad endotherm in the temperature range from 50 to 120°C on the first heating which disappeared on subsequent heating cycles. Microscopic investigations showed a broad enantiotropic mesophase, probably of smectic nature.

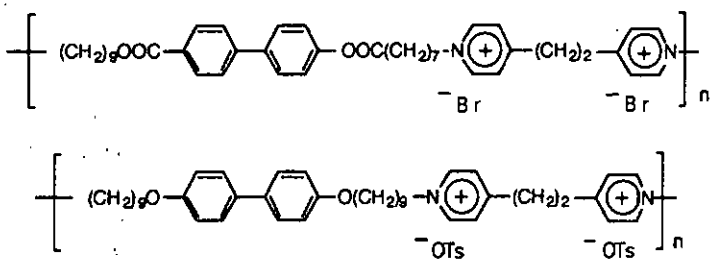

Figure 2.18 *Pyridinium containing main chain polymers with bromide or tosylate anions* [40]

The authors conclude that organic counterions favour the formation of mesophases by lowering the melting point of the ionic polymer. The compound which contains the bromide counterion, is characterised by a high melting point and does not show mesophase behaviour.

Various other investigations on liquid-crystalline pyridinium salts were undertaken [39,41,41-47]. The authors discuss mainly the influence of chain length and the chemical architecture of the cation bearing a pyridinium ring. Liquid-crystalline phases found were always of layered structure.

2.4.4. Silver Stilbazole-Complexes

A great variety of silverstilbazole complexes has been investigated [41,48]. For the complex shown in Figure 2.19. a systematic investigation of the influence of the counterion on the mesomorphic properties was completed [49]. The complexes with X=BF_4 were unstable to light and heat but formed smectic phases at high temperatures. With X=NO_3 smectic A and C phases were observed. For the triflate anion a richer polymorphism was observed. The homologues with n=1-4 showed a nematic phase whereas those for higher homologues exhibited smectic A and C phases, and a crystal smectic G phase. The use of the long chain dodecylsulphate (X=$H_{25}C_{12}OSO_3$) or octylsulphate (X=$H_{17}C_8OSO_3$) as counterions lowered considerably the melting and clearing temperatures. These salts showed a rich polymorphism, such as a nematic, smectic A and C and a cubic phase. In general, the compounds with the octylsulphate counterion, showed similar mesophases.

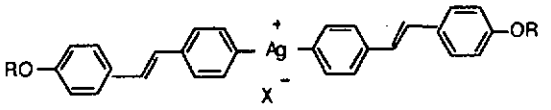

X = BF_4, NO_3, OTf, $H_{25}C_{12}OSO_3$, $H_{17}C_8OSO_3$
R = C_nH_{2n+1} n = 1-12

Figure 2.19. *Silver stilbazoles synthesised by Bruce et al.* [49]

2.4.5. Conclusion

In recent years, there has been continuing interest in ferrocene-containing liquid-crystals. Most of the complexes were disubstituted ferrocenes, either in 1,1'- [50] or in 1,3-position [37,51]. Only some compounds were monosubstituted [52-54]. While these compounds have generated many new liquid-crystalline systems, no attempt was undertaken to oxidise the ferrocene-core in order to study the influence of this process on the liquid-crystalline properties.

In contrast, ferrocene was incorporated into some liquid-crystalline copolymers and these materials were oxidised at the ferrocene core using varying oxidants (hydroquinone / sulphuric acid, $Cu(ClO_4)_2$) [5]. However, due to the small content of ferrocene (only up to 9% of ferrocene-containing monomer was engaged in the polymerisation), the mesophase behaviour of the synthesised copolymers showed only minor changes upon oxidation of the ferrocene core (isotropization temperatures were shifted some degrees to higher temperatures). A liquid-crystalline polymer, based on a ferrocene containing monomer was also oxidised using TCNE [32], but the paramagnetic properties were only investigated at low temperatures. Their liquid-crystalline properties were not investigated. Probably, this was due to the presence of a radical anion which gives rise to decomposition upon heating.

Chapter

3

Objectives

The general purposes of this thesis are to examine liquid-crystalline ferrocenes and mesomorphic ferrocenium containing compounds. We will focus mainly on the effects on the liquid-crystalline properties resulting from the oxidation of the ferrocene unit in a mesogenic compound.

Therefore, the important questions addressed are: which are the factors governing the formation of thermotropic mesophases in ferrocenium-containing compounds and; what is the relation between the molecular architecture and the formation of mesophases. Therefore, we will independently vary the following parameters:

(i) the length of the terminal alkyl chain;
(ii) the length of the flexible spacer connecting the ferrocenium-unit to the mesogenic core;
(iii) the number of aromatic rings in the mesogenic core and,
(iv) the type of counter-anion.

This will enable us to generate some structure-property relationships.
Questions addressed in this thesis are:

(i) what is the relation between the substitution pattern of the ferrocene core and the redox potential of these compounds and;
(ii) which are the factors governing the formation of mesophases in such systems.

Another point to be noticed in this work is the influence of the molecular architecture on the mesophase behaviour in some "monosubstituted" ferrocenes. Structural modifications of the promesogenic core will be particularly examined.

Finally, a series of non-symmetrically disubstituted ferrocenes will be presented. The systematic reduction in symmetry should give rise to lower transition temperatures and an increase of the anisotropic domain.

Chapter

4

Synthesis and Mesomorphism of Liquid-Crystalline Ferrocene and Ferrocenium Derivatives

4.1. Decamethylferrocene (1) and Pentamethylferrocene (2)

Substituents play an important role on the redox properties of ferrocene. They can have either electron-donor or electron-acceptor properties. In order to vary the redox potential of ferrocene, different degrees of substitution with methyl and/or alkyl groups were used. These ferrocenes should be oxidisable under mild conditions to the corresponding ferrocenium ions. Pentamethyl cyclopentadienyl, C_5Me_5, (Cp^*), has been widely used as an electron-donating ligand and convenient synthetic routes to C_5Me_5H (4) have been reported recently [2,55].

Halfsandwich iron(II) complexes (C_5H_5FeR; R=acac, Br, Cl) are versatile starting materials for the synthesis of bileptic dicyclopentadienyl iron(II) compounds. Recently such precursors have been described [9,56]. For example, iron halide complexes are unstable in THF solution above ca. -80°C whereas iron acetylacetonato-complexes, due to the potentially chelating O-donor properties, are more stable. To synthesise the bileptic pentamethylferrocene (2) [10,57-61] and decamethylferrocene (1) [2,62,63] different literature procedures are known. Nevertheless, the synthesis of pentamethylferrocene (2) seems to be not well established.

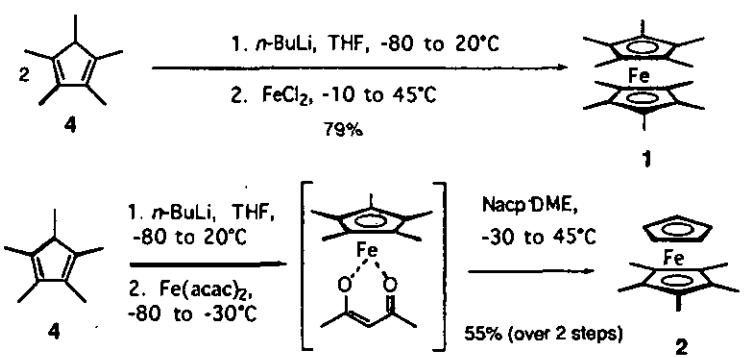

Scheme 4.1.

Pentamethylferrocene (2) has been synthesised following a literature procedure for related ferrocene derivatives [10] (Scheme 4.1.). When a mixture of equimolar amounts of iron(II) acetylacetonate [57,64] and $LiCp^*$ in THF warmed from -78°C to -30°C, a gradual colour change from brown to dark blue/green was observed above -40°C. This indicated the formation of the

acetylacetonato intermediate. However, it was not possible to isolate this intermediate. Following experimental procedures published recently [60] for the synthesis of bileptic ferrocenes, the solution was cooled again to -78°C and reacted with one equivalent of NaCp DME [65], resulting in pentamethylferrocene (2).

Decamethylferrocene (1) was synthesised by reacting two equivalents of $LiCp^*$ with ferrous chloride at -78°C following well established procedures [2,62] (Scheme 4.1.).

4.2. Chemical Oxidation of Ferrocenes

The aim of this work was to investigate the oxidation of ferrocenes, specifically of those substituted with methyl groups. The oxidation of ferrocene (3) with iodine was already reported [66,67] and represents one of the most convenient procedures for the preparation of ferrocenium salts. The reaction leads to ferrocenium polyiodides (5) of variable anion composition (triiodide, pentaiodide or heptaiodide salts have been characterised) [66] (Scheme 4.2.). Ferrocenophanes have also been oxidised with I_2.

In this thesis the triiodide salt 5 was synthesised in order to study its thermal stability. These salts are thermally not stable and decompose on heating.

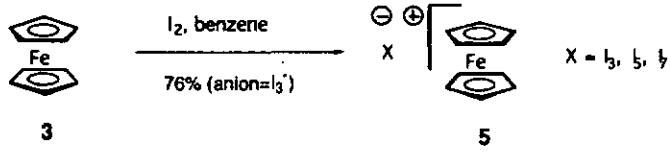

Scheme 4.2.

The aim of this section is to understand the influence of methylation on the redox potential of ferrocene and the search for oxidants. The use of other oxidants should lead to ferrocenium salts containing other counterions and therefore make it possible to investigate the thermal behaviour of salts, which are thermally more stable. The synthesis and structures of the investigated compounds are shown in Scheme 4.3.

For example DDQ can be used for the oxidation of ferrocene [12]. The corresponding charge-transfer complex 11, containing a radical anion as a

counterion, was isolated in good yield. DSC investigations of compound **11** showed a strong exothermic signal upon heating, indicating decomposition.

In contrast the use of silver tosylate did not afford an oxidised ferrocenium species. No change of colour was observed during the reaction period which indicated that ferrocene (3) remained unreacted. These observations underline that the oxidation-potential of ferrocene (3) is too high to be oxidised with a silver salt under these conditions.

In order to obtain further information about the oxidation of ferrocenes, decamethylferrocene (1) and pentamethylferrocene (2) were reacted with silver tosylate. The reaction resulted in the complete oxidation of the ferrocene derivatives 1 and 2 as visualised by a colour change of the reaction mixture from yellow to green. Upon heating, these salts were stable until the melting process began. For decamethylferrocenium tosylate (6) the data obtained from a DSC measurement showed a sharp endothermic melting peak at 290°C. This was followed by a small exothermic peak corresponding to the decomposition of the tosylate-salt 6 in the isotropic melt at about 295°C. The corresponding pentamethylferrocenium tosylate (7) decomposed at 154°C as indicated by DSC measurements.

Pentamethylferrocene (2) was also oxidised with O_2 according to a literature procedure [24]. In this work Duggan and Hendrickson used O_2 for the oxidation of ferrocene in the presence of trichloroacetic acid. This resulted in the formation of a ferrocenium salt as trichloroacetic acid-adduct. The use of pentamethylferrocene (2) under the same experimental conditions (benzene, 5 eq. of pentafluoropropionic acid) revealed a similar result. In this experiment the adduct **10** was isolated. The elemental analyses was consistent with the formula of the compound having structure **10**. Upon heating, compound **10** decomposed at 169°C.

The use of 1eq. of silver heptafluorobutyrate in a mixture of CH_2Cl_2/acetone resulted in the formation of the salt **9**. The counterion was heptafluorobutyrate. A closer look and explanation of the decomposition process of compound 9 upon heating will be discussed in Chapter 5.

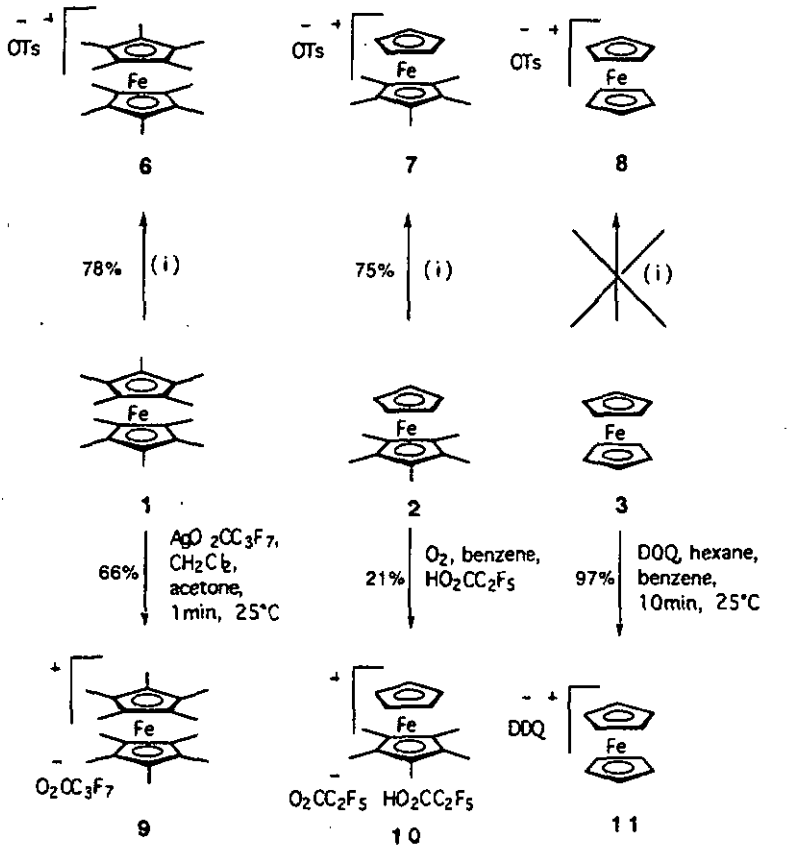

(i) = AgOTs, CH_2Cl_2, acetone, 1min, 25°C

Scheme 4.3.

Table 4.1. *Decomposition temperatures [°C] of salts 6-11*

compound	*dec. [°C]*
6	290-295
7	154
9	140
10	169
11	175

The permethylated ferrocenium derivatives containing a tosylate as counterion seemed to be thermally more stable than those containing other anions. The use of the tosylate counterion in ferrocenium containing liquid crystals seemed therefore to be advantageous. Non-methylated ferrocenes can not be oxidised using silver tosylate. For these reasons we have focused our attention on the development of peralkylated ferrocene precursors.

4.3. The Synthesis of Ferrocene Precursors

The main problem was to develop a method which allows carbon-carbon bond formation between a persubstituted ferrocene and a spacer group. This spacer is believed to connect the mesogenic unit to the ferrocene core. However, in view of the plannified oxidation of the ferrocenyl moiety, an electron donating substituent should be chosen.

As a preferable preparative method the selective oxidation of one methyl group of decamethylferrocene (1) was found. This reaction yields as the main product an aldehyde which itself can be engaged in the second step for carbon-carbon bond formation.

In the first step we prepared, according to a literature procedure [68-72], nonamethylferrocene carboxaldehyde (12)(Scheme 4.4.). The reaction employing barium manganate resulted in the formation of a mixture of three products: compound **12** (42%), octamethylferrocene-1,1'-dicarboxdialdehyde (1%) and octamethylferrocene-1,2-dicarboxdialdehyde (10%). The monoaldehyde **12** was easily separated by column chromatography. The 1,1'- and 1,2-dialdehyde could not be separated by chromatographic techniques and were therefore isolated as mixture. Finally, unreacted decamethylferrocene (1) was recovered in 35% yield.

1',2',3',4',5'-Pentamethylferrocene-1-carboxaldehyde (**14**) was prepared according to a literature procedure by reaction of pentamethylferrocene (2) with phosphoroxychloride and N,N-dimethylformamide under Vilsmeyer conditions in good yield [56].

Ferrocenecarboxaldehyde (16) is commercially available.

The Wittig reaction can be an effective method for stereoselective synthesis of carbon-carbon double bonds. Aldehydes react with non-stabilised

phosphonium-ylides to produce predominantly *cis*-olefines. Reaction of ferrocene carboxaldehyde (16) with an ylide generated from $Ph_3P^+(CH_2)_4CO_2H$ Br^- and KO-^{t}Bu in THF, under conditions that are widely employed for Wittig-reactions, provided a good yield of 6-ferrocenyl-5-hexenoic acid (17) with a 60/40 *cis/trans* ratio. However, in the case of the sterical hindered polysubstituted ferrocene aldehydes 12 and 14, only the *trans*-products 13 and 15 were obtained. The synthetic pathways leading to compounds 13, 15 and 17 are outlined in Scheme 4.4.

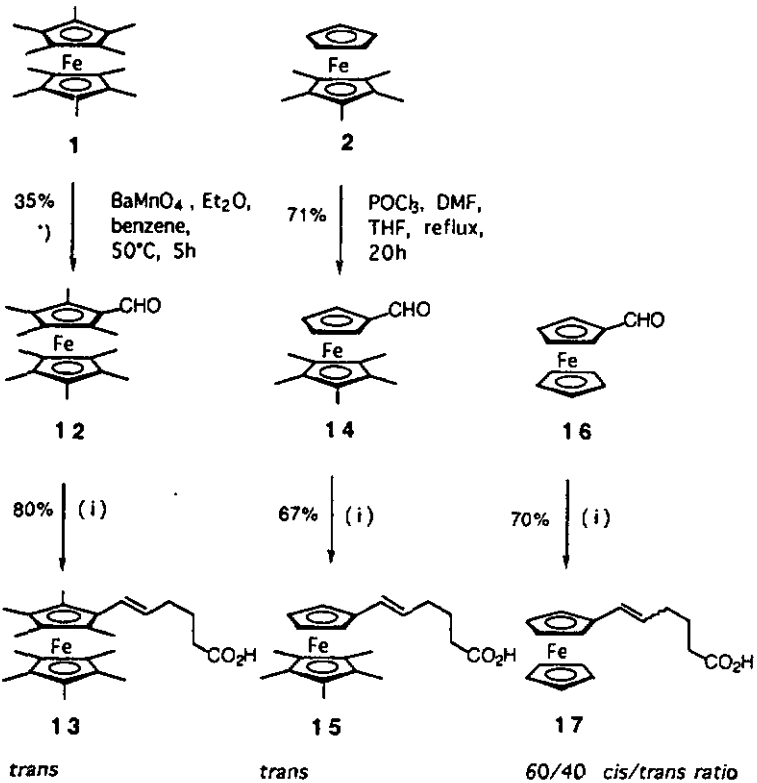

*) Octamethylferrocene-1,2-dicerboxdialdehyde and Octamethylferrocene-1,1'-dicarboxdialdehyde are formed as by-products

Scheme 4.4.

Aldehydes 12 and 14 were also reacted under Wittig reaction conditions in the presence of (4-carboxybenzyl)triphenyl-phosphonium bromide [73]. This reaction provided the acids 18 and 19 (Scheme 4.5.). Both reactions furnished only the *trans*-isomers.

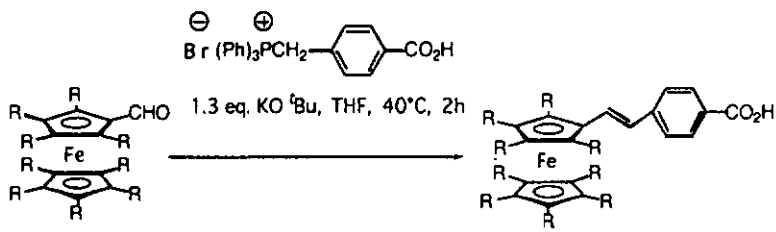

16 R=H
12 R=CH_3

18 R=H, yield: 34%
19 R=CH_3, yield: 15%

Scheme 4.5.

4.3.1. Conclusion

Electron-donating substituents were introduced on the ferrocene unit to lower its oxidation potential.

One methyl group of decamethylferrocene (1) was oxidised according to literature procedures to give the aldehyde 12. At this step the carbonyl function in compound 12 gave way for carbon-carbon bond formation using (4-carboxybutyl)triphenyl-phosphonium bromide under Wittig reaction conditions. In view of the oxidation potential of the targeted ferrocene-derivatives it seemed advantageous to introduce a five membered spacer. This spacer separates the electron withdrawing carboxy function.

However, in a subsequent reaction step, the double bond, in conjugation to the cyclopentadienyl ring, should be transformed to a single bond.

This resulting permethylated ferrocene core displays a redox-active unit and its oxidation potential is considerably lowered in comparison to those of ferrocene (3). In view of calamitic liquid-crystalline phase formation, however, it seemed unfavourable to further increase the steric hindrance of such a molecular fragment.

4.4. Polymethylated Ferrocenes and Ferrocenium Compounds

4.4.1. Ferrocenes and Ferrocenium-Derivatives Bearing Four Aromatic Rings in the Mesogenic Unit

A permethylated ferrocene core undergoes facile oxidation under acidic conditions. Therefore, in the first step the esterification of the acid **13** with the 4-hydroxy-4'-benzyloxy biphenyl (**20**)[74] was realised under mild conditions (Scheme 4.6.). These experimental conditions will be used as standard experimental conditions for esterification [75] (DCC, Ppy, CH_2Cl_2, 25°C, 3 h) unless stated otherwise. It should be noted that the yields of this reaction were normally between 60-80 %.

In the second step the protected biphenyl **21** was deprotected. The double bond was reduced at the same time. The experimental conditions used in this reaction will be used as standard experimental conditions for reactions performed under H_2-atmosphere (deprotection: H_2 4 bars, 10% Pd/C-catalyst, CH_2Cl_2, EtOH, 25°C, 8 h; hydrogenation of double bond: H_2 4 bars, 10% Pd/C-catalyst, CH_2Cl_2, EtOH, 25°C, 30 min).

The main idea behind the use of a molecular architecture bearing four aromatic units in its rigid core, such as in compounds **24-27**, is a long promesogenic core. Instead of the bulkiness of the permethylated ferrocenyl moiety it seemed likely that such a long system should display liquid-crystal behaviour. However, it is known [76,77] that such systems show considerably increased transition temperatures.

Subsequent esterification of **22** with the acids **23a-d** [78,79] led to compounds **24-27**. In the last reaction step the ferrocene core was oxidised with 1eq. of AgOTs, AgOTf or $AgO_2CC_3F_7$, respectively, in CH_2Cl_2/acetone. The experimental conditions used for this oxidation will be used as our standard oxidation procedure (AgX, [X^-=OTs-, OTf-, $C_3F_7CO_2^-$], CH_2Cl_2, acetone, 25°C, some minutes) unless stated otherwise. After purification of the crude products by column chromatography and crystallisation, analytically pure products were obtained.

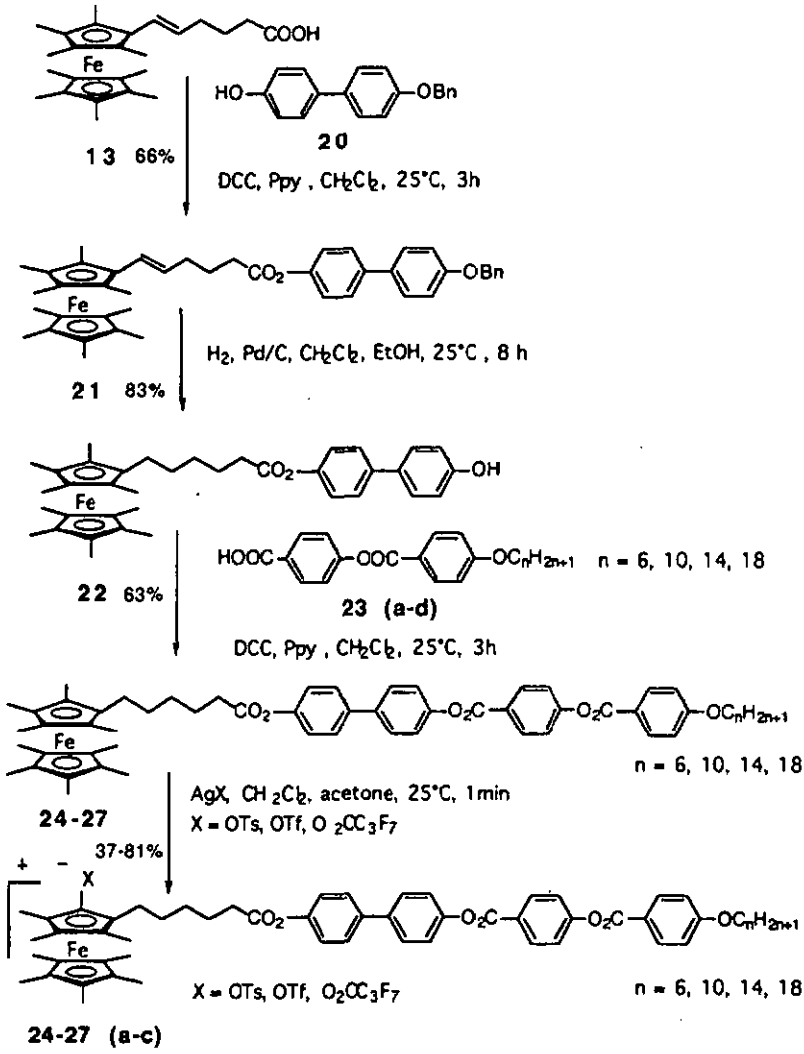

Scheme 4.6. *(For adopted numbers see Table 4.2.)*

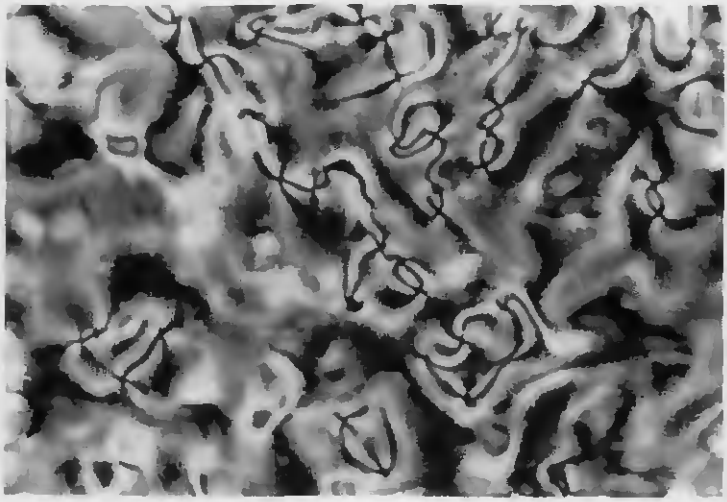

Figure 4.2. *Optical Polarised microphotographs of the nematic phase of compound 27 upon cooling from the isotropic liquid at 155°C; 320 x*

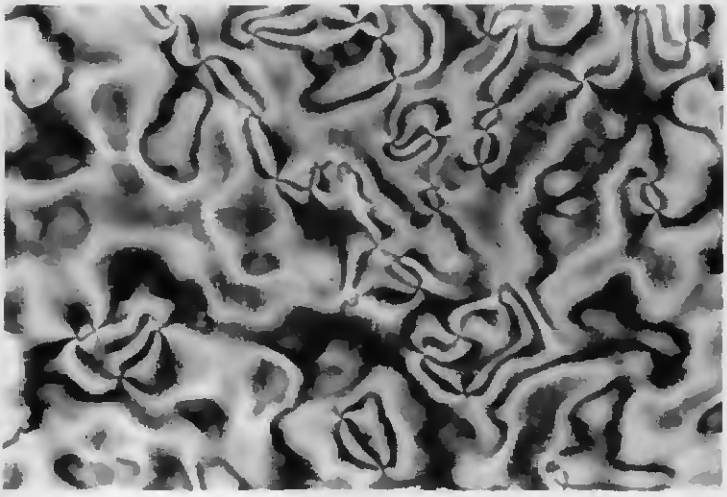

Figure 4.3. *Optical Polarised microphotographs of the smectic C phase of compound 27 upon cooling from the nematic phase at 153°C; 320 x*

Table 4.2. *Adopted numbering scheme for compounds 24-27 (a-c)*

n	*ferrocene*	OTs^-	$C_3H_7CO_2^-$	OTf^-
6	24	24a	24b	-
10	25	25a	25b	25c
14	26	26a	26b	26c
18	27	27a	27b	27c

"Non-oxidised" ferrocenes derivatives (compounds 24-27)

Ferrocenes 24-27 show mesophases with dominating nematic character and relatively high melting and isotropisation temperatures for short alkyl chains. The variation of the terminal groups of the mesogens shows that the alkyl chains have a strong influence on the mesophase behaviour. For longer alkoxy chains both melting and clearing temperatures were lowered considerably. All derivatives showed nematic phases with a mesophase range of about 10°C. The mesophase was characterised by a typical schlieren texture and droplets (Figure 4.2.). The octadecyloxy-derivative (27) exhibits an additional monotropic smectic C phase as indicated by its optical texture (Figure 4.3.). The transition temperatures and enthalpies are summarised in Table 4.3. and the phase diagram is shown in Figure 4.4. The DSC analysis for compound 27 is given in Figure 4.1.

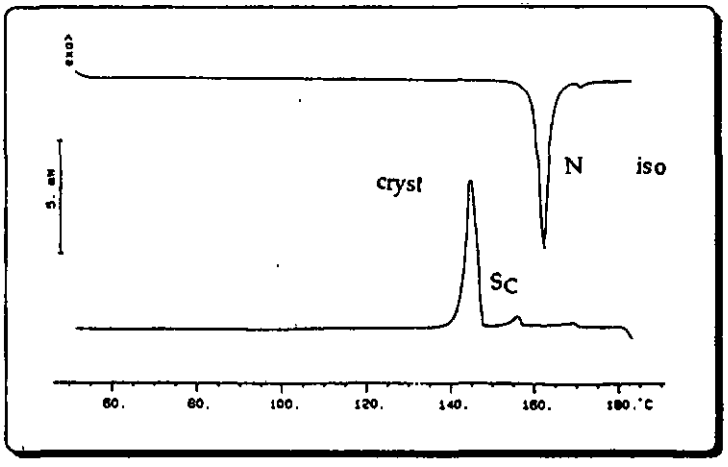

Figure 4.1. *DSC scan obtained of compound 27; first cooling and second heating run; scan rate 10°C min^{-1};*

Table 4.3. *Phase transition temperatures [°C] and enthalpy changes [kJ mol^{-1}] of compounds 24-27*

compound	n	cryst/N	N/iso	N/S_C	S_C/cryst
24	6	199 (35.1)	215 (0.6)	-	-
25	10	189 (49.3)	198 (0.4)	-	-
26	14	167 (43.3)	183 (0.6)	-	-
27	18	161 (57.1)	171 (0.7)	(158) (2.1)	148 (52.8)

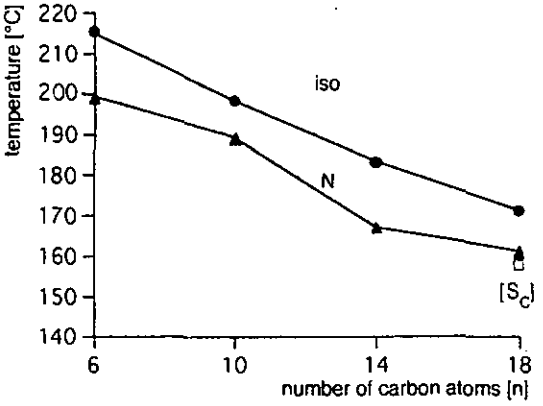

Figure 4.4. *Phase diagram of ferrocene-derivatives 24-27; ▲: melting point ;●: isotropisation, □: N →S_C transition*

Oxidised compounds (compounds 24a,b, 25a-c, 26a-c and 27a-c)

Tosylate as counterion (compounds 24a, 25a, 26a and 27a)

All synthesised salts containing a tosylate counter-anion showed an enantiotropic smectic A phase (Table 4.4.). Compound 27a showed an additional enantiotropic smectic C phase and compound 26a exhibited a monotropic smectic C phase. Upon heating into the isotropic liquid, all substances decomposed. This made it sometimes difficult to observe correct transition temperatures and optical textures. All compounds displayed an oily streak texture with large homeotropic domains (Fig. 4.6.). These textures are

characteristic to smectic A phases. The smectic C phases of 26a and 27a were identified upon cooling the substances from the smectic A phase (without heating before into the isotropic liquid), showing a typical sanded texture (Fig. 4.7.). The results are summarised in Figure 4.5.

Table 4.4. *Phase transition temperatures [°C] and enthalpy-changes [kJ mol^{-1}] of compounds 24a, 25a, 26a and 27a),* [a] *no enthalpy change could be measured*

compound	*n*	*cryst/S_A*	*S_A/S_C*	*S_A/iso*	*cryst/iso*
24a	6	-	-	(148(4.1))	184 (71.2)
25a	10	141 (53.6)	-	159 (3.6)	-
26a	14	129 (56.2)	(100)[a]	170 (2.8)	-
27a	18	133 (59.8)	138[a]	180 (0.9)	-

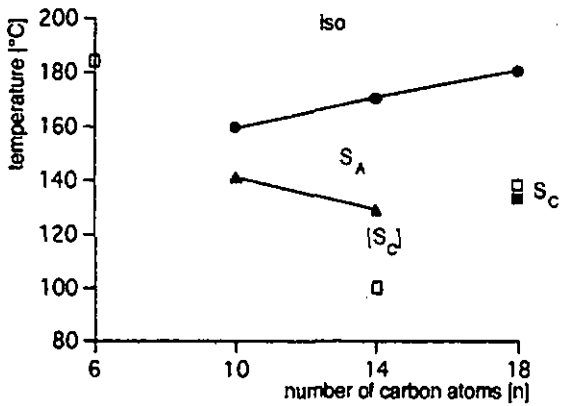

Figure 4.5. *Phase diagram for ferrocenium tosylates 24a, 25a, 26a and 27a;* ▲*: melting point ;* ●*: isotropisation,* ◻ *S_C/S_A*

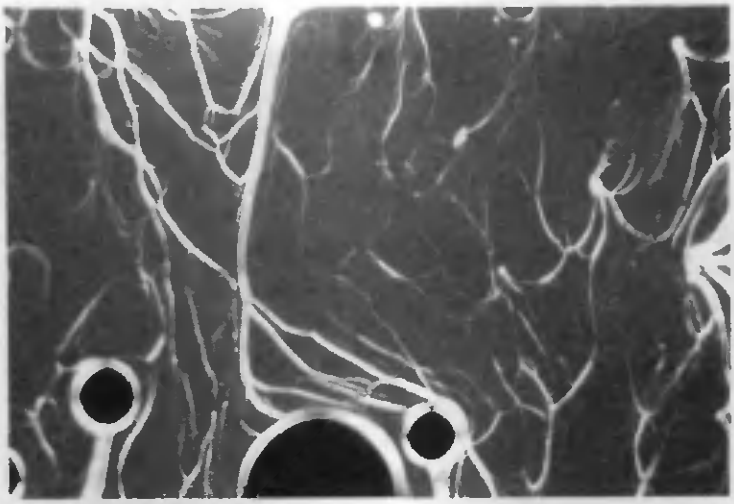

Figure 4.6. *Optical Polurised microphotographs of the smectic A phase of 27a upon cooling from the isotropic liquid at 139°C; 100x*

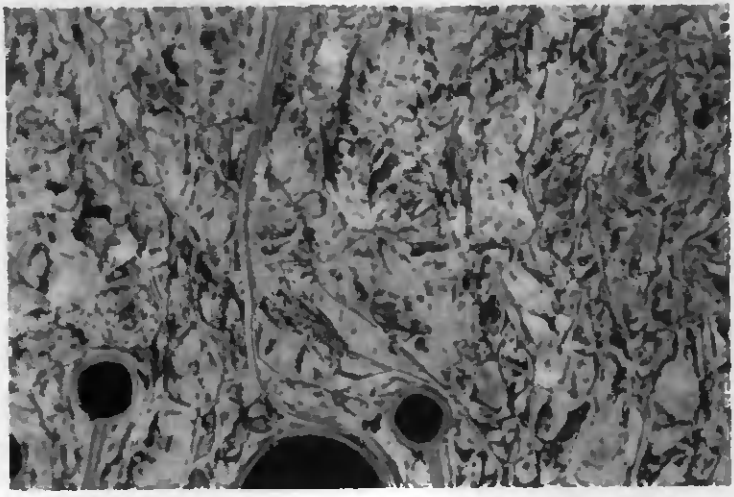

Figure 4.7. *Optical Polarised microphotographs of the smectic C phase of 27a upon cooling from the smectic A phase at 134°C: 100x*

Heptafluorobutyrate as counterion (24b, 25b, 26b and 27b)

When heated, all ferrocenium heptafluorobutyrates showed similar thermal behaviour. Upon heating at about 140°C, a liquid-crystalline-like texture was observed wherein the phase formed a webbing pattern of focal-conic-like defects. In the bounding area decomposed material and gaseous material were observed. The substance turned slowly brown indicating a decomposition process. Thermogravimetric experiments showed a weight loss for each of the heptafluorobutyrate salts between 120 and 150°C (for a closer look see Chapter 5). After reaching a plateau at about 200°C all compounds began to decompose completely. The thermal behaviour of compounds **24b-27b** is summarised in Table 4.5.

Table 4.5. *Decomposition temperatures [°C] of compounds* **24b-27b** *determined by microscopic observations and TG measurements*

compound	*n*	*dec.*
24b	6	~120
25b	10	~120
26b	14	~120
27b	18	~120

Trifluorosulphonate as counterion (compounds 25c, 26c and 27c)

With one exception, the salts containing a triflate counterion did not display mesomorphic behaviour. Only the derivative bearing the octadecyloxy terminal chain displayed a monotropic liquid-crystalline phase. When heated, **27c** melted into an isotropic liquid at 211°C When cooled at 192°C the formation of batonnets was observed, indicating the formation of a smectic A phase. The transition temperatures and enthalpies are summarised in Table 4.6.

Table 4.6. *Phase transition temperatures [°C] and enthalpy-changes [kJ mol^{-1}] of compounds 25c-27c)*

compound	*n*	*cryst$_1$/cryst$_2$*	*cryst$_2$/iso*	*iso/S_A*
25c	10	-	210 (43.7)	-
26c	14	173 (26.1)	207 (28.9)	-
27c	18	168 (31.6)	211 (26.5)	(192) (19.9)

4.4.2. Ferrocene and Ferrocenium Derivatives Bearing Three Aromatic Rings in the Mesogenic Core

4.4.2.1. Derivatives Incorporating a Long Spacer (compounds 31 and 31a-g)

To obtain further information about the influence of the counterion on the liquid-crystalline properties of ferrocenium salts we investigated seven different counter-anions. Specifically, we studied the tosylate, triflate, trifuoroacetate, pentafluoropropionate and heptafluorobutyrate anions and two radical anions ($TCNE^{-}$, $TCNQ^{-}$).

The ferrocenium salts 31a-g were prepared by a synthetic route (Scheme 4.7.) which started with the reaction of nonamethylferrocene-hexenoic acid (13) with 10-(4-benzyloxy-phenoxy)-decan1-1ol (28)[80] to afford the benzyl protected phenol 29. Deprotection of 29 (see standard experimental deprotection procedure) afforded the phenol derivative 30 (the double bond was also reduced in this reaction step). Subsequent esterification of 30 with 4-octadecyloxybenzoic acid-4-carboxyphenyl ester (23d), according to the standard esterification procedure, yielded the liquid-crystalline ferrocene-derivative 31. Oxidation of the ferrocene moiety using different oxidising agents (AgOTs, AgOTf, AgO_2CF_3, $AgO_2CC_2F_5$, $AgO_2CC_3F_7$, TCNQ, TCNE) afforded the ferrocenium salts 31a-g.

Mesomorphic behaviour

When heated, compound 31 melted at 80°C to a smectic C phase which transformed at 89°C tn a smectic A phase. The latter cleared at 95°C into the isotropic melt. At a scanning rate of 10°C min^{-1} the DSC thermogram of 31 showed very broad transitions. Even at a scanning rate of 1°C min^{-1} melting and clearing transitions overlapped and no enthalpy changes could be

determined. The results are compared with those obtained for the non-oxidised ferrocene derivative 31 (see Table 4.7.).

The oxidation of compound 31 with silver tosylate gave only minor changes in the liquid-crystalline properties. Compound 31a exhibited the same mesophases as compound 31. The mesophase range remained nearly unaffected (16°C) whereas transition temperatures were approximately 10°C higher. Figure 4.8. shows a typical example of a DSC thermogram at a scanning rate of 2°C min^{-1}. Upon cooling a partial crystallisation was observed whereas also a glass transition was seen in the DSC.

The salt 31b bearing a triflate counter-anion showed a remarkably different phase behaviour. When heated, compound 31b gave an endotherm at 131°C which corresponded to the formation of an isotropic fluid. On cooling, an exotherm was detected. Polarised optical microscopy revealed the formation of a crystalline phase. .

Oxidation of compound 31 with AgO_2CF_3, $AgO_2CC_2F_5$ and $AgO_2CC_3F_7$, respectively, afforded the salts 31c, 31d and 31e also exhibiting a smectic C and smectic A phase on heating. The mesophase range was slightly broader for compounds 31d (19°C) and 31e (24°C) when compared to the non-oxidised species. Compound 31c was amorphous. No melting peak was registered.

The use of TCNE as an oxidant led to the deeply coloured ferrocenium charge-transfer complex 31f containing the TCNE radical-anion as the counterion. This material was only stable if stored at -30°C, but decomposed slowly at room temperature. DSC measurements of 31f showed only an exothermic signal upon heating with an onset temperature of 50°C, thus indicating decomposition. The analogous oxidation of 31 with TCNQ produced the charge-transfer complex 31g, also not stable upon heating. This compound showed a similar thermal behaviour as the TCNE-complexe.

In conclusion, all liquid-crystalline salts (31a, 31c, 31d and 31e) displayed focal conic textures growing from the isotropic phase as batonnets and/or large homeotropic domains. A smectic C and a smectic A phase were always observed whereas the mesophase range was slightly broader than in the case of the non-oxidised precursor.

The use of a small counter-anion like triflate (compound **31b**) did not favour the formation of liquid-crystalline phases. Salts bearing radical anions as counter-anions were thermally not stable.

At a scanning rate of 10°C min^{-1} all liquid-crystalline compounds showed broad melting peaks and broad isotropisation peaks. Furthermore, crystallisation rarely occurred at a cooling rate of 10°C min^{-1}. On cooling, these salts formed glassy states rather than crystalline states.

The DSC results were thus in agreement with microscopic observations. The transition temperatures and enthalpies, summarised in Table 4.7., were determined either by microscopic investigations and/or DSC measurements.

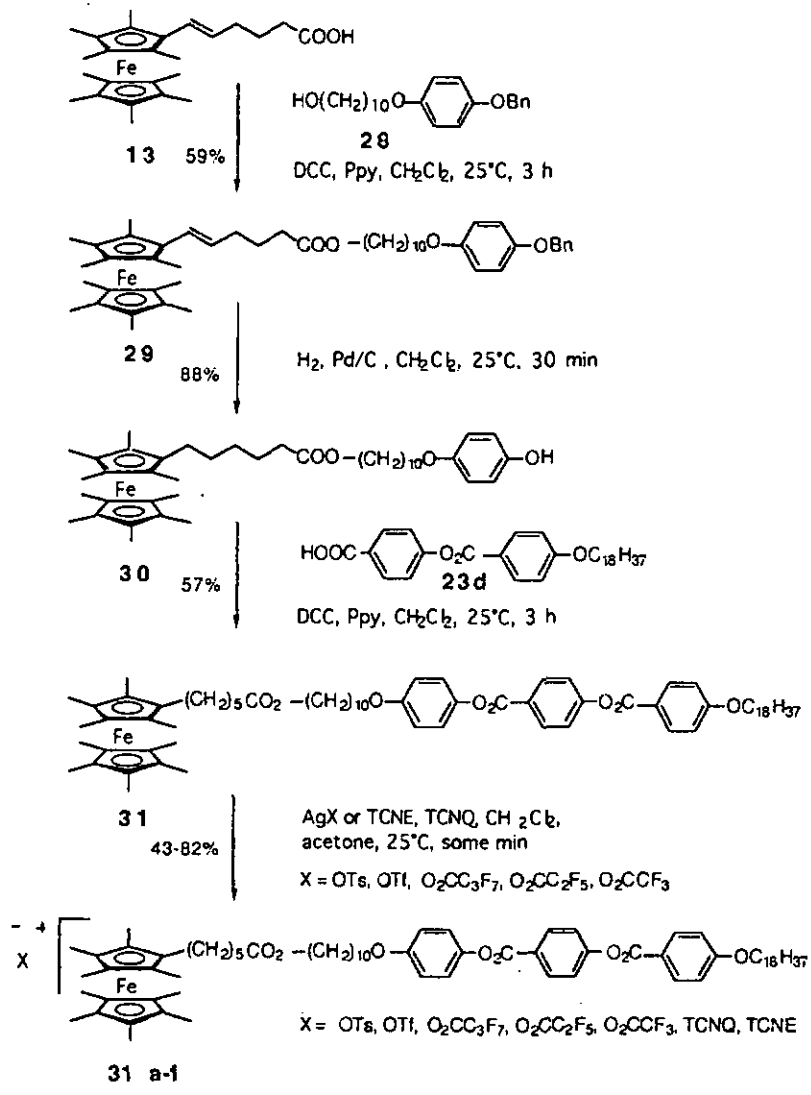
COOH
Fe
13
59%
HO(CH2)10O
OBn
28
DCC, Ppy, CH2Cl2, 25°C, 3 h
COO –(CH2)10O
OBn
29
88%
H2, Pd/C , CH2Cl2, 25°C, 30 min
COO –(CH2)10O
OH
30
57%
HOOC
O2C
OC18H37
23d
DCC, Ppy, CH2Cl2, 25°C, 3 h
(CH2)5CO2 –(CH2)10O
31
43-82%
AgX or TCNE, TCNQ, CH 2Cl2,
acetone, 25°C, some min
X = OTs, OTf, O2CC3F7, O2CC2F5, O2CCF3
X
31 a-1
X= OTs, OTf, O2CC3F7, O2CC2F5, O2CCF3, TCNQ, TCNE

Scheme 4.7.

Table 4.7. *Phase transition temperatures [°C] and enthalpy-changes [kJ mol^{-1}] of compounds x-y; [a] transition enthalpies not measured du to peak overlap; [b] DSC scanning rate: 2°C min^{-1}; [c] phase transitions based on microscopic investigations; [d] compound 31e: no melting peak registered no crystals were obtained; [e] not detectable; [f] from optical microscopy observations*

compound	*anion*	*cryst/S_C*	*S_C/S_A*	*S_A/iso*	*cryst/iso*	*dec.*
31	none[a, b]	80	89	95	-	-
31a	OTs^-[b]	88 (11.4)	94 (2.0)	104 (8.8)	-	-
31b	OTf^-	-	-	-	131 (31.5)	-
31c	$CF_3CO_2^-$[c, d]	e	103	112	-	-
31d	$C_2F_5CO_2^-$[b]	86 (11.7)	97 (0.5)	105 (11.7)	-	-
31e	$C_3F_7CO_2^-$[c]	88	103	112	-	-
31f	$TCNQ^-$	-	-	-	-	~80[f]
31g	$TCNE^-$	-	-	-	-	~90[f]

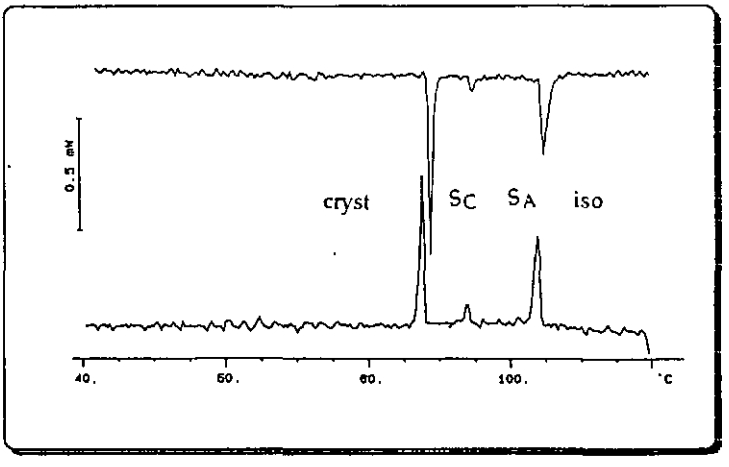

Figure 4.8. *DSC scans obtained of compound 31a, first cooling and second heating run; scan rate 2°C min^{-1}*

4.4.2.2. The Influence of Different Substitution Patterns of Ferrocenes on the Liquid-Crystalline and Redox Properties

The synthesis of compound 34 is shown in Scheme 4.8. Compound 34 was synthesised by esterification of ferrocenecarboxylic acid with the phenol-derivative 33, using the standard esterification method. Compounds 36-43 were synthesised by synthetic routes, shown in Scheme 4.9. The acids 13, 15, 17 and 35 [81] were converted into the esters 36, 38, 40 and 42 in the presence of DCC and Ppy. The final ferrocene-derivatives 37, 39, 41 and 43 were achieved by reduction of the double bond in the presence of H_2 and Pd/C catalyst.

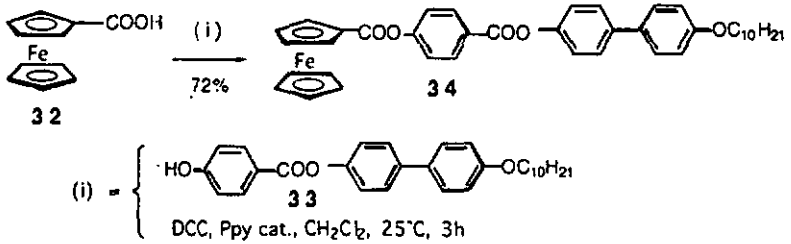

Scheme 4.8.

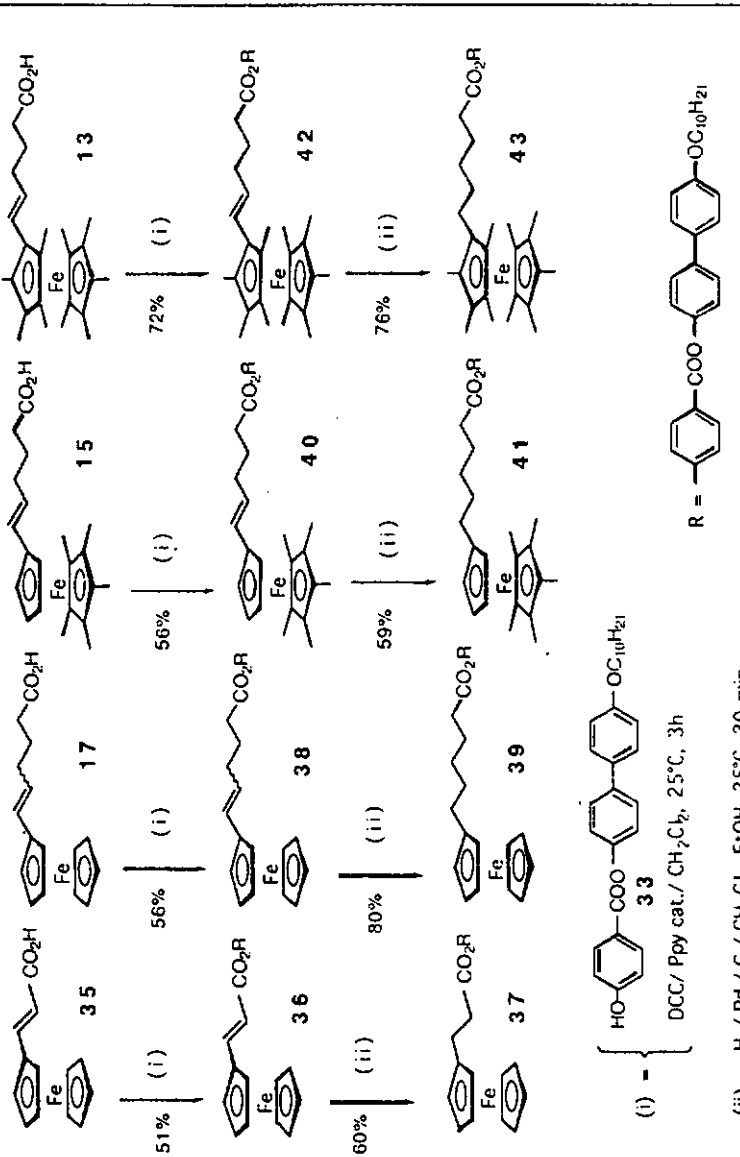
35
36
37
17
38
39
15
40
41
13
42
43
51%
60%
56%
80%
56%
59%
72%
76%
(i)
(ii)
(i) = DCC/ Ppy cat./ CH_2Cl_2, 25°C, 3h
(ii) = H_2/ Pd / C / CH_2Cl_2, EtOH, 25°C, 30 min
R =

Scheme 4.9.

4.4.2.2.1. Electrnchemical Behavinur

Cyclic voltammetry experiments were performed in order to study the electrochemical properties of the seven compounds. These compounds present ferrocene derivatives, fitted with an electroactive ferrocene group for reversible electron exchange. All derivatives contained the same rigid core, so that other effects than those coming from the substitution pattern of the ferrocenyl moiety could be excluded.

All compounds undergo a one-electron reversible oxidation centred at the iron atom. The effects of the substituents on the half-wave oxidation potential is demonstrated in terms of their electronic properties (Table 4.8.). These results are discussed in Chapter 5.

Table 4.8. *Electrochemical data of ferrocenes derivatives differing in their substitution pattern,*

compound	$E_{1/2}$ *[V] vs SCE*	*E [mV]*	E_{AP} *(V)irrev.*
34	0.84	140	+ 1.65
36	0.69	140	+ 1.65
37	0.53	144	+ 1.63
38	0.51	140	+ 1.66
39	0.45	130	+ 1.63
41	0.18	116	+ 1.65
43	-0.07	122	+ 1.69

4.4.2.2.2. Liquid Crystalline Properties

In Scheme 4.9. several mesogenic ferrocene derivatives with different structures and their synthesis are contrasted, but all of them possess the same promesogenic unit. The liquid-crystalline properties of these compounds have been studied. For compound 38 no investigations were undertaken, because this substance represents a *cis/trans*-mixture. Compound 40 was not isolated but engaged without further purification in the following reaction step. Therefore no investigations of the liquid-crystalline behaviour were undertaken. The transition temperatures [°C] and enthalpy changes [kJ mol^{-1}] are summarised in Table 4.9.

- Compound 34 did not show liquid-crystalline behaviour.

- Compound 36 showed an enantiotropic nematic phase.

- By contrast, when heated, compound 37 melted into an isotropic liquid at 149°C. When cooled from the isotropic liquid, a nematic phase appeared as droplets at 145°C. Upon further cooling a smectic C phase appeared at 117°C.

- Compound 39 showed a rich mesomorphism. When heated, compound 39 melted at 96°C to a smectic C phase which transformed on further heating to a nematic phase at 131°C. The isotropic phase occurred at 144°C. On cooling an additional mesophase was observed at 96°C. X-ray diffraction spectra were recorded for compound 39 and a smectic E phase was identified.

- Compound 41 showed the same mesophase types as compound 39, whereas the smectic E phase became enantiotropic.

- Compound 42 did not show liquid-crystalline behaviour.

- Compound 43 did not display liquid-crystalline properties. For a more detailed discussion of the thermal behaviour, see the following Chapter.

Table 4.9. *Phase transition temperatures [°C] and enthalpy changes [kJ mol^{-1}] of compounds 34, 36, 37, 39, 41, 42 and 43*

	cryst1/ cryst2	*cryst/ SE*	*cryst/ SC*	*cryst/ N*	*cryst/ iso*	*SE/ SC*	*SC/ N*	*N/ iso*
34	-	-	-	-	120	-	-	-
					(39.4)			
36	-	-	-	143	-	-	-	156
				(36.8)				*(3.4)*
37	-	-	-	-	149	-	(117)	(145)
					(144.9)		*(8.2)*	*(4.0)*
39	-	-	96	-	-	(96)	131	144
			(90.0)			*(8.0)*	*(10.9)*	(2.5)
41	86	93	-	-	-	108	114	120
	(15.2)	*(18.4)*				*(0.7)*	*(18.4)*	*(5.6)*
42	-	-	-	-	127	-	-	-
43	-	-	-	-	154	-	-	-
					(41.5)			

4.4.2.2.3. Preparation and Characterisation of Ferrocenium Tosylates 41a, 43a, 45a and 46a

The synthetic pathways for the synthesis of compounds 43a, 45, 46, 45a and 46a are similar to those compounds already presented in this thesis and are shown in Schemes 4.10. and 4.11.

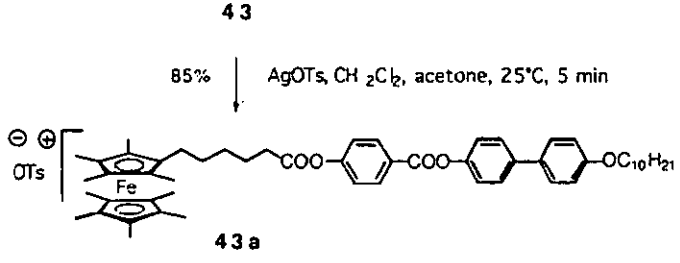

Scheme 4.10.

Generally it is observed that there is a distinct difference in the thermal behaviour between the compounds in their "reduced" form and their oxidised form. Liquid crystallinity was only seen when the peralkylated ferrocenes were oxidised, while none of the "reduced" species exhibited a mesophase. The thermal behaviour of compounds **43**, **45**, **46**, **43a**, **45a** and **46** is summarised in Table 4.10.

Thermal behaviour of compounds **43** *and* **43a**

Compound **43** melted at 154°C into an isotropic fluid.

Upon oxidation the thermal behaviour changed dramatically. During the first heating run the ferrocenium tosylate **43a** gave an endotherm at 132°C, which corresponded to the formation of an isotropic fluid. On cooling from the isotropic melt, an exotherm was detected at 83°C followed by a glass transition temperature at 33°C. Polarised optical microscopy investigations and X-ray investigations revealed the formation of a smectic A phase from 83°C. During the second heating, the liquid-crystalline phase formed at the glass transition temperature (ca. 37°C) and cleared at 83°C. The DSC scan obtained for compound **43a** is shown in Figure 4.9.

X-Ray Investigations of compound **43a**

X-ray diffraction studies, which were performed upon cooling **43a** from the isotropic liquid in a magnetic field of 1.7 T, gave patterns typical of a smectic A phase (the director is parallel to the magnetic field and the layer planes perpendicular to it) with a *d*-layer spacing of 39.5 Å. From CPK models, an approximate length L of 41 Å was measured for **43a** in its fully extended conformation. Upon long irradiation times, solidification of the sample was detected. This result was in agreement with the monotropic character of the mesophase. The isotropic phase was also identified by means of X-ray diffraction.

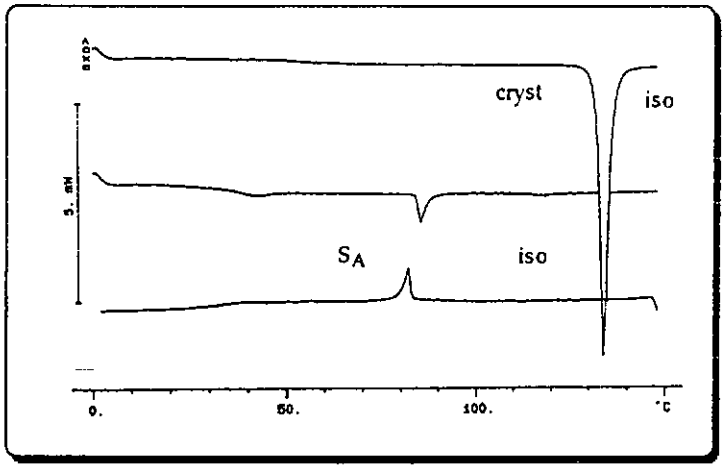

Figure 4.9. *DSC scan obtained for compound 43a; first heating, first cooling and second heating run: scan rate 10°C min^{-1};*

Thermal behaviour of compounds 45 and 45a

Compound **45** represents an isomer of compound **43**, whereas the position of the biphenyl group changes and the direction of one ester group is inverted. Compound **45** melted at 158°C into an isotropic fluid.

As already observed for compound **43**, upon oxidation of compound **45** the thermal behaviour changed dramatically. During the first heating run compound **45a** gave an endotherm at 122°C, which corresponded to the formation an isotropic fluid. Upon cooling the formation of a smectic A phase was detected at 52°C. Upon further cooling no changes of heat capacity were observed in the DSC thermogram, whereas during the second heating run a glass transition temperature was observed at ca. 40°C. This corresponded to the formation of the smectic A phase. On further heating an endotherm was observed at 52°C, which corresponded to the formation of an isotropic fluid.

Thermal behaviour of compounds 46 and 46a

When heated, compound **46** melted at 133°C into an isotropic fluid. A remarkable change in mesophase behaviour was observed in going from **46** to **46a**.

Table 4.10. *Phase transition temperatures [°C] and enthalpy changes [kJ mol^{-1}] of compounds* **43**, **45** *and* **46**; **43a**, **45a** *and* **46a**; [a] *only detectable upon heating; b no enthalpy change during phase transition*

compound	*cryst/iso*	*iso/Col$_h$*	*Col$_h$/S$_A$*	*iso/S$_A$*	*S$_A$/G*
43	154(*11.5*)	-	-	-	-
45	158(*63.3*)	-	-	-	-
46	133(*58.2*)	-	-	-	-
43a	132(*56.3*)	-	-	(83)(*4.5*)	33
45a	122(*68.7*)	-	-	(52)(5.7)	35[a]
46a	124(*81.2*)	(102)[b]	(85)(*1.7*)	-	35

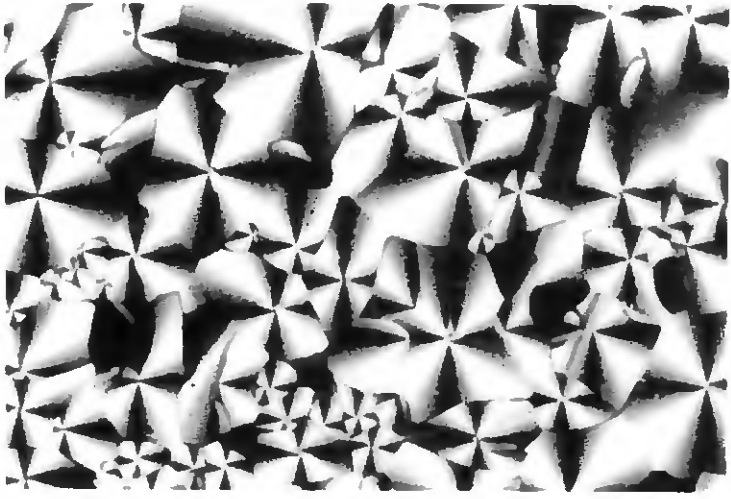

Figure 4.10. *Optical Polarised microphotographs of the columnar (Col$_h$) phase of* **46a** *upon cooling from the isotropic liquid at 102°C; 320 x*

The DSC scan of compound **46a** is shown in Figure 4.12. During the first heating **46a** gave an endotherm at 124°C This corresponded to the formation of an isotropic fluid, while during the first cooling an exotherm was registered at 85°C. In contrast, optical polarising microscopy showed on cooling the formation of a liquid-crystalline phase at 102°C. At a slow cooling rate of 0.2°C min^{-1} an optical texture developed, indicating the formation of a columnar phase (Figure 4.10.). This microphotograph can be a representative example of the texture of a hexagonal columnar phase (Col_h). Upon further cooling a texture developed, shown in Figure 4.11., indicating the formation of a smectic A phase at 85°C. A glass transition was observed at 35°C. The second heating scan for the same compound showed a cold crystallisation at 90°C followed by isotropisation at about 120°C (very broad melting peak). In summary the DSC results do not show the formation of a columnar phase, detected by optical polarising microscopy, whereas the transition $Col_h \rightarrow S_A$ was also observed in the DSC thermogram.

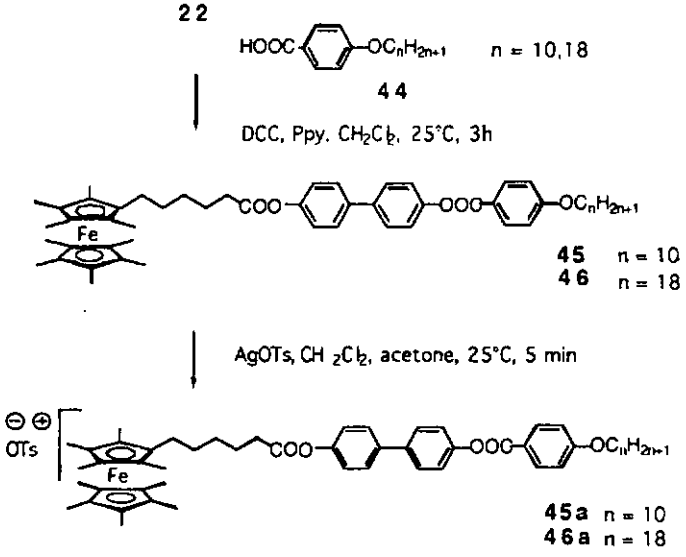

Scheme 4.11.

Figure 4.11. *Optical Polarised microphotographs of the smectic A (S_A) phase of* **46a** *upon cooling from the columnar phase (Col_h) at 84°C, 320 x*

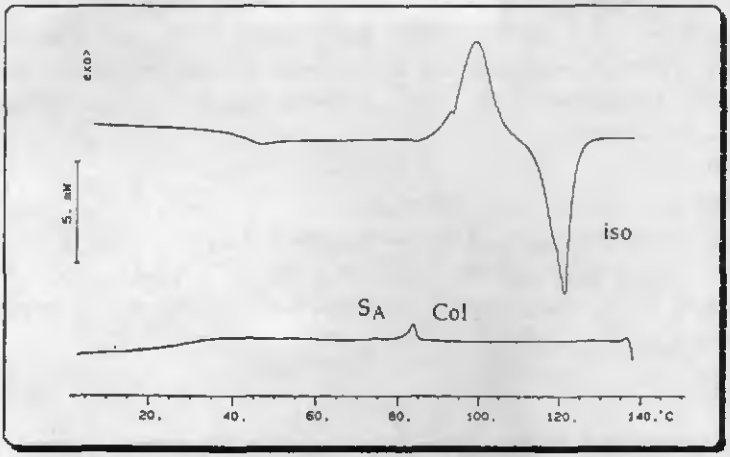

Figure 4.12. *DSC scan obtained for compound* **46a**:
first cooling and second heating run; scan rate 10°C min^{-1};

Compound **41** was oxidised according to the standard experimental procedure using silver tosylate to give **41a** (Scheme 4.12.).

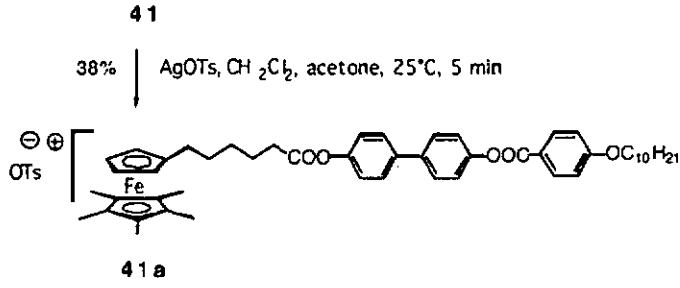

Scheme 4.12.

Thermal behaviour of Compound ***41a***

When heated, compound **41a** melted at 84°C into a smectic A phase followed by isotropisation at 131°C. During further heating and cooling cycles DSC measurements detected degradation, while microscopic observations also showed the formation of decomposed material. Compound **41a** is an example of a liquid-crystalline salt, which exhibited enantiotropic mesomorphism. Unfortunately, this hexa-alkylated ferrocenium-salt decomposed in the vicinity of the smectic A phase and no characteristic enthalpy changes could be measured. Due to this reason, upon subsequent thermal scans, no reproducible results were obtained.

X-ray investigations of compound ***41a***

X-ray diffraction studies, which were performed upon cooling **41a** from the isotropic liquid, gave patterns typical of a smectic A phase with a *d*-layer spacing of 39.5 Å. When heated into the liquid-crystalline phase decomposition was detected.

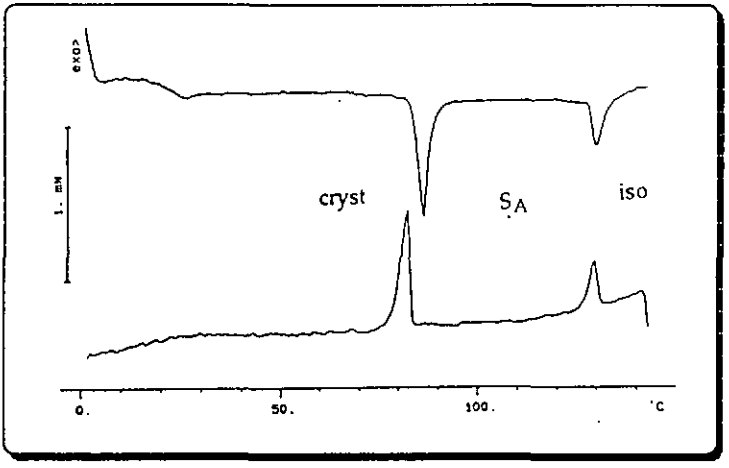

Figure 4.13. *DSC scan obtained for compound 41a: first cooling and second heating run; scan rate 10°C min^{-1}; for further thermal scans a considerably change was registered due to decomposition of the material*

4.4.3. Ferrocene and Ferrocenium Derivatives Bearing Two Aromatic Rings in the Mesogenic Unit

This section is aimed at discovering the properties of permethylated ferrocenes and ferrocenium salts which contain only a short promesogenic group as rigid core. Due to the fact that these compounds show lower tendencies for liquid crystal formation, our attention focused on only two examples. The synthetic routes leading to compounds 51 and 52a are shown in Scheme 4.13. The synthetic methods are well established following esterification, hydrogenation and oxidation experimental procedures.

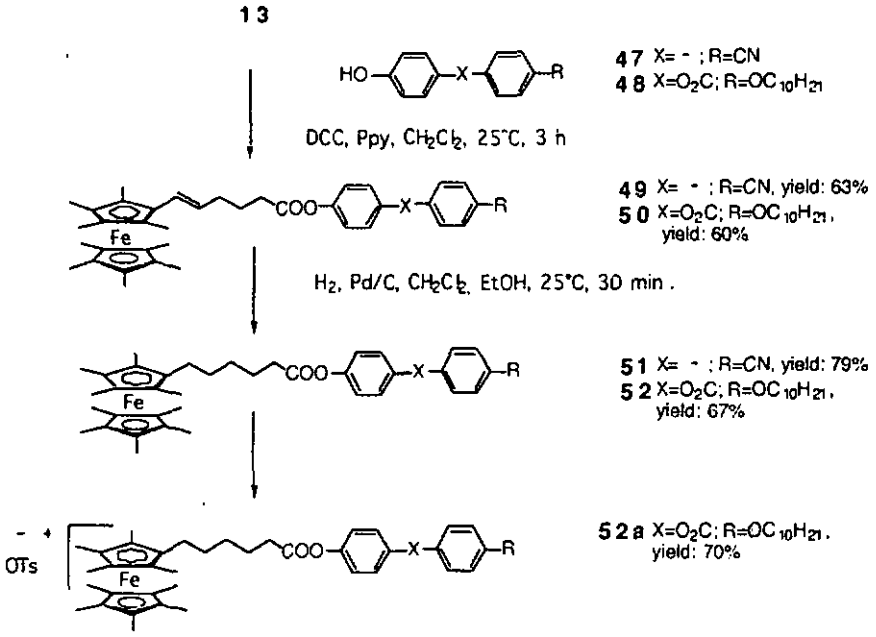

Scheme 4.13.

Table 4.11. *Isotropisation temperatures [°C] and enthalpy changes [kJ mol^{-1}] of compounds 51-52(a)*

compound	*cryst/iso*
51	135(22.2)
52	103(46.0)
52a	104(102.0)

Both ferrocene derivatives, 51 and 52, exhibited low melting temperatures. No liquid-crystalline phases were observed. This behaviour confirms our assumption that a bulky peralkylated ferrocene core is disadvantageous for the mesomorphic properties of compounds bearing a short promesogenic core. Compound 52 was oxidised with AgOTs giving the ferrocenium salt 52a. When heated, compound 52a melted at 104°C into an isotropic fluid When cooled, a glass transition was detected.

In conclusion, none of the ferrocene-derivatives 51-52(a) showed mesomorphic behaviour.

4.5. Monosubstituted Derivatives

4.5.1. Chiral Derivatives

The aim of this work was to investigate the effect on the mesomorphic behaviour caused by the chiral butyl-2-oxy-propionate group. The synthetic routes to the ferrocene derivatives 53-56 are shown in Scheme 4.14. These compounds consist of a ferrocene moiety connected via a spacer to a long rod-like core containing a terminal butyl-2-oxy-propionate group. The esters were prepared by reacting the phenol-derivative 57 with the acid intermediates 18 and 19. Subsequent catalytic reduction of the double bond yielded the final ferrocene derivatives 54 and 56.

Figure 4.14. *Optical polarised microphotographs of the chiral nematic phase of compound* 53 *upon cooling from the isotropic liquid at 164°C; 200 x*

Figure 4.15. *Optical Polarised microphotographs of the chiral nematic phase of compound 54 upon cooling from the isotropic liquid at 155°C; 200 x*

Compound 53, containing a longer promesogenic core, exhibited a chiral nematic phase which was identified by its typical optical texture (Figure 4.14.). The catalytic reduction of the double bond caused a moderate decrease in the melting point for compound 54 in comparison to 53. Compound 54 also exhibited a chiral nematic phase (Figure 4.15.). Next it was of interest to oxidise the ferrocene moiety in such a chiral compound. In order to investigate this matter we synthesised a ferrocene with a lowered redox potential also bearing a butyllactate substituent. This gave compounds 55 and 56.

When heated, both, compound 55 and 56 melted into an isotropic fluid and when cooled, they crystallised. For compound 55 (isotropisation: 146°C) it was found that the persubstituted ferrocene unit causes marked reductions in the clearing point in comparison to the non-methylated ferrocene 53 (isotropisation: 221°C).

The persubstituted ferrocene-derivative was oxidised using silver tosylate, silver dodecylsulphonate and silver heptafluorobutyrate. The resulting ferrocenium-salts were obtained as amorphous compounds. Thus, no melting points were detected. Microscopic investigations for compounds 56(a-c) did not reveal the formation of a mesophase. Finally, the amorphous and hygroscopic

character of oxidised compounds did not allow to obtain satisfying elemental analyses.

The transition temperatures and enthalpies of compounds 53-56 are summarised in Table 4.12.

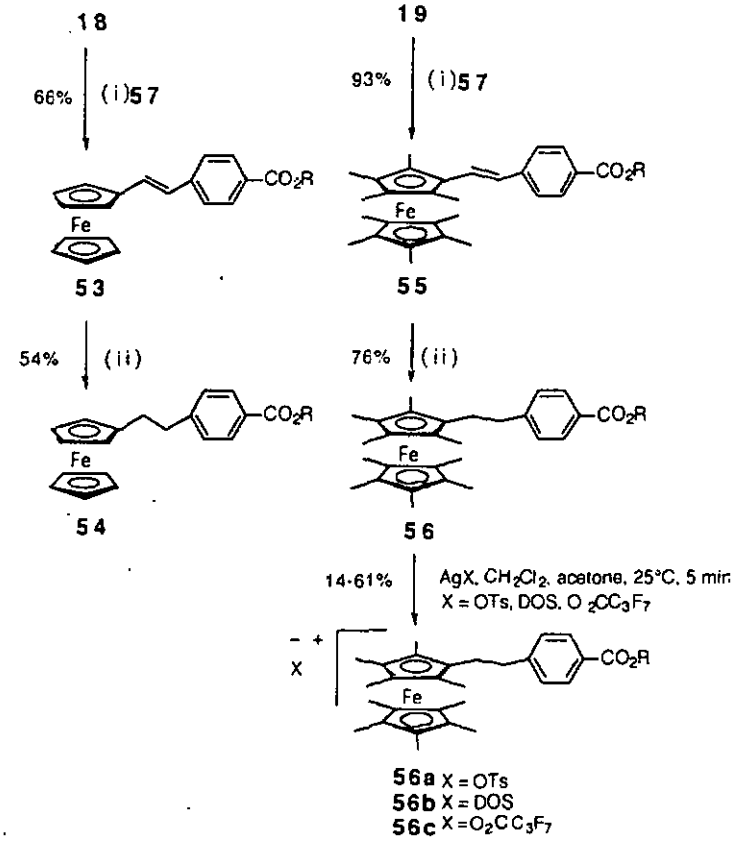

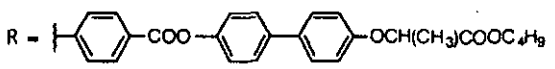

(i) = DCC, Ppy cat., CH_2Cl_2, 25°C, 3h
(ii) = H_2, Pd/C, CH_2Cl_2, EtOH

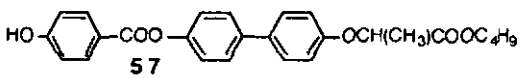

Scheme 4.14.

Table 4.12. *Phase transition temperatures [°C] and enthalpy changes [kJ mol^{-1}] of compounds 53-56*

compound	*cryst/N**	*cryst/iso*	*N*/iso*
53	144(36.6)	-	221(1.0)
54	122(38.7)	-	164(0.7)
55	-	146	-
56	-	166	-

4.5.2. Influence of the Orientation of the Ester Group on the Mesomorphic Properties

The esterification of the acid 18 with 4-(decyloxy)phenyl 4-hydroxybenzoate (58d) [50] resulted in the formation of compound 59, showing a nematic phase over a temperature range of 29°C. Upon treatment of compound 59 with H_2 and Pd/C as catalyst the double bond was reduced resulting in compound 61. Compound 61 showed a nematic phase having only a very narrow mesophase range of 6°C.

The ferrocene derivatives 60 and 62 were synthesised following the same experimental procedures as for compounds 59 and 61 using the acid derivative 18 and 4-hydroxyphenyl-4(decyloxy) benzoate (48) [50]. The structural motive of the mesogenic unit in compounds 59 and 61 shows striking similarity with the rigid core in compounds 60 and 62, whereas the "orientation" of one ester group is inverted. Upon heating, compound 60 gave an enantiotropic nematic phase (ΔT=2°C). The subsequent reduction of the double bond led to compound 62, showing also a very narrow nematic mesophase range (ΔT=3°C). All nematic phases of compounds 59-62 were identified by a typical schlieren texture, which developed on cooling from the isotropic melt to the liquid-crystalline phase. The synthesis of compounds 59-62 are shown in Scheme 4.15. and the thermal behaviour is summarised in Table 4.13.

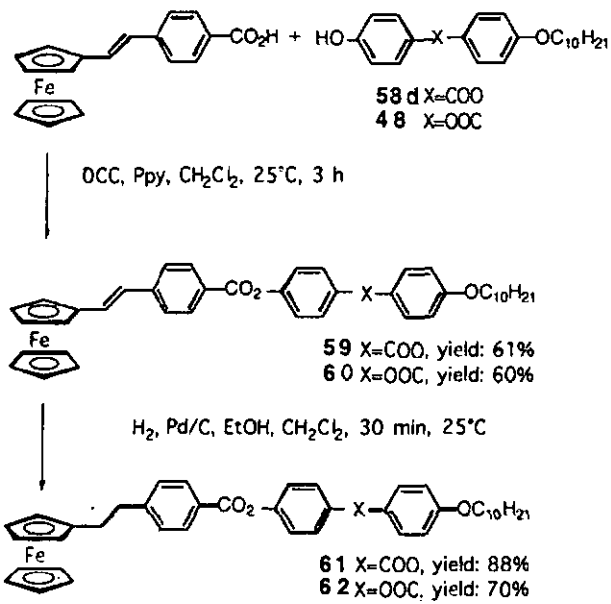

Scheme 4.15.

Table 4.13. *Phase transition temperatures [°C] and enthalpy changes [kJ mol^{-1}] of compounds 59-62*

compound	*X=*	*cryst/N*	*N/iso*
59	COO	143(29.3)	172(1.7)
60	OOC	179(52.9)	181(1.6)
61	COO	125(50.1)	131(1.4)
62	OOC	134(46.7)	137(1.6)

4.5.3. Variation of the Terminal Chain Length in Monosubstituted Ferrocenes

These compounds were prepared by a synthetic route using an esterification/deprotection cycle three times (Scheme 4.16.). Standard procedures as already described in this thesis were used for all reactions. All derivatives of the series 67 exhibited an enantiotropic nematic phase. For compounds 67b (n=5) and 67c (n=10) an additional monotropic smectic A phase was observed, whereas for those compounds incorporating longer terminal

alkyl chains (67d, 67e), the smectic A phase became enantiotropic. The forked ferrocene 67f did not display mesomorphic behaviour. The thermal behaviour of compounds 67a-f is summarised in Table 4.14. and the phase diagram of the series 67 is shown in Figure 4.16.

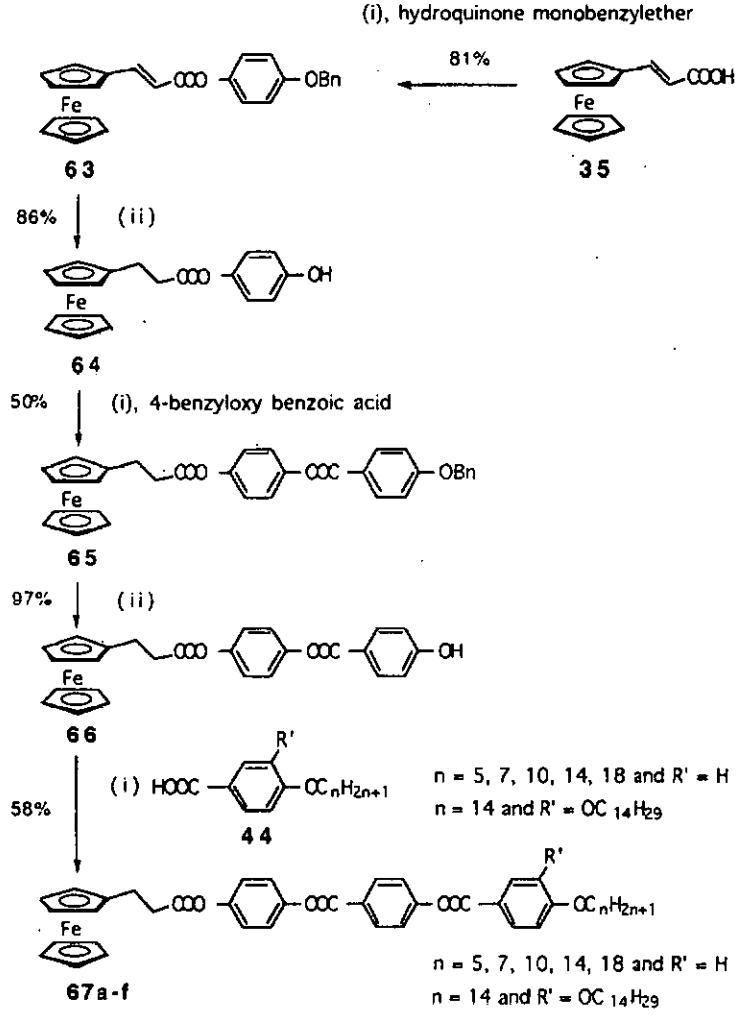

(i) = DCC, Ppy, CH_2Cl_2, 25°C, 3 h (ii) H_2, Pd/C, CH_2Cl_2, EtOH, 25°C, 8 h

Scheme 4.16. *(For adopted numbers see Table 4.14.)*

Table 4.14. *Phase transition temperatures [°C] and enthalpy change [kJ mol^{-1}] of compounds 67a-67f; [a] cold crystallisation*

compound	*n*	*cryst$_1$/ cryst$_2$*	*cryst/S_A*	*cryst/N*	*cryst/ iso*	*S_A/N*	*N/S_A*	*N/iso*
67a	5	-	-	149(45.5)	-	-	-	171(0.9)
67b	7	-	-	142(44.0)	-	-	(119)(0.6)	162(0.7)
67c	10	-	-	132(46.0)	-	-	(121)(0.9)	151(1.0)
67d	14	109[a]	110(3.5)	-	-	115(0.5)	-	138(0.8)
67e	18	-	102(54.7)	-	-	121(1.2)	-	132(1.2)
67f	14	-	-	-	87(80.0)	-	-	-

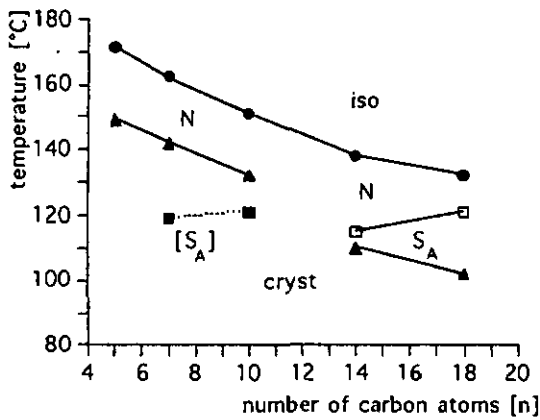

Figure 4.16. *Dependence of the transition temperatures on the number of carbon atoms of the alkyl chain in ferrocene-derivatives 67a-67e; ▲: melting point ; ●: isotropisation, □: $S_A \rightarrow N$ transition : ■ $N \rightarrow S_A$ transition*

4.5.3.1. Oxidation of Compound 67c with Iodine or DDQ

The ferrocene 67c was oxidised with iodine or DDQ in hexane/benzene to yield dark-brown crystals. The charge-transfer complex 68b (anion=DDQ$^{\cdot-}$) was deeply coloured, whereas the dark green colour in the complex 68a (anion=I_3^-)

came from charge transfer interactions in the triiodide anion. The synthesis of the complexes 68a and 68b are shown in Scheme 4.17.

DSC analyses were carried out for both complexes showing large exotherms at about 150°C (68a) and 110°C (68b) indicating thermal decomposition. Microscopic investigations also showed the formation of decomposed material. Furthermore, upon long storage at room temperature (3-4 weeks) some enclosures of yellow material were found in compound 68b indicating the formation of the "reduced" component 67c. The decomposition temperatures upon heating compounds 68a and 68b are summarised in Table 4.15.

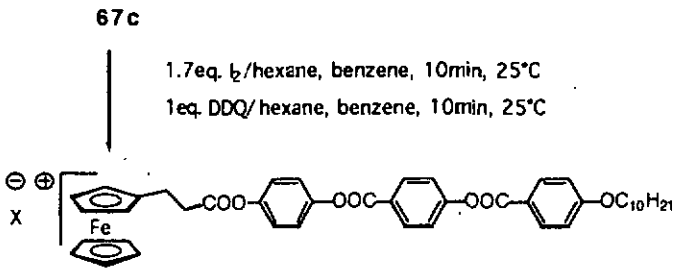

68a X = I_3, yield: 74%
68b X = DDQ, yield: 80%

Scheme 4.17.

Table 4.15. *Decomposition temperatures [°C] of compounds 103a and 103b*

compound	*anion*	*dec.*
68a	I_3^-	150
68b	DDQ$^{\cdot-}$	110-118

4.6. Disubstituted Ferrocene Derivatives

Ferrocene-1,1'-dicarbonyl dichloride (69)[50] was treated with 1eq. of 4(decyloxy) phenyl 4-hydroxybenzoate [50] (58d) in benzene, at reflux for 36 h. The mono-ester intermediate 70 was isolated in moderate yield (32%) due to the formation of the disubstituted by-product. This mono-ester intermediate was converted into the acid chloride 71 by reaction with oxalyl chloride in CH_2Cl_2 at reflux, in the presence of pyridine. The investigated non-symmetrically substituted ferrocenes 72a-g were synthesised by esterification of 71 with the

hydroxy esters **58a-g**. The reactions were performed in CH_2Cl_2 under reflux in the presence of NEt_3. Purification by column chromatography and crystallisation gave the targeted ferrocene derivatives in good yields. The synthetic pathways are shown in Scheme 4.18.

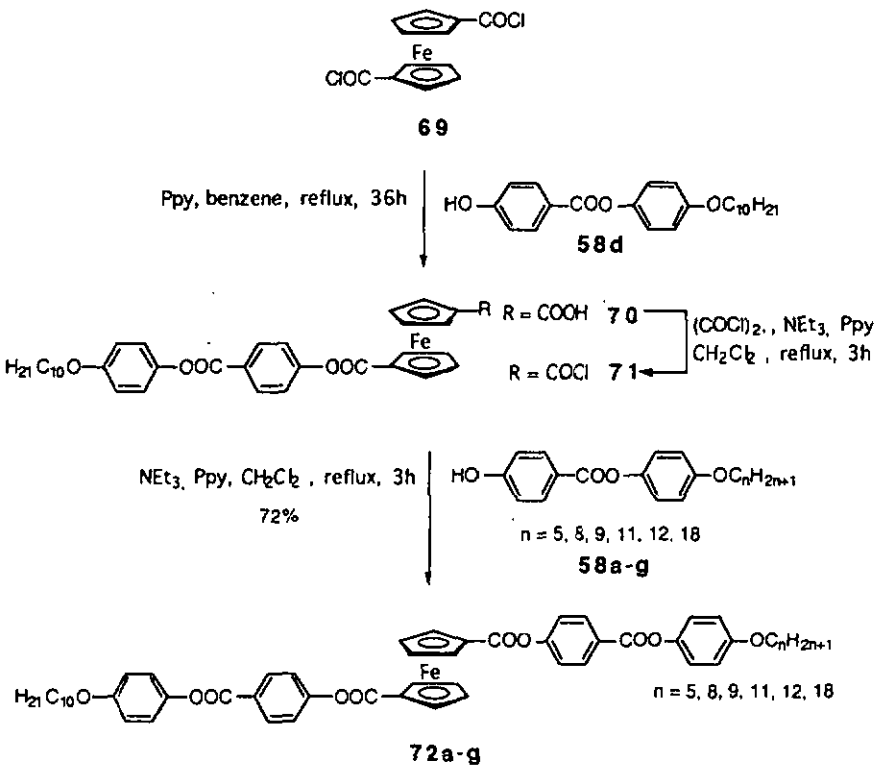

Scheme 4.18.

The transition temperatures and enthalpy changes are reported in Table 4.16. When heated, all members of the family **72** gave enantiotropic S_A phases. It is noteworthy to point out that the derivatisation with longer alkyl chains does stabilise the mesophase range. On increasing the alkyl chain length the smectic A range broadened constantly (ΔT=2°C for n=5, ΔT=12°C for n=11 and ΔT=20°C for n=18). The phase diagram of series **72** is shown in Figure 4.17.

Table 4.16. *Phase transition temperatures [°C] and enthalpy changes [kJ mol^{-1}] of compounds 72a-72g;* [a] *for the symmetrically disubstituted compound see ref.* [50]

compound	*n*	*cryst/S_A*	*S_A/iso*
72a	5	159 (59.1)	161 (5.5)
72b	8	156 (62.4)	163 (9.0)
72c	9	157 (61.0)	164 (9.4)
72d	10	156 (70.4)	165 (9.9)
72e	11	155 (72.7)	167 (10.2)
72f	12	155 (64.0)	168 (10.7)
72g	18	150 (34.7)	170 (11.7)

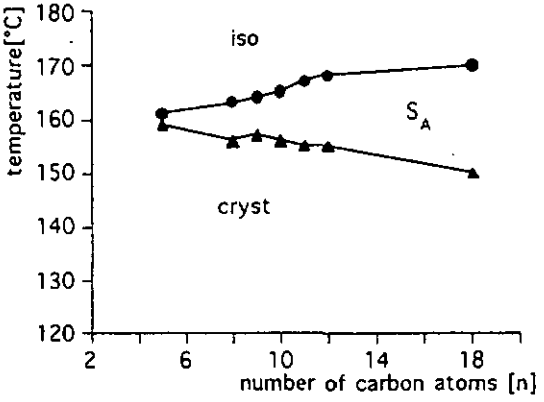

Figure 4.17. *Dependence of the transition temperatures on the carbon number of the alkyl chain in ferrocenes 72a-72g;* ▲: *melting point;* ● *isotropisation*

4.7. Precursors

The phenol derivatives 33 and 57 were prepared using a similar experimental procedures. The synthetic pathways are given in Scheme 4.19. The esterification of compounds 73 [82] and 74 using the standard experimental method led to the benzyl protected esters 75 [74] and 76. These were subsequently reacted with H_2 resulting in the deprotected phenol-derivatives 33 and 57.

The decyloxy derivative **33** exhibited a monotropic nematic phase characterised by its recognisable schlieren texture. For compound **57** no mesomorphic behaviour was seen. The phase behaviour of the obtained compounds is listed in Table 4.17.

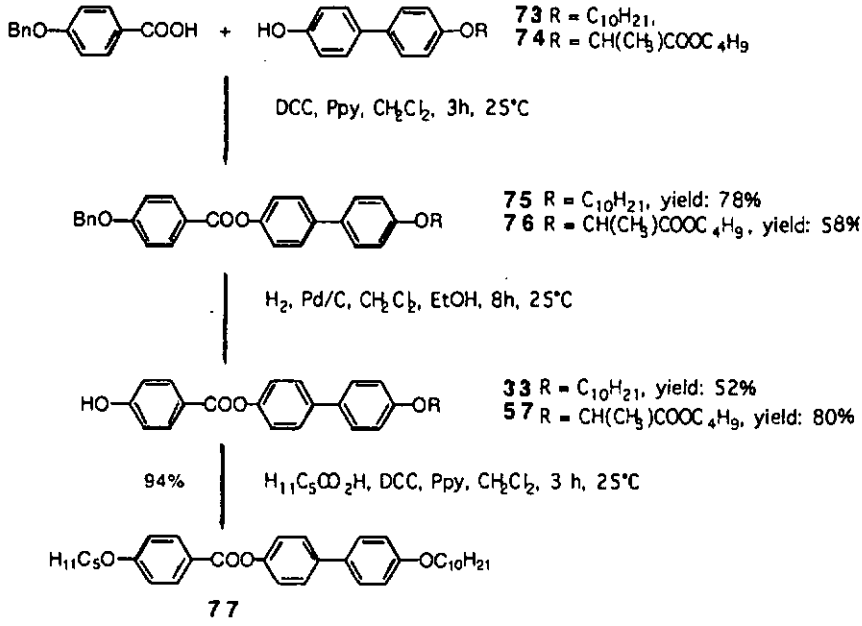

Scheme 4.19.

Compound **77** was synthesised according to our standard esterification procedure and exhibited three mesophases. When heated, it melted at 106°C into a liquid-crystalline phase (non-identified smectic phase). On further heating, a smectic C phase formed at 124°C followed by a nematic phase at 166°C which cleared at 197°C into the isotropic liquid. The nematic phase was identified by the formation of a typical schlieren texture.

Table 4.17. *Phase transition temperatures [°C] and enthalpy changes [kJ mol^{-1}] of compounds 33, 57 and 77*

compound	*cryst/iso*	*cryst/S_X*	*S_X/ S_C*	*S_C/ N*	*N/iso*
33	206(*50.6*)	-	-	-	[204(*7.7*)]
57	186	-	-	-	-
77	-	106(*45.1*)	124(*5.9*)	166(*4.6*)	197(*2.9*)

Chapter

5

Discussion

This discussion of mesomorphic and electrochemical properties focuses primarily on polysubstituted ferrocene derivatives. Secondly, "monosubstituted" ferrocene-derivatives are discussed, including some chiral derivatives. Finally, a series of non-symmetrically 1,1'-disubstituted ferrocenes is discussed.

5.1. Thermal Behaviour of Ferrocenium-Salts Bearing Four Aromatic Rings in the Promesogenic Core

All the non-oxidised homologues having four aromatic rings in the promesogenic core gave rise to enantiotropic phase behaviour. A nematic phase was observed for all the derivatives whereas for compound 27 (n=18) an additional monotropic smectic C phase was seen. Regarding the chain length of the terminal alkoxy groups the mesophase range remained nearly unaffected.

In this case it was obvious that the formation of enantiotropic liquid-crystalline phases was due to the long promesogenic part. Comparison with compounds 45 and 46, which both showed no mesophase, suggested that the bulky persubstituted ferrocene moiety decreases the tendency for formation of liquid-crystalline phases.

Tosylate-salts (compounds 24a, 25a, 26a and 27a)

As can be seen from Figures 4.4. and 4.5., the mesophase range of the tosylate salts was generally larger than for non-oxidised ferrocenes. All salts showed a smectic A phase which was monotropic for 24a and enantiotropic for compounds containing longer alkyl chains. The tetradecyloxy derivative (compound 26a) showed an additional monotropic smectic C phase. The smectic C phase was enantiotropic for the derivative bearing the long octadecyloxy chain (compound 27a). However, none of the tosylate salts seemed to be thermally stable in the isotropic phase as indicated by the formation of decomposed material. Also, as revealed on subsequent thermal cycles, DSC measurements showed a slow decomposition of all tosylate-salts in the vicinity of the isotropic liquid. Therefore, investigations of the smectic C phase were undertaken on heating compounds not into the isotropic phase but only until the smectic A phase formed.

It is proposed that steric interactions of persubstituted ferrocenium head groups demand an antiparallel correlation in order to achieve a dense packing. The amphiphilic properties of the ferrocenium-salts and the packing dominate

the structure and lead to smectic A and smectic C phases of monolayer type. If the chains are elongated a smectic C phase results and the antiparallel alignment is presumed to result again. A general schematic model of the antiparallel organisation of the ferrocenium-salts in the smectic A phase is proposed for compound **43a** (Fig. 5.6.).

Heptafluorobutyrate-salts (compounds 24b, 25b, 26b and 27b):

When heated, ferrocenium-salts containing a heptafluorobutyrate anion gave rise to decomposition. Microscopic investigations showed the formation of a gaseous material upon heating. At about 120°C, bubbles formed and a webbing pattern of oily-streak-like defects at the bounding area was seen. Upon further heating the gaseous substance formed vigorously. It was assumed that upon heating the heptafluorobutyrate anion gains a proton (most probably liberated from the cation) and concurrently the boiling point of the heptafluorobutyric acid (bp.: 120°C) is reached.

TG measurements were undertaken in order to prove this assumption. The TG scan for compound **27b**, typical for all salts containing a heptafluorobutyrate anion, is shown in Figure 5.1. The DSC scan for the first heating run of compound **27b** is shown additionally in Figure 5.2. In the thermogravimetric experiment a weight-loss is observed between 120°C and 240°C. This effect most probably corresponds to the formation of heptafluorobutyric acid. The measured weight-loss of 15.1% in the given temperature range is equal to 1 eq. of heptafluorobutyric acid (bp.: 120°C). Thus, the liberated acid evaporates quickly at temperatures higher than 120°C. Between 240°C and 360°C an additional weight-loss was observed (10.5%), whereas complete degradation was seen at temperatures higher than 360°C.

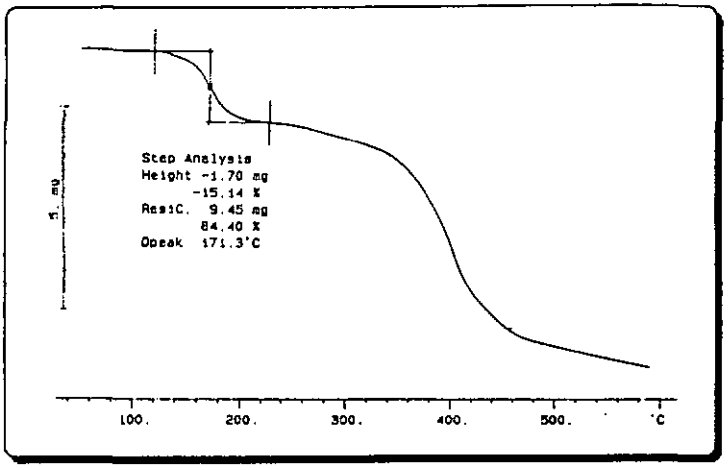

Figure 5.1. *TG scan of compound 27b at a heating rate of 20°C min^{-1} under N_2*

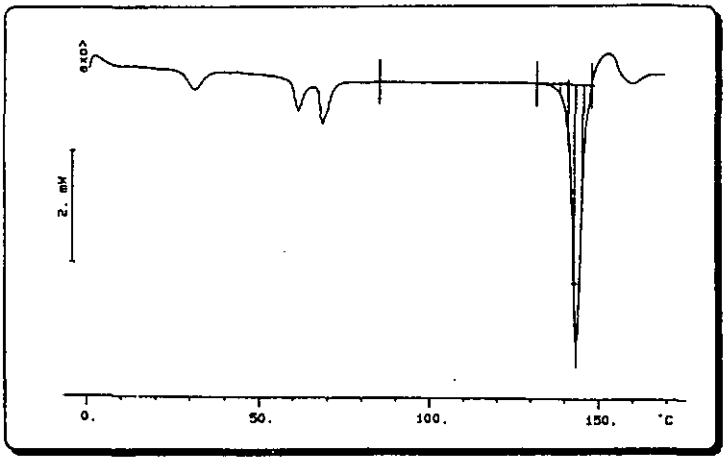

Figure 5.2. *DSC scan of compound 27b at a heating rate of 10°C min^{-1} under N_2*

In contrast, the DSC measurements of compound **27b** showed during the first heating a strong endotherm at 141°C whereas optical microscopy and thermogravimetric investigations revealed that decomposition occurs already

at temperatures higher than 120°C. Furthermore, no investigations were undertaken to clarify the nature of the ferrocenium-containing intermediate which was formed at temperatures higher than 120°C. Nevertheless, from these results it seemed evident that the thermal decomposition of ferrocenium-salts containing a heptafluorobutyrate anion can best be described by the following equation (Figure 5.3.):

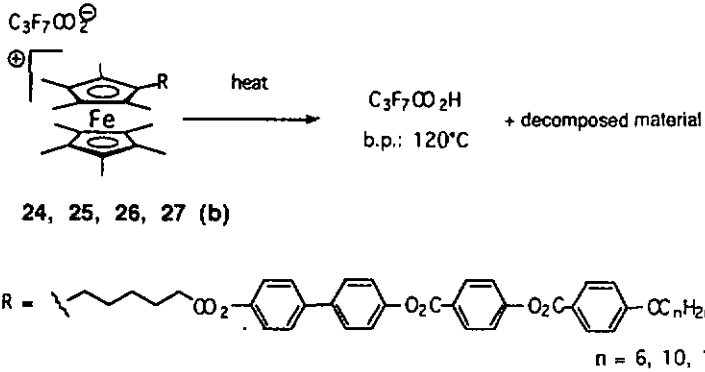

Figure 5.3. *Equation describing the thermal decomposition of compounds 24b, 25b, 26b and 27b*

The triflate-salts (compounds 25c, 26c and 27c)

With one exception this series did not show liquid-crystalline properties. Only the ferrocene-derivative **27c**, containing the long octadecyloxy terminal chain, exhibited a monotropic smectic A phase. All salts melted at higher temperatures than the corresponding tosylate-salts. Perhaps, due to the high crystallinity of the triflate-anion, the ionic forces between the ions are much stronger, thus resulting in non-liquid-crystalline salts with high melting points. Only for compound **27c**, bearing the long octadecyloxy terminal chain, the lateral interactions and segregation between the aromatic and aliphatic part are strong enough to produce a liquid-crystalline arrangement. Thus, for compounds **25c** and **26c**, these interactions seem to be considerably reduced.

5.1.1. UV/vis-Electronic Absorption Spectrum of non-Oxidised and Oxidised Compounds

Absorption spectra of ferrocene and related ferrocenium derivatives have been investigated by several authors [24]. Of particular interest is that absorption

bands in the visible region change upon oxidation of ferrocene to ferrocenium, visualised by a colour change from yellow to dark-green or blue.

The bands in the visible region always have intensities of $100<\varepsilon<1000$, whereas the ε-values in the ultraviolet region are much higher. The differences upon oxidation in the visible region (350-800 nm) of compounds **27** and **27a** are displayed in Figures 5.4. and 5.5. The band positions and intensities are given in Table 5.1.

Furthermore the UV/vis-spectra of the ferrocenium-salts, either bearing a tosylate, triflate or heptafluorobutyrate counter-anion, were all remarkably superimposable, which is what would be expected in view of the absence of anion bands in the region of 350-800 nm.

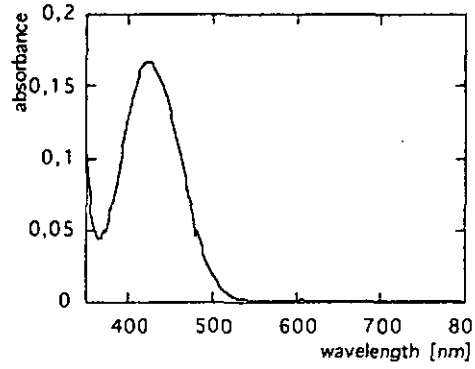

Figure 5.4. *Electronic absorption spectrum of compound 27*

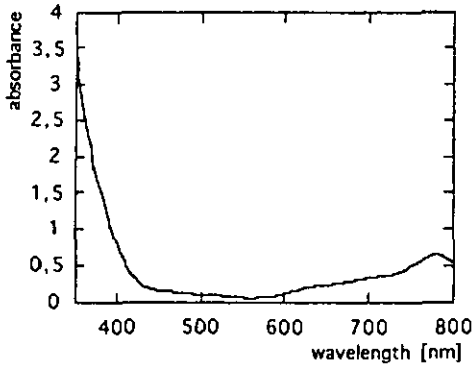

Figure 5.5 . *Electronic absorption spectrum of compound 27a*

Table 5.1. *The electronic absorption spectra of compound 27 and 27a*

compound	*absorption bands* λ_{max} *[nm]*
27	274 (67750); 425 (130)
27a	274 (66390); 642 (228); 705 (352); 778 (622)

5.1.2. Conclusion

Due to their amphiphilic character all oxidised derivatives which displayed liquid-crystalline properties formed layered phases (smectic A and / or smectic C). Within the smectic phase a head-to-tail arrangement is assumed.

Upon oxidation of non-oxidised ferrocenes the mesomorphic properties were transformed from a nematic phase to a layered phase. Furthermore, the thermal behaviour of the resulting ferrocenium-salts depends essentially on the type of counter-anion and the length of the terminal alkyl chain.

The thermal behaviour can be summarised as follows:

- *non-oxidised ferrocenes:*
- the homologous series shows a strong dependence of the transition temperatures on the terminal chain length;
- n=6,10 and 14: enantiotropic nematic phase;
- n=18: enantiotropic nematic phase, monotropic smectic C phase.

- *tosylate salts:*
- n=6 and 10: enantiotropic smectic A phase;
- n=14: enantiotropic smectic A phase and monotropic smectic C phase;
- n=18: enantiotropic smectic A and smectic C phases.

- *heptafluorobutyrate salts:*
- n=6, 10, 14 and 18: decomposition, formation of a gaseous compound

- *triflate salts:*
- n=10 and 14: not liquid-crystal;
- n=18: monotropic smectic A phase.

5.2. The Influence of the Counter-Anion on the Mesophase Behaviour (Compound 31)

In this series the influence of the oxidation and the type of counter-anion are examined.

In order to extend the study of liquid-crystalline ferrocenium-salts, the synthesis of a series having different counter-anions was undertaken. These new complexes would allow to better understand the role of the counter-anion in mesophase formation and, if possible, to evaluate some structure-property relationships. It was thought that owing to the different size and structure of anions, these salts would yield materials having different mesomorphism. Previous studies on mesomorphic ionic silver stilbazoles showed that when the counter-anion was small and globular, such as nitrate and tetrafluoroborate, the transition temperatures were high and the complexes decomposed in the vicinity of the isotropic liquid [49,83]. We therefore investigated the thermal behaviour of six salts having counter-anions with an increased volume (CH_3-C_6H_4-$5O_3^-$, $CF_3SO_3^-$, $C_nF_{2n+1}CO_2^-$ with n=1,2 and 3) but also the charge-transfer salts having radical anions (TCNE, TCNQ).

The non-oxidised ferrocene-derivative 31 gave rise to enantiotropic mesomorphism, including smectic C and smectic A phases.

Compound 31a having the tosylate counter-anion showed enantiotropic smectic C and smectic A phases.

In the present system, a rather small counter-anion seems to prevent the formation of a liquid-crystalline phase. This absence of liquid-crystalline behaviour for the triflate-salt (compound 31b) was expected at this stage. In comparison, only one of the ferrocenium-salts of series 25c-27c (bearing four aromatic rings and a triflate counter-anion) showed a monotropic phase behaviour. Thus no mesophases were observed, probably due to the high crystallinity of the triflate anion. This could be due to the attractive ionic interactions winning out over the decreased structural anisotropy, resulting from the presence of a smaller anion.

The mesomorphic properties of the ferrocenium-salts having a perfluorinated carboxylate as a counter-anion (compounds 31c, 31d and 31e) were found to be slightly different than those found in the non-oxidised ferrocene. Enantiotropic smectic A and smectic C phases were observed in these systems and the melting temperatures were slightly shifted to higher temperatures (6-8°C). The smectic A phase existed over a wider temperature range than for the non-oxidised compound and consequently the smectic C phase cleared at slightly higher temperatures. However, one has to take into consideration that these compounds rapidly decomposed when heated above 120°C. In contrast, if heated in several heating and cooling cycles only to 110°C, DSC measurements were reversible. This indicates the thermal stability of investigated salts at temperatures below 110°C.

Some compounds were not obtained as powders but rather as amorphous solids since the DSC hardly showed the melting transition.

TG measurements were undertaken for compounds 31c-e, which revealed the same thermal behaviour as already seen for compounds 24-27(b). Upon heating a weight-loss was observed for all salts bearing an anion of type $C_nF_{2n+1}CO_2^-$. This weight-loss corresponded most probably to the formation of 1 eq. $C_nF_{2n+1}CO_2H$. Optical observations suggested that these salts also liberate a gaseous substance when heated above 120°C. Upon further heating (360°C) only a minor weight-loss was observed, probably due to the formation of a thermally more stable species.

Table 5.2. summarises the results from thermogravimetric measurements for compounds 31c-e.

Table 5.2. *Results from thermogravimetric experiments of compounds 31c-e*

compound	anion	weight-loss at		
		220°C	340°C	460°C
31c	CF_3CO_2	10.0%	16.7%	75.8%
31d	$C_2F_5CO_2$	12.6%	15.4%	79.9%
31e	$C_3F_7CO_2$	15.4%	18.8%	81.4%

The two charge-transfer complexes **31f** and **31g** did not show liquid-crystalline properties. It may be that the radical anion is the origin of the decomposition process which already occurs at room temperature. When heated, the DSC scan also revealed a constant degradation for both compounds, as indicated by a strong exothermic signal over a large temperature range. However, it seemed that decomposition is connected with the presence of ester-groups in the charge-transfer complex. By contrast, the charge-transfer salts of decamethylferrocene with TCNE or TCNQ are known to be stable [84].

5.2.1. Conclusion

The type of counter-anion and its ionic-strength governed the mesomorphism of this series. Mesomorphic salts were obtained with the tosylate anion and anions of perfluorocarboxy acids. The phase behaviour of the resulting salts showed only minor changes upon oxidation. In contrast, the oxidation of compound **31** with silver triflate yielded a non-mesomorphic ferrocenium-salt. The reason for the different mesophase behaviour of salts bearing trifluorosulphonate (**31b**) or trifluoroacetate (**31e**) counter-anion is still unclear.

5.3. Thermal Behaviour of Ferrocenium-Salts Bearing Three Aromatic Rings in the Promesogenic Core, Compounds 41(a), 43(a), 45(a) and 46(a)

The persubstituted ferrocene-derivatives **43**, **45** and **46** were not mesomorphic. These materials melted to the isotropic liquid upon heating and crystallised upon cooling. The absence of liquid-crystalline behaviour for these systems was expected since the bulky persubstituted ferrocene-moiety reduces the mesogenic properties in calamitic mesogens. By contrast, the pentamethylated

ferrocene-derivative **41** exhibited a rich mesomorphism including a smectic E, smectic C and nematic phase.

Upon oxidation dramatic changes in the thermal behaviour are induced. All persubstituted ferrocenium-salts (compounds **43a**, **45a** and **46a**) gave rise to a monotropic mesomorphism, including a layered (smectic A) and in one case a columnar phase (Col_h) Both phases were characterised on the basis of their optical textures. The smectic A phases of compounds **41a** and **43a** were determined by X-ray measurements. All salts showed a strong dependence of the thermal behaviour on the thermal history. On first heating the crystals melted directly to the isotropic liquid. On cooling, an interesting mesomorphism was observed. Due to the ionic character of the ferrocenium-salts, these compounds showed the tendency to form lamellar or micellar structures, thus resulting in a monotropic behaviour. Furthermore, on cooling, all salts showed a rather strong hindrance for crystallisation as evidenced by strong supercooling effects but sometimes they partially crystallised after a few hours. Most probably a large supercooling was due to the high viscosity of salts in the liquid-crystalline phase.

The length of the terminal alkoxy chain was found to greatly influence the occurrence of mesophases: the mesomorphism obtained for compounds **43a** and **45a** (terminal decyloxy chain) is quite comparable. Due to their ionic character they showed strong supercooling effects and exhibited a monotropic smectic A phase. In this system one can assume that the anions are located close to the ferrocenium head groups. However, no precise statement about the location of the anions can be given at this point. By X-ray investigations the layer thickness was determined to 39.5Å and this was found to be comparable to the length of the cation (41Å) in its fully extended conformation. In this layer the molecules are estimated to organise themselves due to the electrical repulsions antiparallel in a head-to-tail arrangement. The structure model of compound **43a** in the smectic A phase is shown in Figure 5.7. In this representation no counter-anions are displayed.

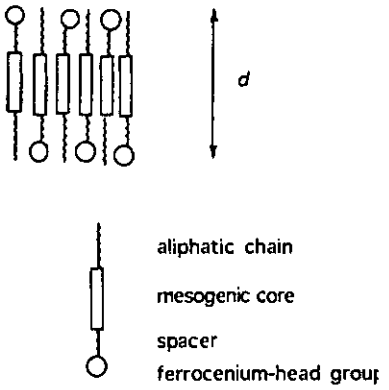

Figure 5.6. *Possible arrangement of compound 43a in the smectic A phase*

5.3.1. Magnetic Measurements of Compound 43a

The aim of this section is to report on the temperature depending magnetic susceptibility measurements of compound 43a. This measurements and observations act as preliminary conclusions to this point and were conducted at the University of Marburg (D).

An analysis of the magnetic susceptibility data can offer the possibility to detect changes due to the formation of liquid-crystalline phases. The temperature dependent magnetic susceptibilities, the effective magnetic moment and the magnetisation of the ferrocenium-salt 43a are displayed in Figures 5.7. and 5.8. On heating, a phase transition at about 127°C is visible. On cooling, an additional change in the magnetic susceptibility occurred at about 87°C. In contrast, X-ray investigations revealed clearly the existence of an isotropic phase at this temperature upon cooling. The change in the magnetic susceptibility may therefore be due to some degradation of the compound at this temperature.

From the experimental magnetisation values (e_μ), the known sample mass and the molecular weight of the sample, the molar susceptibility was calculated to 1.1 10^{-3} cm^3 mol^{-1} at room temperature. Correction for the diamagnetic contribution of the single atoms adds about 650 10^{-3} cm^3 mol^{-1} to this value, yielding a final result of 1.67 10^{-3} cm^3 mol^{-1} for the molar susceptibility at T=25°C. The inverse susceptibility shows a Curie-Weiss type behaviour up to

temperatures of about 120°C The Curie-constant was determined to 0.516 cm^3 K mol^{-1}.

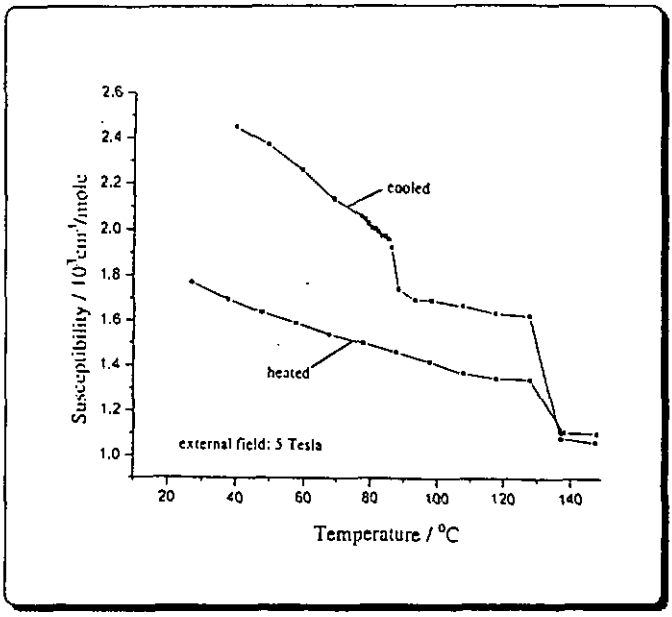

Figure 5.7. *Experimental magnetic susceptibility (χ) as a function of temperature for compound 43a. Data for polycrystalline sample*

5.3.2. Mesomorphism of Compound 46a

The optical textures of compounds 43a and 45a were very similar to each other. This suggested also a smectic A phase for compound 45a. It is interesting to note that the phase behaviour of these two ferrocenium-salts, after passing the first thermal cycle, was completely reproducible on subsequent heating-cooling cycles. This indicates good thermal stability of permethylated ferrocenium-tosylate salts up to 130°C.

Compound 46a showed an interesting mesomorphism. The optical observations suggested that upon cooling from the isotropic melt a columnar phase of hexagonal symmetry (Figure 4.10.) formed. In contrast, the DSC measurements showed no signal for the iso→Col_h transition at 102°C. This low

transition enthalpy could probably be due to some preorganisation effects of the salt already in the isotropic phase.

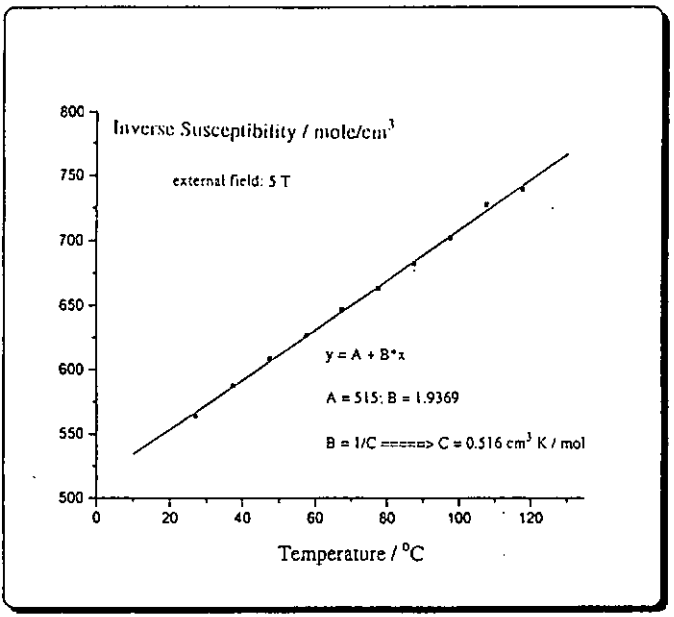

Figure. 5.8. *Magnetisation (M) of compound 43a as a function of temperature*

It can be assumed that the molecular packing in the columnar phase is as shown in Figure 5.9. (anions not displayed). The ionic heads arrange themselves in the centre of a column, whereas the aromatic core and the aliphatic tails fill the space around the columns. Upon further cooling, optical observations, in addition to the DSC traces, suggested the formation of a smectic A phase at 85°C. This mesophase was identified by its optical texture (focal-conic texture, Figure 4.11.), which was formed in a small non-covered droplet at a cooling rate of 0.1°C min^{-1}. Another observation was that upon cooling a glassy state was formed, as evidenced by DSC measurements. Most probably, the high viscosity of the material in the smectic A phase at lower temperatures prevented crystallisation. A cold crystallisation was observed in the second heating run.

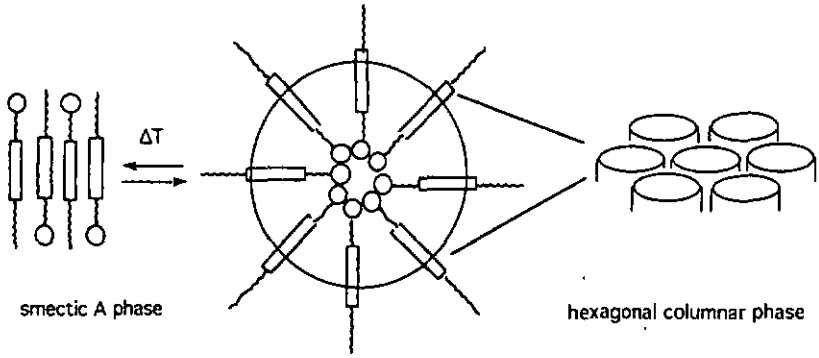

Figure 5.9. *Schematic representation of the proposed structure of compound 46a in the smectic A phase, and in the columnar phase*

Thermal behaviour of compound **41a**

The introduction of six alkyl substituents to the ferrocenyl core gave rise to a ferrocene derivative, having also a lowered oxidation potential, when compared to "monosubstituted" derivatives. Consequently, compound **41a** was oxidised using silver tosylate. Interestingly, upon heating an enantiotropic smectic A phase was observed. This behaviour can demonstrate the steric influence of substitution on the cyclopentadienyl ring. In comparison with compound **43a**, having a persubstituted ferrocenyl core and showing only a monotropic smectic A phase, it was indicated that the bulky ferrocenyl moiety reduces the tendency for mesophase formation.

Another important point to discuss is the thermal stability. Whereas the persubstituted ferrocenium-salts were thermally stable up to 150°C, the hexasubstituted derivative **41a** decomposed in the vicinity of the liquid-crystalline phase (100°C). Furthermore, DSC scans where not reproducible on subsequent thermal cycles.

5.3.2.1. Conclusion

Mesomorphic properties have been induced through the oxidation of the non-mesomorphic ferrocene-derivatives (**43**, **45** and **46**) with silver tosylate. The thermal behaviour of the resulting salts depended essentially on the length of the terminal alkoxy chain. A layered mesophase was found for all three oxidised derivatives (smectic A phase) which was explained by the presence of

electric charges. Ionic pairs can hinder the molecules to form a nematic phase. Upon cooling all compounds formed glassy states rather than crystalline states. These states were evidenced by the retention of the liquid-crystalline texture on cooling which did not give way to a crystalline form. The increased viscosity of liquid-crystalline salts was used to explain the formation of glassy states.

The columnar phase (Col_h) was only observed for compound **46a**, having the long octadecyloxy terminal chain, but the reasons of its occurrence still remain uncertain at the present time. Furthermore, in order to obtain thermally stable ferrocenium-salts, it seems necessary to synthesise derivatives which are permethylated at the ferrocene core.

5.3. Thermal Behaviour of Ferrocenium-Salts Bearing Two Aromatic Rings, Compounds 51, 52 and 52(a)

Only two persubstituted mesogenic ferrocene derivatives were synthesised. The non-oxidised species were proposed to be non-mesomorphic because of their short mesogenic part. Compounds **51** and **52** did not display mesomorphism. Even oxidation of compound **52** with silver tosylate resulting in **52a** did not give a mesomorphic salt. Comparing now the thermal behaviour of compounds **25**, **45** and **52** and of the related oxidised species, it seems obvious that mesomorphism can be interpreted in terms of the length of the rigid part. All derivatives incorporate the same terminal decyloxy chain, but have different numbers of aromatic rings in the mesogenic part. The results can be summarised as follows:

- 2 aromatic rings in the rigid part: not liquid crystal
- 3 aromatic rings in the rigid part: the non-oxidised derivative did not display liquid-crystallinity. By contrast, a monotropic mesophase was seen for the corresponding salt.
- 4 aromatic rings in the rigid part: enantiotropic mesomorphism was seen for both derivatives

This demonstrates the necessity of a longer rigid part in mesogenic ferrocene derivatives for enantiotropic liquid crystal phase formation.

5.4. The Substitution Pattern of Ferrocene and its Influence on the Redox-Potential and Mesomorphic Properties

In the first part of our studies we concentrated on the investigation of structural parameters on the liquid crystalline properties. In the second part the substitution pattern of the ferrocene core was investigated in order to understand its role on the redox potentials. The molecular structures of ferrocene-derivatives **34**, **36**, **37**, **39**, **41** and **43** discussed in this Chapter are compared in Figure 5.11.

This Chapter is aimed at understanding the role of structural parameters in both the linking unit and the ferrocene core on the mesophase behaviour. Firstly, the linking unit will be varied. Secondly, different degrees of methylation for the ferrocene core are used. The mesogenic part of all molecules is consistent. Therefore, other effects than those coming from the substitution pattern of the ferrocene core can be excluded.

5.4.1. Mesomorphic Behaviour

Starting from compound **34**, which exhibited no liquid-crystalline phase, the introduction of an additional linking unit between the ferrocenyl-moiety and mesogenic group led to compound **36** which exhibited an enantiotropic nematic phase. The elongation of the molecule in comparison to compound **34** seems to be the origin of liquid-crystallinity. In going from **36** to **37**, the double bond is reduced and the resulting molecule incorporates a more flexible linking unit. At the same time the conjugation between the ferrocenyl-moiety and the mesogenic core is broken. This led to a monotropic phase behaviour of **37**, including smectic C and nematic phases. These relationships between the molecular structure and the anisotropic phase behaviour show that the liquid-crystalline behaviour of these compounds cannot only be explained in terms of *d*/L-ratio of the molecules (*d*=distance between the two cyclopentadienyl rings; l=length of the rigid core). Most probably the origin of the monotropic phase behaviour is the lowered dipole moment in compound **37**.

Ferrocene derivative **38** represents a *cis/trans* mixture. No thermal investigations were undertaken.

Interestingly, ferrocene derivative **39**, wherein the ferrocenyl moiety is attached to the mesogenic core by means of a five membered spacer, exhibited a

rich mesomorphism. X-ray investigations revealed the formation of a monotropic smectic E phase whereas the smectic C and nematic phases were enantiotropic. The mesophase range was 48°C. This shows that lengthening the aliphatic spacer, located between a mesogenic group and a ferrocenyl moiety, causes a clear increase in the mesophase stability. The clearing point was not affected.

Introduction of five methyl substituents (compound **41**) caused two effects: the mesophase range was decreased (ΔT=27°C) and the smectic E phase was enantiotropic.

Further substitution of the cyclopentadienyl ring led to the permethylated ferrocene-derivative **43**. Consequently, this was accompanied by a loss of liquid-crystalline properties and an increase of the melting point.

In order to compare the influence of ferrocenyl substitution, compound **77** has been synthesised. It incorporates the same mesogenic core as the compounds discussed in this Chapter whereas the ferrocenyl moiety is replaced by a hydrogen atom. The mesophase range was considerably larger (ΔT=91°C) when compared to ferrocenyl substituted compounds. When heated, compound **77** exhibited three mesophases: a non-identified smectic phase, a smectic C phase and a nematic phase. This shows that the mesophase stability is additionally influenced by the size of the ferrocenyl group attached to the five membered spacer, *e.g.* the ferrocenyl moiety causes a strong reduction in mesophase stability.

5.4.1.1. Conclusion

The observed mesophase types depended on the linking unit and the substitution pattern of ferrocenyl moiety. The appearance of mesophases is generally assumed to be influenced by the *d*/L-ratio of the mesogens investigated. A richer mesomorphism was observed for derivatives, containing a five membered spacer group, which separates the ferrocenyl moiety from the mesogenic group. In summary, liquid-crystalline materials obtained showed a rich mesomorphism including smectic E, smectic C and nematic phases. The rather short ferrocene derivative **34** exhibited no mesophase. Derivatives with decreased *d*/L-ratio displayed mesomorphism. In contrast, for compound **43**, incorporating the bulky ferrocenyl-unit, no mesophase was observed. The observed properties confirm our assumption

that the *d*/L-ratio is of great importance in the mesophase-formation of such molecules.

5.4.2. Electrochemical Investigations

Ferrocene complexes can typically undergo a one-electron reversible anodic process. The oxidation potential is dependent on the substituents. Its redox properties and those of its derivatives have been widely studied by electrochemical methods. The anodic behaviour of seven ferrocene derivatives versus a saturated calomel electrode was studied by cyclic voltammetry at a Pt-electrode in dichloroethane. Figure 5.11. displays derivatives for which electrochemical investigations were undertaken. The voltammograms of compounds **34**, **36**, **37**, **39**, **41** and **43** are shown in Figures 5.12. and 5.13., respectively.

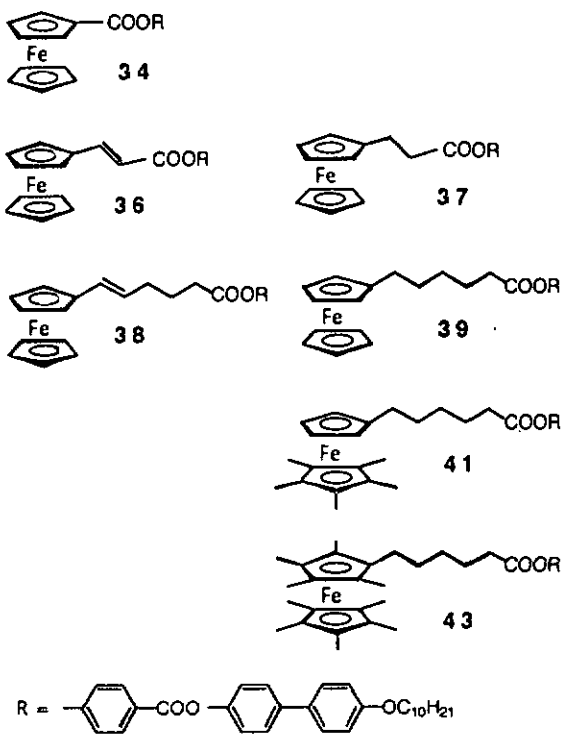

Figure 5.11. *Ferrocene derivatives for which electrochemical investigations were undertaken*

Compound **34** was oxidised reversibly at 0.84 V. For this derivative, containing an ester group connected to the ferrocene moiety, the highest oxidation potential of all compounds investigated was observed. This higher value can be attributed to the electron-withdrawing effect of the carboxy-group. A lower value was found for compound **36** (0.69 V), incorporating a double bond which separates the ferrocene core and the carboxy function. This lower value, in comparison to compound **34**, can be attributed to the separation of the strongly electron-withdrawing carboxy-group from the ferrocene core. However, the effect of the electron-withdrawing -CO_2R-group is transmitted by resonance to the ferrocene core.

For compound **37** an oxidation potential of 0.53 V was found. Firstly, the incorporation of the saturated two-carbon bridge lowers the oxidation potential considerably in comparison to compound **36**, which contains the unsaturated

bridge -C≡C-. Secondly, the -$(CH_2)_2$COOR substituent behaves as an electron acceptor relative to hydrogen.

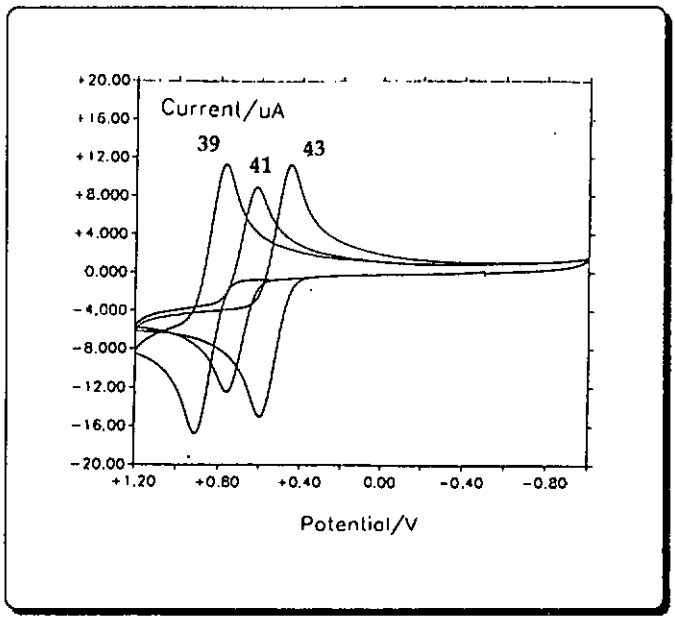

Figure 5.12. *Cyclic voltammogram for the oxidation of the ferrocene-derivatives 34, 36 and 37; scanning rate=200 mV* s^{-1} *(vs SCE)*

For compound 39 an oxidation potential of 0.45 V was observed. In contrast to compound 37, the -$(CH_2)_5$COOR substituent behaves as a very weak electron acceptor relative to hydrogen ($E_{1/2}$=0.44 V). This is due to the distance between the strong electron-acceptor -COOR group and the ferrocene moiety, and to the combined effect of the five methylene groups that have donor properties. This result agrees with those reported by Silva et al. [17,18] and Bolm et al. [85] for series of ferrocenylcarboxylic acids with interposed methylene groups (Fc$(CH_2)_n$COOH: n=1,2,3 or 4; $\partial\Delta E_{1/2}$= 0.02, -0.005, -0.02 or -0.04 mV respectively; in comparison to non-substituted ferrocene). The authors state that the introduction of each methylene group in the bridge (n= 1-4) results in a cathodic shift of $E_{1/2}$ of ca. 20 mV. For n≥2, the complex becomes easier to oxidise than the hydrogen substituted compound. In comparison to the

electron-withdrawing properties of the aromatic-ring connected to the ester group, it can be understood that the -$(CH_2)_5COOR$ group shows weak donor properties.

For compound **38** a value of 0.51 V was found. Therefore, compound **38** is harder to oxidise than compound **39** and the electron-withdrawing ability of the double bond is displayed in the substituted ferrocene **38**. Consequently, the resonance effect of the negatively charged cyclopentadienyl ring with the unsaturated bond is displayed by means of electrochemical investigations.

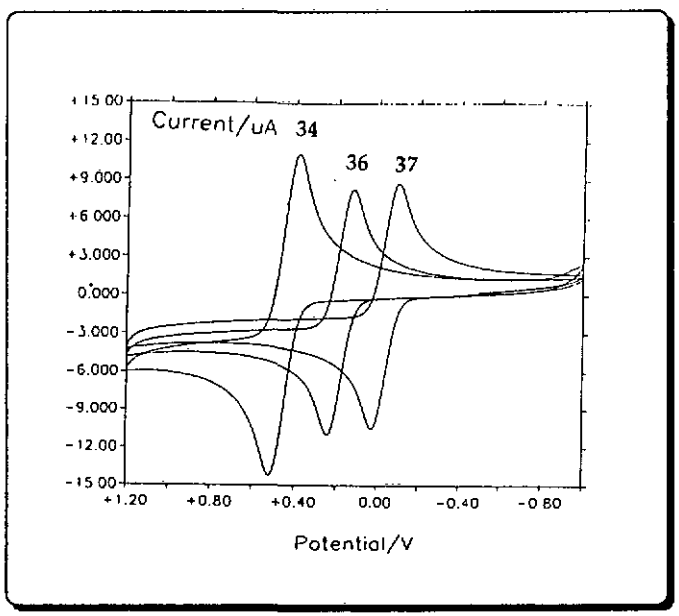

Figure 5.13. *Cyclic voltammogram for the oxidation of the ferrocene-derivatives 39, 41 and 43; scanning rate=200 mV s^{-1} (vs SCE)*

Finally, compounds **41** and **43** had oxidation potentials at considerably lower values than the other investigated compounds. The obtained values of 0.18 V for compound **41** and -0.07 V for compound **43** are consistent with the electron-donating effect of 6 respectively 10 alkyl substituents.

5.4.2.1. Conclusion

In view of the oxidation potential of investigated ferrocene derivatives only compounds 41 and 43 should be oxidisable with silver salts. By contrast, non-methylated derivatives, having an increased oxidation potential, should not react under these experimental conditions. Consequently, preliminary essays with compounds having a non-methylated ferrocene core did not yield an oxidised species but left the ferrocene derivative unreacted. However, in the electrochemical experiments *all* investigated ferrocene-derivatives showed a reversible one-electron oxidation. This is important in view of obtaining stable ferrocenium-salts.

5.5. Variation of Structural Parameters of the Mesogenic Core

5.5.1. A Series of Monosubstituted Ferrocene-Derivatives (Compounds 67a-f)

Only a few complexes in this series were synthesised and two types of mesophases were observed: a nematic phase and a smectic one. Melting and clearing points decreased on increasing the alkoxy chain length. The temperature range exhibited by the nematic phase remained nearly constant on increasing the alkoxy chain length. Only derivative 67e, having the octadecyloxy chain, showed a reduced nematic phase range. Smectic A phase formation may be due to microphase separation in which the mesogenic cores form one region while the alkoxy chains constitute another. Thus, for shorter chains the smectic phase was not observed (n=5) nor was monotropic (n=7, 10). For longer chains it was enantiotropic (n=14,18) and for compound 67e (n=18) the smectic phase was stabilised with respect to the nematic phase.

The forked ferrocene-derivative 67f (two tetradecyloxy chains in 3- and 4-position) was not liquid-crystalline. In this case it was obvious that the destabilisation of the liquid-crystalline properties is due to the alkoxy chain in 3-position. Comparison with compound 67d (one tetradecyloxy chain in 4-position), which showed an enantiotropic nematic and smectic A phase, suggested that strong steric effects may be the origin of this behaviour.

Therefore, the lateral chain in 3-position strongly reduced the lateral interactions between two adjacent molecules.

5.5.1.1. Oxidised Compounds

Only some oxidants (for example: I_2, DDQ, $FeCl_4^-$, H_2SO_4) are known to oxidise ferrocene (3)(ΔE=0.45 V). Due to this reason only two oxidised derivatives were synthesised. Compound 67c (no electrochemical investigations of this derivative were undertaken) was chosen because its oxidation potential was assumed to be nearly equal to that of compound 37 and that of ferrocene (3). The electron-donating effect of the two methylene units is compensated by the electron-withdrawing effect of the carboxy function (which influences the redox-potential of the ferrocene-derivative). Thus, strong oxidants have to be engaged in order to oxidise the ferrocene-moiety of compound 67c. Two complexes were synthesised incorporating a I_3^-(68a) or DDQ (68b) counter-anion. When heated, both ferrocenium-salts gave rise to decomposition whereas only for the triiodide salt a defined decomposition temperature was determined. In contrast, the charge-transfer complex 68b, having a radical anion as counter-anion, decomposed constantly when heated. Even at room-temperature, compound 68b was not stable as indicated by the formation of yellow material, which formed during some weeks. This indicated that the non-oxidised ferrocene (compound 67c) probably re-formed under these conditions. Thus, no further thermal investigations of present ferrocene-derivatives were undertaken.

5.5.2. Compounds 59-62

The observed mesophases in ferrocene derivatives 59-62 were always nematic whereas a remarkable difference in the thermal behaviour was seen. This difference depended on the linkage of the ferrocenyl moiety to the core unit and the orientation of the external ester function. Compound 59 showed the nematic phase over a wider temperature range (ΔT=29°C) than compounds 60, 61 and 62 (ΔT=2°C, 6°C and 3°C, respectively). It can be noted that for compounds incorporating a flexible linking unit (61 and 62), such as -CH_2-CH_2, liquid-crystalline tendencies are lowered. In contrast, for compounds 59 and 60

(linking unit: -CH=CH-), a higher melting point was observed. In the case of compound 59 a stabilisation of the mesophase was observed.

Firstly, considering the chemical structure of all compounds it can be noted that the shape of all molecules is nearly similar. Secondly, the chemical reduction of the double bond led to an increased molecular flexibility which can also effect mesophase behaviour. Therefore, the phase behaviour has to be explained from another point of view. A broader mesophase range was observed only for compound 59. For this compound a high dipole moment is considered. This is due to the orientation of the two ester groups and the electron rich ferrocenyl moiety, which is in conjugation with the rigid core. This higher dipole moment is most probably the origin of the broader anisotropic domain when compared to compounds 60, 61 and 62. Compound 60 was prepared by hydrogenation of compound 59. In this reaction the conjugation between the electron-donating ferrocenyl moiety and the rigid core was broken. This caused a clear decrease in the thermal stability of the mesophase and can demonstrate the contribution of the ferrocenyl moiety to the dipole moment of a liquid crystal. Figure 5.14. illustrates schematically the resultant dipole moments of the investigated compounds. It is displayed as a function of the orientation of the "external" ester group. Two possible conformations are viewed for each isomer.

For ferrocene-derivatives 61 and 62 a smaller dipole moment was estimated, as can be seen from Figure 5.14. Consequently, a decreased mesophase stability was found for these two compounds.

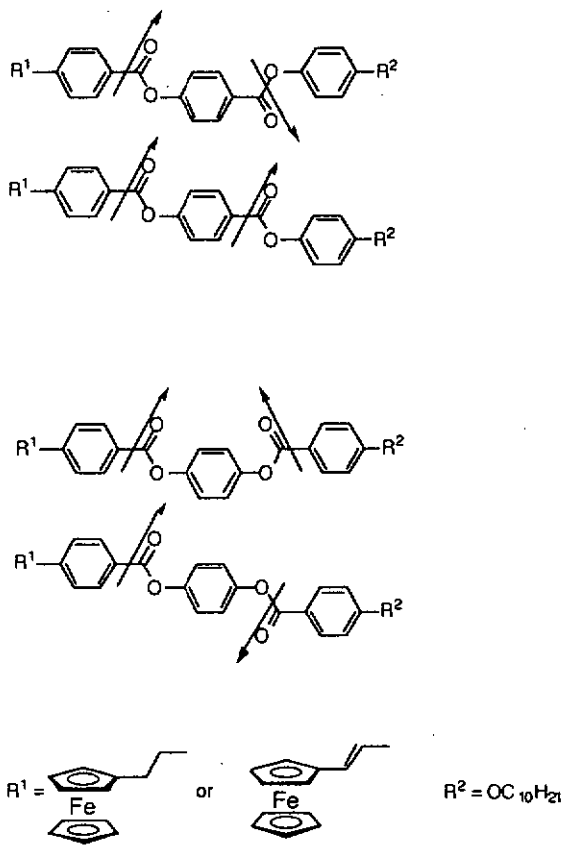

Figure 5.14. *Schematic representation of the resultant dipole moment of compounds 59-62 depending on their conformation*

5.5.3. Chiral Compounds

Chiral liquid-crystalline ferrocene derivatives have already been reported by Deschenaux et al.[86] and Imrie et al. [54]. Chiral substituents were used to give mono- or di-substituted ferrocenes and these authors found smectic B and smectic C phases. The possibility of planar-chiral mesogenic ferrocene derivatives has been discussed recently [87]. This Chapter deals with the discussion and the comparison of the mesomorphic behaviour of four chiral

ferrocene derivatives having the same mesogenic unit but are either monosubstituted or permethylated.

Among these four compounds only the two monosubstituted derivatives **53** and **54** displayed mesomorphic properties. Ferrocene derivative **53**, incorporating a -CH=CH- function, exhibited an enhanced liquid-crystalline behaviour when compared with compound **54**. The temperature range exhibited by the chiral nematic phase is decreased on going to the $-CH_2-CH_2-$ linking unit. This behaviour may be understood by considering the role played by the two different linking units. For the more rigid species **53** the transition temperatures were higher and the mesophase range was increased. Thus, a flexible linking unit induced a more limited anisotropic phase behaviour.

Despite the rules established by Vorländer on the necessity for the elongated shape of the molecules to induce calamitic mesophases, the permethylated ferrocene derivatives **55** and **56** did not show liquid crystallinity. This behaviour was somehow unexpected because other persubstituted ferrocene derivatives, incorporating longer promesogenic parts (such as compounds **24-27**), showed liquid crystallinity. This indicated that persubstitution can lead to a complete loss of the mesomorphic properties. This is probably due to the reduction of the lateral interactions and the segregation between the aliphatic and aromatic parts of the molecules. However, preliminary essays to oxidise the persubstituted derivatives **55** and **56** with silver salts (AgOTs, AgOTf, $AgO_2CC_3F_7$) did not yield liquid-crystalline materials. Another point to be noticed is that incorrect elemental analysis of obtained oxidised substances indicated the presence of solvent residues. Even heating them over several days under reduced pressure did not yield substances which gave satisfying microanalytical data.

In conclusion, in view of liquid-crystalline phase formation the chiral butyl-propionate group does not seem comparable with persubstituted ferrocene or ferrocenium moieties. Even the oxidation to ferrocenium-derivatives did not induce mesomorphic behaviour.

5.6. Disubstituted Liquid-Crystalline Ferrocenes

A series of monosubstituted, non-symmetrically substituted ferrocenes was synthesised (compounds 72a-g). All synthesised compounds exhibited an enantiotropic smectic A phase, whereas for shorter chain length *n* only a very narrow anisotropic domain was observed. On going to longer alkoxy-chains the liquid-crystalline domain broadened considerably.

Chapter

6

Conclusion

Our conclusion may be summarised as follows: structural variations that effect the ironcyclopentadienyl core lead to changes in the mesomorphic behaviour and the redox potentials of ferrocenes and ferrocenium salts.

Structural modifications (degree of methylation on the cyclopentadienyl rings) have a large effect on the thermal behaviour. For persubstituted ferrocenes it was found that incorporation of a rigid core containing two or three aromatic rings produces non-mesomorphic derivatives. In contrast, the use of a longer promesogenic core bearing four aromatic rings, leads to enantiotropic mesophases, predominantly of nematic character.

In this study electrochemical investigations were performed on several compounds and the measured values of the oxidation potentials agreed with the estimated values. Interestingly, only permethylated ferrocenium salts seem to be thermally stable upon heating, whereas pentamethyl-substitution of one cyclopentadienyl ring leads to an oxidised compound which decomposed upon heating. Furthermore, non-methylated ferrocene-derivatives could not be oxidised by the use of silver salts, but had to be treated with stronger oxidants such as I_2 or DDQ. The resulting ferrocenium salts were also thermally unstable.

The liquid-crystalline phases observed for ferrocenium-salts were always of layered structure; smectic A and/or smectic C in type. These results were explained by electrostatic head-group repulsions of the ferrocenium cations. For one compound a columnar mesophase (Col_h) was observed. A model of the molecular arrangement of the salts in the layered and in the columnar phase is proposed.

In a further investigation the influence of the counterion on the mesomorphic properties of ferrocenium salts was examined. Seven different counter-anions were studied. The ferrocenium-salts containing the tosylate counterion showed predominantly smectic phases. In contrast, for compounds containing the smaller triflate anion, generally no mesophases were observed. This difference between the two sulphonate counterions is explained by the different size and in terms of their interdigitation between the ferrocenium head groups. Small counterions seem therefore to be unfavourable in terms of mesomorphic properties. All charge-transfer ferrocenium complexes which

contain radical anions (TCNE, TCNQ, DDQ) were thermally unstable. Therefore, due to its aromatic nature (interdigitation between ferrocenium head groups), the size (low crystallinity of salts) and the type of ionic group (sulphonate group as conjugate base of a strong acid) the tosylate counterion seems to favour the most pronounced mesomorphic properties in ferrocenium-salts.

Since we had no precise information on the molecular structure of investigated ferrocenium salts (crystal growth was not successful either to poor tendency to crystallisation or decomposition of salts) it was not possible to clarify the position of the counter-anion with respect to the ferrocenium cation in a crystal state.

Moreover, molecules of amphiphilic type are known to show lyotropic phase behaviour which was not studied in this thesis. In this respect it could be interesting to compare the lyotropic mesomorphism of those salts with their thermotropic phase behaviour.

We therefore suggest that future studies of mesomorphic redox-active ferrocene systems should focus on the improvement of liquid-crystallinity. This could be done either by varying the promesogenic core or by searching further anions which favour mesophase formation.

We believe that the amphiphilic character of ferrocenium salts can give rise to further interesting properties, namely the formation of columnar phases. This may lead to a better understanding of the molecular organisation of ferrocenium-salts within the liquid-crystalline state.

Chapter

7

Experimental Part

7.1. General Remarks

7.1.1. Analytical Methods and equipment

Chromatography

Column Chromatography (CC) was conducted on Silica Gel 60 (0.060-0.200 mm, SDS). Thin Layer Chromatography (TLC) used Silica Gel Plates 60 F_{245} (Merck).

Differential-Scanning-Calorimetry (DSC) Measurements

Transition temperatures (°C) and enthalpies (kJ mol^{-1}) were determined with a Differential Scanning Calorimeter (Mettler DSC 30) connected to a Mettler TA 4000 processor. For the treatment of the data Mettler TA 72.2/5 Graphware was used. The apparatus was calibrated with Indium (mp.=156.6°C, ΔH_{fusion}=28.45 $kJmol^{-1}$). The DSC curves were recorded under nitrogen at a rate of 10°C min^{-1} if not stated otherwise. The melting, transition, isotropisation and crystallisation temperatures are reported as onset temperatures and refer to the second heating-cooling cycle if not stated otherwise.

Elemental-Analyses

The purity of all new compounds was verified by elemental analyses, to an accurancy of within ±0.3% (C and H). Elemental Analyses were conducted in the Analytical Department, Ciba (Marly) or at the ETH Zürich.

Infrared-Spectroscopy

Infrared spectra were recorded on a Perkin-Elmer 1720 FTIR spectrometer.

Magnetic Measurements

These measurements were conducted at the Universität Marburg (D). A powdered sample of a compound **43a** was measured with a Quantum Design MPMS5 SQUID (Superconducting Quantum Interference Device) magnetometer in the temperature range 25<T<150°C and an external field of H=5 T. The sample was measured in a quartz tube for which no correction was applied. The sample was heated to 150°C, kept there for 10 min and then cooled to r.t.

Mass-Spectroscopy

Mass spectra were recorded on a Nermag RC 30-10 (EI: 70eV; CI: NH_4^+) spectrometer. The intensities are given in brackets. The signals are given in m/e and in percent of the basis-peak (100%). The FAB (Fast Atom Bombardment)-spectra were recorded on a Vacuum Generators Micromass 7070 E at the Université de Fribourg (CH).

Melting points

Melting points were measured on a Büchi melting point apparatus Büchi 530 and were uncorrected.

Microscopic Investigations

Optical studies were conducted using a Zeiss-Axioscop polarising microscope equipped with a Linkham-THMS 600 variable temperature stage; under nitrogen.

NMR-Spectroscopy

Proton and Carbon NMR spectra were recorded on a Varian Gemini 200 spectrometer or on a Bruker AMX 400 spectrometer. HETCOR spectra were recorded on a Bruker AMX 400 spectra. The residual solvent peaks were used as internal reference ($CDCl_3$: δ 7.26 [^{1}H] or 77.0 [^{13}C] ppm; CD_2Cl_2: δ 5.32 [^{1}H] or 53.8 [^{13}C] ppm; d_6-acetone: δ 2.04 [^{1}H] or 206 [^{13}C] ppm; d_6-DMSO: δ 2.49 [^{1}H] or 39.5 [^{13}C] ppm.) Abbreviations: *s*: singulet; *d*: doublet; *t*: triplet; *q*: quartet; *quint*: quintet; *sept*: septet; *m*: multiplet.

Thermogravimetric Analyses

Thermogravimetric Analyses were performed with a Mettler TG 50 thermobalance connected to a Mettler TA 4000 processor at a rate of 20°C min^{-1}.

UV/vis Measurements

UV spectra were obtained with a uvikon 930 spectrophotometer in CH_2Cl_2, contained in 1.0 cm quarts cells. Measurements were carried out between 200 and 800 nm.

X-ray measurements

X-ray measurements were conducted by Dr. Anne-Marie Levelut at the Université de Paris-Sud (F).

7.1.2. Chemical Substances

Substance	*Abbreviation*	*Quality*
(-)-Butyl-L-lactate, $[\alpha]_D^{20} = -12\pm1$		Fluka97%
1-Bromoalkanes		Fluka 95-97%
2-Bromo-2-butene (mixture of cis and trans)		Aldrich 98%
2,3-Dichloro-5,6-dicyano-1,4-benzoquinone	DDQ	Fluka 97%
(4-Carboxybutyl)triphenylphosphonium bromide		Fluka 99%
4'-Hydroxy-4-biphenylcarbonitrile		Aldrich
4-Hydroxyacetophenone		Fluka 97%
4-Pyrrolidinopyperidine	Ppy	Aldrich 98%
4,4'-Dihydroxybiphenyl		Fluka 98%
7,7,8,8-Tetracyanoquinodimethane	TCNQ	Fluka 98%
α-Bromo-*p*-toluic acid		Fluka 98%
Bariummanganate	$BaMnO_4$	Fluka pract.
Benzylbromide	BrBn	Fluka 98%
Borontrifluoride diethyletherate	$BF_3\,Et_2O$	Fluka 98%
Butyllithium 1.6M in hexane	*n*-BuLi	Aldrich
Chromium(IV)oxide	CrO_3	Fluka 99%
Dicyclopentadiene		Fluka 85-90%
Diethylazodicarboxylate solution, Assay 40% in toluene	DEAD	Fluka
Dimethylformamide	DMF	sds 99.8%
Ferrocenecarboxaldehyde	FcCHO	Fluka 98%
Glutaric anhydride		Fluka 95%
Hydroquinone monobenzylether		Fluka 99%
Iodine	I_2	Fluka 99.8
Iron(II)chloride anhydrous	$FeCl_2$	5trem 98%
Lithium, wire, high sodium	Li(Na)	Aldrich 98%
Malonic acid		Fluka 98%
N,N'-Dicyclohexylcarbodiimide	DCC	Fluka 99%
N,N,N',N'-Tetramethylethylenediamine	TMEDA	Fluka99%
Oxalylchloride	$(COCl)_2$	Fluka 98%
Palladium on activated Charcoal (Assay 10% Pd)	Pd/C	Fluka
Phosphorousoxychloride	$POCl_3$	Fluka 98%

Substance	*Abbreviation*	*Quality*
Piperidine		Fluka 99%
Silver hexafluorophosphate	$AgPF_6$	Aldrich 98%
Silver toluene-4-sulfonate	AgOTs	Fluka 96%
Silver trifluoromethanesulfonate	AgOTf	Aldrich 99%
Silverheptafluorobutyrate	$AgO_2CC_3F_7$	Aldrich 97%
Silverpentafluoropropionate	$AgO_2CC_2F_5$	Aldrich 98%
Silvertrifluoroacetate	AgO_2CF_3	Aldrich98%
Sodiumhydride 60% Dispersion in Mineral Oil	NaH	Aldrich
tert-Butyllithium 1.5M in pentane	*t*-BuLi	Fluka
Tetracyanoethylene	TCNE	Fluka 97%
Triethylamine	NEt_3	Fluka 99.5%

Solvents

The following solvents were distilled before use. Petroleum ether refers to the 90-110°C fraction.

Solvent	*Distillation over*
Dibutylether	NaH
Dichloromethane	P_2O_5
Diethyl ether	$LiAlH_4$
Ethyl acetate	P_2O_5
Heptane	Na
Hexane	Na
t-Butylmethylether	NaH
Tetrahydrofurane	Na, benzophenone

7.2. Synthesis

7.2.1. Standard Experimental Procedures

7.2.1.1. Esterification

A solution of dichloromethane (20 ml) which contains the phenol derivative (0.01 mol), the acid derivative (0.01 mol), DCC (0.01 mol) and Ppy (catalytic amount: 10 mol-%) is stirred for 6 h under nitrogen at room temperature. After the reaction is complete (TLC) insoluble dicyclohexylurea is filtered off and the filtrate is evaporated. The residue is projected to column chromatography (dichloromethane/SiO_2) and the ester is eluted (solvent for column chromatography in case of alkylated ferrocene derivatives: CH_2Cl_2-NEt_3 (98:2)). The ester is recrystallised (solvent: see experimental section). The yields are normally between 60-80%.

7.2.1.2. Deprotection

A solution of CH_2Cl_2-EtOH (300 ml, 5:1) containing the benzyl protected derivative (0.1 mol) and Pd/C catalyst (10% by weight) is shaken overnight under H_2 (4 bars). The solution is filtered and the filtrate is evaporated. The product is recrystallised (solvent: see experimental section).

7.2.1.3. Hydrogenation

A solution of CH_2Cl_2 (50 ml) containing the derivative to be hydrogenated (0.1 mol) and Pd/C catalyst (10% by weight) is shaken 30 min under H_2 (4 bars). The solution is filtered and the filtrate is evaporated. The product is recrystallised from dichloromethane-ethanol or acetone (see experimental section).

7.2.1.4. Oxidation

To a solution of dichloromethane-acetone (10 ml, 1:1) containing the ferrocene derivative (1 eq.) a solution of AgX (0.95-1 eq., X= OTs, OTf, $F_{2n+1}C_nCO_2$ [n = 1, 2, 3]) in acetone (10 ml) is given dropwise at room temperature. The colour changes rapidly from bright yellow to green, indicating the oxidation of the ferrocene core. After 5 min the reaction is complete (TLC) and the solution is

filtered over celite and the filtrate is evaporated. The residue is projected to column chromatography (CH_2Cl_2 + 2% *MeOH*) and a bright yellow zone of unreacted ferrocene is eluted first. Using a solvent gradient (CH_2Cl_2 + up to 10% MeOH) a green zone containing the product is eluted. The solvent is evaporated and the crude ferrocenium salt is recrystallised (solvent AcOEt).

7.2.2. Chemical Substances

7.2.2.1. Decamethylferrocene (1)

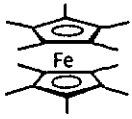

Pentamethylcyclopentadiene (4) (10 g, 0.0735 mol) under Ar in THF (100 ml) is cooled to -78°C. 1.6 M BuLi (150 ml, 0.118 mol, 1.6 eq.) is added slowly and the reaction mixture is allowed to warm to r.t. The mixture is cooled to -78°C and $FeCl_2$ (14.7 g, 0.118 mol, 1.6 eq.) is added. The solution is allowed to warm to r.t. and turns from grey to dark green colour. To insure complete reaction the mixture is refluxed overnight. The brown mixture is poured onto water and ether and filtered. The organic phase is separated and the aqueous layer is washed twice with ether. The combined organic extracts are dried over $MgSO_4$ and evaporated. The residue is recrystallised from methanol to give orange Decamethylferrocene (1). mp: 290°C. Yield: 18.9 g (0.058 mol, 79%). ^{1}H-NMR (200 MHz, d_6-acetone): δ 1.67 (*s*, 30H). ^{13}C-NMR (100 MHz, d_6-acetone): δ 9.8 (CH_3); 79.0 (Cp-C). Anal. calc. for $C_{20}H_{30}Fe$ (326.30): C 73.62 H 9.27; found: C 73.52 H 9.48.

7.2.2.2. Pentamethylferrocene (2)

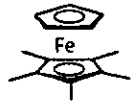

Cyclopentadien (4)

Mineral oil (100 ml) is placed in a 4 necked flask equipped with a vigreux column, thermometer, magnetic stirring bar and dropping funnel. The vigreux column is connected to a water cooled condenser and a second thermometer allowing to control vapour temperature. An ice cooled trap is placed at the outlet of the condenser.

The mineral oil is heated to 240-250°C and with fast stirring dicyclopentadien is added through the dropping funnel with a rate of approx. 10 ml min^{-1}. The temperature at the top of the vigreux column should not be higher than 45°C. Cyclopentadien (4) is collected in the ice-cooled trap and is stored at -75°C.

Cyclopentadienylsodium DME [65]:

In a 4-necked flask equipped with a reflux-condenser, thermometer, KPG-stirrer and a dropping funnel, sodium (11.5 g, 0.5 mol) is suspended in toluene (70 ml). The mixture is heated under reflux. After all sodium is molten the mixture is stirred vigorously in order to generate a fine dispersion of sodium. Immediately after the suspension has formed the solution is cooled rapidly by using an ice-NaCl bath. A fine suspension of sodium has formed and the solvent is removed by using a canula an a slight positive pressure of N_2. THF (170 ml) is added to the flask and cyclopentadiene (4)(36.5 g, 0.55 mol) is dropped to the mixture during 2h. The temperature of the mixture should not be higher than 40°C. The solution turns to purple and is stirred for additional 2h until no sodium is left. Dimethoxyethane (54 g, 0.6 mol) is added to the reaction mixture. A precipitate forms immediately. This product is filtered off and washed twice with small portions of hexane to give colourless cyclopentadienylsodium-DME which is used without further characterisation. Yield: 4.37 g (0.0246 mol, 34%).

Bis-iron(II)acetylacetonate

A mixture of ironpentacarbonyl (14.3 g, 10 ml, 0.0732 mol, 1eq.) and acetylacetone (7.32 g, 0.0732 mol, 1 eq.) in dibutylether (100 ml) is heated under reflux for 36 h. The orange solution rapidly turns dark red and a precipitate is formed. After complete reaction the mixture is cooled under a slight pressure of Ar to 0°C and the product is filtered off. The crystals are washed twice with small portions of ether to give yellow-orange bis-iron(II)acetylacetonate which is engaged without further characterisation. The product is very sensitive to moisture and air. Yield: 6.24 g (0.0246 mol, 34%).

Pentamethylferrocene

Pentamethylcyclopentadiene (4) (3.32 g, 0.0246 mol 1 eq.) in THF (20 ml) under Ar is cooled to -78°C and 1.6 M *tert*-BuLi (18.1 ml, 0.027 mol) is added during 20 min. The mixture is allowed to warm to r.t. and stirred for further 10 min to insure complete reaction. A pale yellow precipitate forms and the suspension is cooled again to -78°C. Solid bis-iron(II)acetylacetonate (6.24 g, 0.0246 mol, 1 eq.) is added at this temperature at once to the reaction mixture while the flask is flushed by a strong stream of Ar in order to protect the solution from oxidation. The mixture is allowed to warm slowly to 0°C during 1h. At about -30°C the colour changes from red-orange to brown, indicating the formation of the pentamethylcyclopentadienyl iron(II) acetylacetonate (10) intermediate. After reaching 0°C the mixture is cooled again to -20°C and the cyclopentadienylsodium-DME (4.37 g, 0.0246 mol, 1 eq.) is added in the same manner to the flak as bis-iron(II)acetylacetonate before. The solution is carefully heated to 40°C for 30 min.

Water (20 ml) and ether (40 ml) are added to the brown solution and the mixture is filtered through SiO_2 (6x3 cm). The phases are separated and the aqueous layer is extracted with ether until the washings remain colourless. The combined organic extracts are washed with water (3x100ml) and the solution is dried over $MgSO_4$ and evaporated.

The residue is projected to column chromatography (hexane-ether, 1:1; 2x40 cm) and an orange zone is eluted to give after evaporation a mixture of ferrocene (3), pentamethylferrocene (2) and decamethylferrocene (1) (1 : 23 : 3; determined by the integral intensities in the ^{1}H-NMR-spectra). Recrystallisation from EtOH gives a mixture of pentamethylferrocene (2) and decamethylferrocene (1) (11 : 1) and a second recrystallisation from EtOH-hexane (10:1) leads to pure pentamethylferrocene (2). mp. 87-98°C. Yield: 3.46 g

(0.0135 mol, 55%, calc. for NaCp DME). R_f(ether)=0.83. ^{1}H-NMR (200 MHz, $CDCl_3$): δ 1.94 (*s*, 15 H, CH_3); 3.70 (*s*, 5H, Cp-H). ^{13}C-NMR: (100 MHz, $CDCl_3$): δ 11.5 (CH_3); 71.3 (Cp-C); 80.2 (*tert*-C). Anal. calc. for $C_{15}H_{20}Fe$ (256.17): C 70.33 H7.87; found: C 70.81 H 8.15.

7.2.2.3. Ferrocenium triiodide (5)

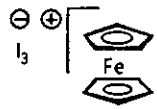

Ferrocene (3) is oxidised with I_2. Compound 5 is prepared using a procedure similar to that described for compound 68a. Amounts used: Ferrocene (3) 300 mg (1.61 mmol, 1eq.) in benzene-hexane (8:2) (80 ml); I_2 (695.4 mg, 2.74 mmol, 1.7 eq.) in benzene (100 ml). mp. 186°C (dec.). Yield: 0.69 g (1.22 mmol, 76%). Anal. calc. for $C_{10}H_{10}FeI_3$ (566.75): C 21.19 H 1.78; found: 20.29 H 1.77.

7.2.2.4. Decamethylferrocenium tosylate (6) and decamethylferrocenium heptafluorobutyrate (9)

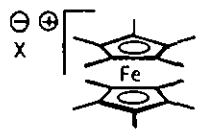

X = $C_3F_7CO_2$, OTs

Decamethylferrocene (1) is oxidised with silver tosylate or silver heptafluoro butyrate. The standard experimental procedure is used.

X=OTs (compound 6)

Amounts used: Decamethylferrocene (1) (160 mg, 0.491 mmol, 1 eq.); silver tosylate (116 mg, 0.414 mmol, 0.9 eq.). CH_2Cl_2 15 ml. mp.: 243°C (dec.). Yield: 160 mg (0.322 mmol, 78%). Anal. calc. for $C_{27}H_{37}FeO_3S$ (497.49): C 65.19 H 7.50; found: C 65.00 H 7.64.

X=$C_3F_7CO_2$ (compound 9)

Amounts used: Decamethylferrocene (1) (110 mg, 0.337 mmol, 1 eq.); silverbutyrate (97 mg, 0.303 mmol, 0.9 eq.). CH_2Cl_2 15 ml. mp.: 140-160°C (dec., difficult to determine). Yield: 120 mg (0.222 mmol, 66%). Anal. calc. for $C_{24}H_{30}F_7FeO_2$ (539.35): C 53.45 H 5.61; found: C 53.43 H 5.70.

7.2.2.5. Pentamethylferrocenium tosylate (7)

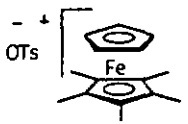

Silver tosylate (109 mg, 0.391 mmol) is suspended in acetone (10 ml) and a solution of pentamethylferrocene (2) (100 mg, 0.391 mmol) in CH_2Cl_2 (10 ml) is added dropwise to this suspension. The stirred reaction mixture immediately turns black. To insure complete reaction the mixture is heated under reflux for 2h. The solution is filtered over celite. The solvent is removed under reduced pressure and the residue is carefully washed with several portions of ether. Yield: 125 mg (0.293 mmol, 75%). mp. 154 (dec.). Anal. calc. for $C_{22}H_{27}FeO_3S$ (427.37): C 61.83 H 6.37; found: C 61.29 H 7.03.

7.2.2.6. Pentamethylferrocenium pentafluoro propionate-pentafluoro propionic acid adduct (10)

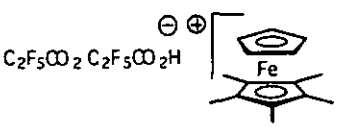

Pentamethylferrocene (2) (105 mg, 0.410 mmol, 1 eq.) and Pentafuoropropionic acid (202 mg, 0.128 ml, 1.230 mmol, 3 eq.) are dissolved in benzene (20 ml) and O_2 is bubbled through this solution. The colour rapidly changes to dark brown. After 2 h this solution is poured onto hexane (50 ml). The precipitated product is filtered off and washed several times with ether an hexane. Yield: 50 mg (0.086 mmol, 21%). mp. 169 (dec.). Anal. calc. for $C_{21}H_{21}F_{10}FeO_4$ (583.24): C 43.25 H 3.63; found: C 43.68 H 3.64.

7.2.2.7. Oxidation of ferrocene (3) with DDQ (compound 11)

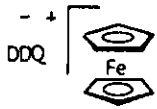

Ferrocene (3) is oxidised with DDQ. Compound 11 is prepared using a procedure similar to that described for compound 68b. Amounts used: Ferrocene (3) (372 mg, 2 mmol); DDQ (454 mg, 2 mmol); CH_2Cl_2 (10ml). Yiefd: 800 mg (1.937 mmol, 97%). mp. 175°C (dec.). Anal. calc. for $C_{18}H_{10}Cl_2FeN_2O_2$ (413.05): C 52.34 H 2.44 N 6.78; found: C 51.82 H 2.38 N 6.93.

7.2.2.8. Oxidation of Decamethylferrocene (1) with $BaMnO_4$ [68-72,88] (compound 12)

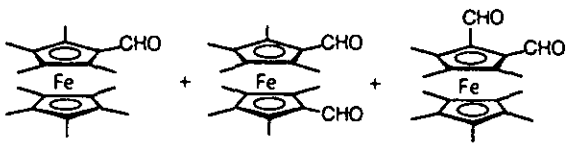

Decamethylferrocene (1) (19 g, 0.0583 mol) is dissolved in a mixture of ether and benzene (1:1, 1000 ml) and powdered $BaMnO_4$ (100 g) is added. The suspension is heated under reflux for 6 h. After cooling to r.t. the mixture is filtered. The solvent is evaporated and the residue is projected to column chromatography (CH_2Cl_2+1%NEt_3; 5x100 cm). A bright yellow zone of unreacted decamethylferrocene (1) is eluted first. The desired aldehyde 12 is eluted as a first dark red zone. A second dark red zone is eluted containing a mixture of the 1,1'- and 1,2- dialdehydes.

Yield: 8.0 g decamethylferrocene (2) (recovered, 0.0245 mol, 42%).

Yield: 7.0 g nonamethylferrocene carboxaldehyde (12) (0.0206 mol, 35%). mp. 330°C. $R_f(CH_2Cl_2)$=0.58. ^{1}H-NMR (200 MHz, d_6-acetone) δ 1.65 (s, 15H, CH_3); 1.79 (*s*, 6H, CH_3); 1.98 (*s*, 6H, CH_3); 9.98 (*s*, 1H, CHO). Anal. calc. for $C_{20}H_{28}FeO$ (340.28): C 70.59 H 8.29; found: C 70.65 H 8.39.

Yield: 2.0 g octamethylferrocene-1,2-dicarboxdialdehyde and octamethyl ferrocene-1,1'-dicarboxdialdehyde (0.056 mol, 10%). $R_f(CH_2Cl_2)$=0.19. ^{1}H-NMR (200 MHz, d_6-acetone): δ 1.62 (*s*, 15H, γ-CH_3, 1,2-isomer); 1.67 (*s*, 6H, β-CH_3, 1,1'-isomer); 1.84 (*s*, 3H, β-CH_3, 1,2-isomer); 1.97 (*s*, 6H, α-CH_3, 1,1'-isomer); 2.10 (*s*, 6H, α-CH_3, 1,2-isomer); 10.01 (*s*, 2H, CHO, 1,1'-isomer); 10.28 (*s*, 2H, CHO, 1,2-isomer).

7.2.2.9. 6-(1',2,2',3,3'4,4',5,5'Nonamethylferrocenyl)-5-hexenoic acid (13)

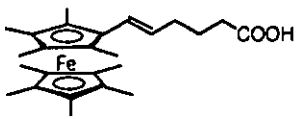

(4-Carboxybutyl) triphenylphosphonium bromide (0.98 g, 2.21 mmol) is suspended under N_2 in THF (5 ml). A solution of potassium-*tert*-butoxide (0.49 g, 4.41 mmol) in THF (4 ml) is added during 5 min at r.t. while the reaction mixture turns from colourless to dark orange colour. After 20 min a solution of nonamethylferrocene carboxaldehyde (12) (0.5 g, 1.47 mmol) in THF (5 ml) is added dropwise while the colour of the mixture turns to brown. After 3 h the reaction is complete and the mixture is poured onto water and ether. The aqueous layer is separated and the organic layer is washed once with water. The combined aqueous extracts are washed once with AcOEt and acidified with HCl (2 *N*) until the product precipitates. The precipitate is re-extracted with AcOEt and the organic solution is washed with water until the aqueous layer remain neutral. The organic layer is dried over $MgSO_4$. The solvent is evaporated and the residue is recrystallised from hexane to give 6-(1',2,2',3,3'4,4',5,5' nonamethylferrocenyl)-5-hexenoic acid (13). Yield: 0.5 g (1.18 mmol, 80%). mp. 116°C. $R_f(CH_2Cl_2)$=0.33. ^{1}H-NMR (200 MHz, d_6-acetone): δ 1.63 (*s*, 15H, CH_3); 1.69 (*s*, 6H, CH_3); 1.78 (*s*, 6H, CH_3); 1.78 (*m*, 2H, CH_2), 2.18 (*m*, 2H, CH_2), 2.37 (*t*, 2H, CH_2), 5.70 (*dt*, 1H, sp^2-C-H, J=15.8 Hz); 6.09 (*d*, 1H, sp^2-C-H, J=15.8 Hz).

7.2.2.10. 1-Formyl-1',2',3',4',5'-pentamethylferrocene (14)

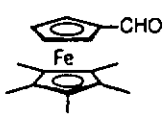

Pentamethylferrocene (2) (0.768 g, 3 mmol, 1 eq.) is dissolved in CH_2Cl_2 (10 ml). To this solution $POCl_3$ (1.15 g, 0.69 ml, 7.5 mmol, 2.5 eq.) and DMF (0.986 g, 1.04 ml, 13.5 mmol, 4.5 eq.) are added. The mixture is heated under reflux for 24 h. The dark purple solution is allowed to cool to r.t. and cold water (15 ml) and K_2CO_3 (2.42 g, 17.4 mmol, 5.8 eq.) are added. This suspension is stirred for 1 h at r.t. Ether (30 ml) is added and the organic phase is separated. The aqueous phase is extracted twice with ether and the combined organic extracts are washed with water and dried over Na_2SO_4. The solvent is evaporated and the residue is recrystallised from hexane to give 1-Formyl-1',2',3',4',5'-pentamethylferrocene (**13**). Yield: 0.604 g (2.13 mmol, 71%). mp. 52°C. **^{1}H-NMR** (200 MHz, $CDCl_3$): δ 1.84 (*s*, 15H, CH_3); 4.17 (*t*, 2H, Cp-H); 4.26 (*t*, 2H, Cp-H); 9.70 (*s*, 1H, CHO). **^{13}C-NMR** (100 MHz, APT, $CDCl_3$): δ 11.0 (CH_3); 71.9 (Cp-C); 77.5 (Cp-C); 82.3 (Cp-*tert*-C); 128.4 (Cp-*tert*-C-CHO); 193.9 (CHO). Anal. calc. for $C_{16}H_{20}FeO$ (284.18): C 67.62 H 7.09; found: C 67.61 H 7.06.

7.2.2.11. (1',2',3,'4',5'-Pentamethylferrocenyl)-5-hexenoic acid (15)

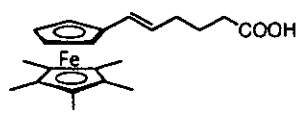

(1',2',3,'4',5'-Pentamethylferrocenyl)-5-hexenoic acid (**15**) is synthesised from pentamethyl ferrocene carboxaldehyde (**14**) and (4-carboxybutyl)triphenylphosphonium bromide. It is prepared using a procedure similar to that described for compound **13**. The crude product was obtained. Amounts used: (4-Carboxybutyl) triphenylphosphonium bromide 148 mg (0.334 mmol); potassium-*tert*-butoxide 38 mg (0.334 mmol); (1',2',3,'4',5'-pentamethyl ferrocenyl)-5-hexenoic acid (**15**) 95 mg (0.334 mmol); THF 25 ml. Yield: 80 mg (0.224 mmol, 67%); R_f(AcOEt)=0.72. **^{1}H-NMR** (200 MHz, $CDCl_3$): δ 1.59 (*s*, 15H, Cp-CH_3); 2.20-2.49 (*m*, 6H, CH_2); 3.65-4.12 (*m*, 4H, Cp-H); 5.32-5.58 (*m*, 1H, sp^2-CH); 5.69-5.91 (*m*, 1H, sp^2-CH).

7.2.2.12. 6-Ferrocenyl-5-(*E*/*Z*)-hexenoic acid (17)

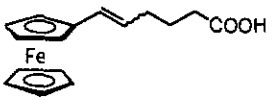

(4-Carboxybutyl)triphenylphosphonium bromide (4.42 g, 0.01 mol) is suspended under N_2 in THF (15 ml). A solution of potassium-*tert*-butoxide (3.52 g, 0.02 mol) in THF (10 ml) is added during 5 min at r.t. while the reaction mixture turns from colourless to dark orange colour. After 20 min a solution of ferrocenecarboxaldehyde (16) (2.14 g, 0.01 mol) in THF (10 ml) is added dropwise while the colour of the mixture turns to brown. After 45 min the reaction is complete and the mixture is poured onto water and ether. The aqueous layer is separated and the organic layer is washed once with water. The combined aqueous extracts are washed once with AcOEt and acidified with HCl (10%) until the product precipitates. The precipitate is extracted with AcOEt and the organic solution is washed with water and dried over $MgSO_4$. The solvent is evaporated and the residue is projected to column chromatography (AcOEt; 1x20 cm). A dark red zone is eluted to give after evaporation pure 6-Ferrocenyl-5-hexenoic acid (17) as a mixture of *cis-trans* isomers (2:1). Yield: 2.1 g (0.007 mol, 70%). R_f(AcOEt)=0.61. **^{1}H-NMR** (200 MHz, $CDCl_3$): δ 1.81 (*q*, 2H, CH_2); 2.11-2.48 (*m*, 4H, -CH_2-); 4.12 (*s*, 5H, Cp-H); 4.21 (*s*, 2H, Cp-H); 4.33 (*s*, 2H, Cp-H); 5.42 (*dt*, 1H, J^1_{cis}=11.4 Hz, sp^2-CH); 5.74 (*dt*, 1H, J^1_{trans}=15.5 Hz, sp^2-CH); 6.12 (*d*, 1H, sp^2-H, cis- and trans-isomer). **^{13}C-NMR** (100 MHz, APT, $CDCl_3$): δ 24.7 (CH_2); 28.3 (CH_2); 32.2 and 33.7 (CH_2, *cis*- and *trans*-isomer); 66.5 (Cp-H); 68.6 (Cp-H); 69.2 (Cp-H); 82.1 (*tert*-C); 127.1 (sp^2-C); 128.0 (sp^2-C); 180.0 (COOH). **EI-MS** (70 eV): 298 (M^+, 11); 84 (90); 49 (100). **Anal. calc.** for $C_{16}H_{18}FeO_2$ (298.13): C 64.45 H 6.08; found: C 64.36 H 6.16.

7.2.2.13. 1-Ferrocenyl-2-(4'-carboxyphenyl)ethylene (18)

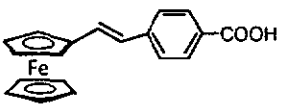

1-Ferrocenyl-2-(4'-carboxyphenyl)ethylene (18) is synthesised from ferrocene carboxaldehyde (16) and (4-carboxybenzyl)triphenyl-phosphonium bromide. It

is prepared using a procedure similar to that described for compound 19. Amounts used: Ferrocene carboxaldehyde (16) 1.37 g (8.06 mmol, 1eq.); (4-carboxybenzyl)triphenyl-phosphonium bromide 5 g (10.48 mmol, 1.3 eq.); potassium-*tert*-butoxide 2.55 g (20.98 mmol, 2.6 eq.); THF 20 ml. Yield: 0.91 g (2.74 mmol, 34%). mp. 272°C. ^{1}H-NMR (200 MHz, d_6-DMSO): δ 4.16 (*s*, 5H, Cp-H); 4.37 (*t*, 2H, Cp-H), 4.62 (*t*, 2H, Cp-H); 6.84 (*d*, 1H, J=16.1Hz, sp^2C-H); 7.17 (*d*, 1H, J=16.5Hz, sp^2C-H); 7.60 (*d*, 2H, arom-H); 7.90 (*d*, 2H, arom-H). Anal. calc. for $C_{19}H_{16}FeO_2$ (332.18): C 68.70 H 4.85; found: C 68.63 H 5.06.

7.2.2.14. 1-Nonamethylferrocenyl-2-(4'-carboxyphenyl)ethylene (19)

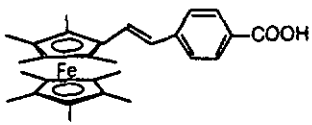

(4-Carboxybenzyl)triphenyl-phosphonium bromide (2.86 g, 6 mmol) is suspended under N_2 in THF (10 ml). A solution of potassium-*tert*-butoxide (1.35 g, 12 mmol) in THF (12 ml) is added during 5 min at r.t. while the reaction mixture turns from colourless to dark orange colour. After 30 min a solution of 1-nonamethylferrocenyl-2-(4'-carboxyphenyl)ethylene (19) (2.0 g, 6 mmol) in THF (12 ml) is added dropwise while the colour of the mixture turns to brown. The reaction mixture is heated under reflux for 4 h. After cooling to r.t. the mixture is poured onto water (25 ml) and ether (25 ml). The aqueous layer is separated and the organic layer is washed twice with water. The combined aqueous extracts are washed with AcOEt and acidified with HCl (10%). The aqueous layer is re-extracted once with AcOEt and the combined organic layers are dried with $MgSO_4$ and evaporated. The solid residue is washed with hexane, filtered off and dried. Yield: 0.42 g (0.915 mmol,15%). mp. 301°C. ^{1}H-NMR (200 MHz, $CDCl_3$): δ 1.39 (*s*, 15H, Cp-CH_3); 1.54 (*s*, 6H, Cp-CH_3); 1.67 (*s*, 6H, Cp-CH_3); 6.67 (*m*, 2H, sp^2-CH); 7.45 (*d*, 2H, arom-H); 8.03 (*d*, 2H, arom-H). EI-MS (70eV): 459 ($M^{+\cdot}$, 16), 135 (100), 119 (70), 91 (70).

7.2.2.15. 6-Nonamethylferrocenyl-5-hexenoic acid (4-biphenyl-4'-benzyloxy) ester (21)

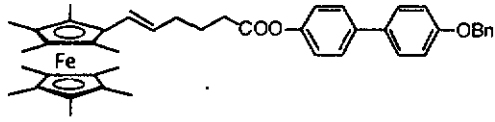

6-Nonamethylferrocenyl-5-hexenoic acid (4-biphenyl-4'-benzyloxy) ester (21) is synthesised from ferrocene derivative 13 and 4-benzyl-4'-hydroxy biphenyl [74]. It is prepared using the standard experimental procedure for esterification. Amounts used: (1',2,2',3,3'4,4',5,5' nonamethylferrocenyl)-5-hexenoic acid (13) 3.9 g (8.89 mmol); 4-benzyl-4'-hydroxy biphenyl 2.46 g (8.89 mmol); DCC 1.83 g (8.89 mmol); Ppy 0.13 g (0.89 mmol); CH_2Cl_2 100 ml. Recrystallisation from EtOH-hexane. Yield: 4 g (5.85 mmol, 66%). mp. 135°C. $R_f(CH_2Cl_2)$=0.77. ^{1}H-NMR (200 MHz, d_6-acetone): δ 1.67 (*s*, 15H, Fc-CH_3); 1.72 (*s*, 6H, Fc-CH_3); 1.82 (*s*, 6H; Fc-CH_3); 1.91 (*quint*; 2H; CH_2); 2.29 (*dt*; 2H, CH_2); 2.70 (*t*, 2H, O_2-CH_2); 5.19 (*s*, 2H, Ar-CH_2); 5.74 (*dt*, 1H, J=15.7Hz, sp^2-CH); 6.17 (*d*, 1H, J=16.1Hz, Fc-CH); 7.11 (*d*, 2H, J=8.8Hz, arom-H); 7.17 (*d*, 2H, J=8.8Hz, arom-H); 7.33-7.65 (*m*, 9H, arom-H). Anal. calc. for $C_{44}H_{50}FeO_3$: C 77.41 H 7.38; found: C 76.70 H 7.32.

7.2.2.16. 6-Nonamethylferrocenyl-5-hexenoic acid (4-biphenyl-4'-hydroxy) ester (22)

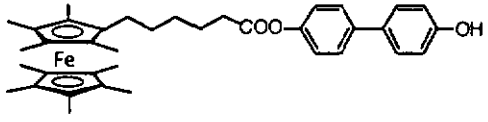

6-Nonamethylferrocenyl-5-hexenoic acid (4-biphenyl-4'-hydroxy) ester (22) is synthesised from compound 21. It is prepared using the standard experimental procedure for deprotection. Amounts used: 21 4 g (5.85 mmol); Pd/C 0.4 g; CH_2Cl_2 100 ml. Recrystallisation from hexane-EtOH. Yield: 2.9 g (4.88 mmol, 83%). mp. 181°C. $R_f(CH_2Cl_2)$=0.21 ^{1}H-NMR (200 MHz, d_6-acetone): δ 1.34-1.44 (*m*, 6H, CH_2); 1.67-1.71 (*m*, 27H, Cp-CH_3); 2.24 (*t*, 2H, Cp-CH_2); 2.57 (*t*, 2H, CH_2-CO_2); 6.94 (*d*, 2H, J=8.8Hz, arom-H); 7.12 (*d*, 2H, J=8.8Hz, arom-H); 7.51 (*d*, 2H, J=8.8Hz, arom-H); 7.63 (*d*, 2H, J=8.8Hz, arom-H).

7.2.2.17. Compounds 24-27

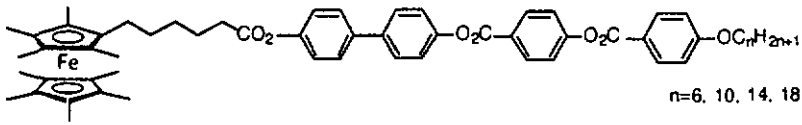

Compounds **24-27** are synthesised from 6-nonamethylferrocenyl-5-hexenoic acid (4-biphenyl-4'-hydroxy) ester (**22**) and the corresponding 4-alkyloxybenzoic acid-4-carboxyphenyl esters (alkyl=hexyl, decyl, tetradecyl or octadecyl) **23a-d**. They are prepared using the standard experimental procedure for esterification.

Characterisation and experimental details for compound **27**, (n=18): Amounts used: 6-Nonamethylferrocenyl-5-hexenoic acid (4-biphenyl-4'-hydroxy) ester (**22**) 3.56 g (5.98 mmol); 4-octadecyloxybenzoic acid-4-carboxyphenyl ester (**23d**) 3.05 g (5.98 mmol); DCC 1.23 g (5.98 mmol); Ppy 0.088 g (0.598 mmol). **Yield**: 4.1 g (3.77 mmol, 63%). Recrystallisation from EtOH-CH_2Cl_2. **27**. R_f (CH_2Cl_2)=0.73. ^{1}H-NMR (200 MHz, $CDCl_3$): δ 0.89 (*t*, CH_3, 3H); 1.28 (*m*, 38H, CH_2); 1.50 (*m*, 27H, Fc-CH_3); 1.81 (*m*, 2H, O-CH_2-CH_2); 2.59 (*t*, 2H, O_2C-CH_2); 4.07 (*t*, 2H, O-CH_2); 7.00 (*d*, 2H, J=8.8Hz, arom-H); 7.17 (*d*, 2H, J=8.8Hz, arom-H); 7.31 (*d*, 2H, J=8.8Hz, arom-H); 7.39 (*d*, 2H, J=8.8Hz, arom-H); 7.60 (*d*, 2H, J=8.8Hz, arom-H); 7,64 (*d*, 2H, J=8.8Hz, arom-H); 8.17 (*d*, 2H, J=8.8Hz, arom-H); 8.31 (*d*, 2H, J=8.8Hz, arom-H).

Table 7.1. *Elemental analyses of compounds*

compound	*n*	*formula*	*MW*	*%C (calc.)*	*% H (calc.)*	*%C (found)*	*% H (found)*
24	6	$C_{57}H_{66}FeO_7$	918.99	74.49	7.24	74.36	7.24
25	10	$C_{61}H_{74}FeO_7$	975.09	75.14	7.65	75.14	7.66
26	14	$C_{65}H_{82}FeO_7$	1031.20	75.71	8.01	75.86	7.95
27	18	$C_{69}H_{90}FeO_7$	1087.31	76.22	8.34	76.26	8.38

7.2.2.18. Compounds 24(a-b)-27(a-c)

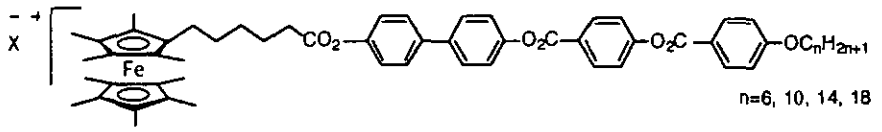

X = OTs, OTf, $C_3F_7CO_2$

The ferrocene derivatives 24-27 are oxidised with different silver salts (silver tosylate, silver triflate, silver heptafluorobutyrate). Tosylate and triflate salts crystallise well whereas the heptafluorobutyrate salts sometimes have to be recrystallised twice in order to obtain satisfying microanalytical data. The standard experimental procedures for these oxidations are depicted in Chapter 7.2.1.4. Whether or not the compounds crystallise well the yields of all products are between 37-81%. All compounds are recrystallised from AcOEt.

Table 7.2. *Elemental analyses of compounds*

com-pound	X^-	*n*	*formula*	*MW*	%C *(calc.)*	%H *(calc.)*	%C *(found)*	%H *(found)*
24a	OTs	6	$C_{64}H_{73}FeO_{10}S$	1090.19	70.51	6.75	70.07	6.86
24b	$C_3F_7CO_2$	6	$C_{69}H_{82}F_7FeO_9$	1244.24	66.60	6.64	66.72	6.68
25a	OTs	10	$C_{68}H_{81}FeO_{10}$	1146.29	71.25	7.12	71.17	7.32
25b	$C_3F_7CO_2$	10	$C_{65}H_{74}F_7FeO_9$	1188.14	65.71	6.28	65.46	6.34
25c	OTf	10	$C_{62}H_{74}F_3FeO_{10}S$	1124.17	66.24	6.63	66.11	6.69
26a	OTs	14	$C_{72}H_{89}FeO_{10}$	1262.40	71.92	7.46	71.76	7.47
26b	$C_3F_7CO_2$	14	$C_{61}H_{66}F_7FeO_9$	1132.03	64.72	5.88	64.58	5.80
26c	OTf	14	$C_{66}H_{82}F_3FeO_{10}S$	1180.28	67.16	7.00	67.09	6.89
27a	OTs	18	$C_{76}H_{97}FeO_{10}$	1258.51	72.53	7.77	72.42	7.92
27b	$C_3F_7CO_2$	18	$C_{73}H_{90}F_7FeO_9$	1300.35	67.43	6.98	67.29	7.03
27c	OTf	18	$C_{70}H_{90}F_3FeO_{10}S$	1236.39	68.00	7.34	67.93	7.33

Table 7.3. *Experimental details of compounds 24-27(a-c)*

Synthesis of compound	*Amounts used Starting ferrocene*			*Amounts used Oxidant (AgX)*			*Yield Product*		
		mg	*mmol*		*mg*	*mmol*	*mg*	*mmol*	*%*
24a	24	200	0.217	AgOTs	60	0.217	140	0.134	62
24b	24	200	0.217	$AgO_2CC_3F_7$	69	0.217	130	0.108	50
25a	25	200	0.205	AgOTs	57	0.205	100	0.084	41
25b	25	200	0.205	$AgO_2CC_3F_7$	65	0.205	90	0.076	37
25c	25	200	0.205	AgOTf	52	0.205	120	0.111	54
26a	26	200	0.194	AgOTs	54	0.194	190	0.157	81
26b	26	200	0.194	$AgO_2CC_3F_7$	62	0.194	130	0.116	60
26c	26	200	0.194	AgOTf	49	0.194	170	0.145	75
27a	27	500	0.459	AgOTs	128	0.459	330	0.266	58
27b	27	200	0.184	$AgO_2CC_3F_7$	59	0.184	130	0.099	54
27c	27	200	0.184	AgOTf	47	0.184	160	0.132	72

7.2.2.19. 10-(4-benzyloxy-phenoxy)-decan-1-ol (28) [80]

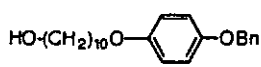

A solution of monobenzyloxy hydroquinone ether (10 g, 0.049 mol, 1 eq.), potassium carbonate (14.8 g, 0.147 mol, 3 eq.), and 1-bromodecanol (11.6 g, 0.049 mol, 1 eq.) in DMF (200 ml) is heated at 120°C for 3 h. After cooling to r.t. insoluble potassium carbonate is filtered off and the solvent is evaporated. The crude product is recrystallised from heptane and 10-(4-benzyloxy-phenoxy)-decan-1-ol (28) is isolated as a colourless powder. Yield: 14.3 g (0.04 mol, 82%). m.p. 94°C. $R_f(CH_2Cl_2)$=0.16. ^{1}H-NMR (200 MHz, $CDCl_3$): δ 0.1.32 (*m*, 12H, CH_2); 1.57 (*q*, 2H, CH_2-CH_2-OH); 1.76 (*q*, 2H, CH_2-CH_2-OPh); 3.65 (*t*, 2H, HO-CH_2); 3.91 (*t*, 2H, CH_2-O-Ph); 5.02 (*s*, 2H, Bn-CH_2); 6.81-6.94 (*m*, 4H, arom-H); 7.35-7-43 (*m*, 5H, arom-H). Anal. calc. for $C_{23}H_{32}O_3$ (356.50): C 77.49 H 9.05; found: C 77.43 H 9.16.

7.2.2.20. 6-Nonamethylferrocenyl-5-hexenoic acid (1-decyl-10 (1'-phenyloxy-4'-benzoyl)) ester (29)

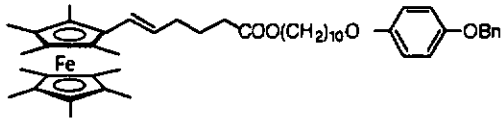

6-Nonamethylferrocenyl-5-hexenoic acid (1-decyl-10 (1'-phenyloxy-4'-benzoyl) ester (**29**) is synthesised from compound **13** and compound **28**. It is prepared using the standard experimental procedure for esterification. Amounts used: 6-(1',2,2',3,3'4,4',5,5' Nonamethylferrocenyl)-5-hexenoic acid (**13**) 3 g (7.07 mmol, 1 eq.); 10-(4-benzyloxy-phenoxy)-decan-1-ol (**28**) 2.77 g (7.78 mmol, 1.1 eq.); DCC 1.6 g (7.78 mmol, 1.1 eq.); Ppy 115 mg (0.778 mmol); CH_2Cl_2 160 ml. Recrystallisation from EtOH-CH_2Cl_2. Yield: 4.77 g (6.25 mmol, 88%). mp. 45°C. $R_f(CH_2Cl_2)$=0.68. ^{1}H-NMR (200 MHz, $CDCl_3$): δ 1.32 (*m*, 12H, CH_2); 1.49 (*s*, 15H, Fc-CH_3); 1.56 (*s*, 6H, Fc-CH_3); 1.63 (*s*, 6H, Fc-CH_3); 1.76 (*quint*, 4H, O-CH_2-CH_2); *q*, 2H, sp^2-CH_2); 2.36 (*t*, 2H, O_2C-CH_2); 3.91 (*t*, 2H, O-CH_2); 4.08 (*t*, 2H, O-CH_2); 5.02 (*s*, 2H, Ar-CH_2); 5.65-5.94 (*m*, 2H, sp^2-CH); 6.81-6.94 (*m*, 4H, arom-H); 7.32-7.46 (*m*, 5H, arom-H). Anal. calc. for $C_{48}H_{66}FeO_4$ (762.89): C 75.57 H 8.72; found: C 75.63 H 8.86.

7.2.2.21. 6-Nonamethylferrocenyl hexanoic acid (1-decyl-10 (1'-phenyloxy-4'-hydroxy)ester (30)

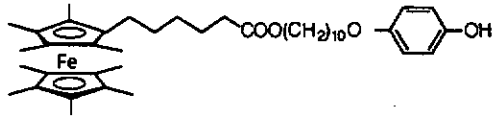

6-Nonamethylferrocenyl hexanoic acid (1-decyl-10 (1'-phenyloxy-4'-hydroxy) ester (**30**) is synthesised from compound **29**. It is prepared using the standard experimental procedure for deprotection. Amounts used: **29** 4.77 g (6.25 mmol); Pd/C 0.5 g, CH_2Cl_2 250 ml. Recrystallisation from hexane. Yield: **4** g (5.945 mmol, 88%). mp. 53°C. $R_f(CH_2Cl_2)$=0.19 ^{1}H-NMR (200 MHz, d_6-acetone): δ 1.45 (*m*, 18H, CH_2); 1.60 - 1.73 (*m*, 6H, CH_2); 1.62 (*m*, 27H, Fc-CH_3); 2.27 (*t*, 2H, O_2C-CH_2); 3.89 (*t*, 2H, O-CH_2); 4.03 (*t*, 2H, O-CH_2); 6.75 (*s*, 4H, arom-H). Anal. calc. for $C_{41}H_{62}FeO_4$ (674.78): C 72.97 H 9.26; found: C 73.16 H 9.57.

7.2.2.22. Compound 31

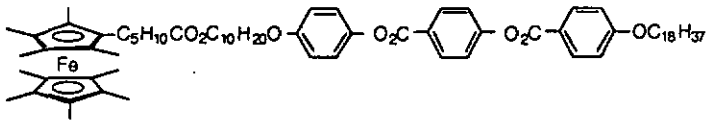

Compound 31 is synthesised from compound 30 and 4-octadecyloxybenzoic acid-4-carboxyphenyl ester (23d). It is prepared using the standard experimental procedure for esterification. Amounts used: 30 4 g (5.945 mmol, 1 eq.); 4-octadecyloxybenzoic acid-4-carboxyphenyl ester (23d) 3.63 g (7.13 mmol, 1.2 eq.); DCC 1.47 g (7.13 mmol, 1.2 eq.); Ppy 105 mg (0.713 mmol); CH_2Cl_2 150 ml. Recrystallisation from EtOH-CH_2Cl_2. Yield: 3.5 g (2.99 mmol, 50%). $R_f(CH_2Cl_2)$=0.89. ^{1}H-NMR (200 MHz, $CDCl_3$): δ 0.89 (*t*, 3H, CH_3); 1.27 (*m*, CH_2) and 1.32 (*m*, CH_2) (∑54H); 1.57 (*s*, 27H; Cp-CH_3); 1.80 (*m*,2H, CH_2); 2.29 (*t*, 2H, CH_2-CO_2); 3.97 (*t*, 2H, O-CH_2); 4.06 (*t*, 4H, CO_2 and O-CH_2); 6.93 (*d*, 2H, J=8.8Hz, arom-H); 6.99 (*d*, 2H, J=8.8Hz, arom-H); 7.13 (*d*, 2H, J=8.8Hz, arom-H); 7.36 (*d*, 2H, J=8.8Hz, arom-H); 8.16 (*d*, 2H, J=8.8Hz, arom-H); 8.27 (*d*, 2H, J=8.8Hz, arom-H). Anal. calc. for $C_{73}H_{106}FeO_8$ (1167.48): C 75.10 H 9.15; found: C 75.24 H 9.26.

7.2.2.23. Compounds 31a-g

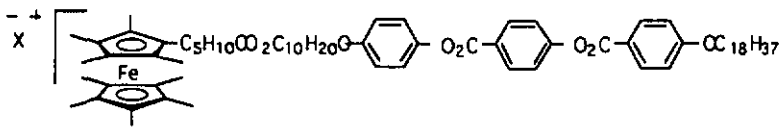

X=OTs, OTf, CF_3CO_2, $C_2F_5CO_2$, $C_3F_7CO_2$ TCNQ, TCNE

The ferrocene derivative 31 is oxidised by different oxidants (silver tosylate, silver triflate, silver trifuoroacetate, silver pentafluoropropionate, silver heptafluorobutyrate, TCNE, TCNQ) to give the corresponding ferrocenium-derivatives. The standard experimental procedures for these oxidations are depicted in Chapter 7.2.1.4. Compounds 31a-e are recrystallised from AcOEt. The charge-transfer salts 31f and 31g are not purified by column chromatography but recrystallised from hexane.

Table 7.4. *Elemental analyses of compounds*

com-pound	*anion*	*formula*	*MW*	*%C (calc.)*	*%H (calc.)*	*%C (found)*	*%H (found)*
31a	OTs	$C_{80}H_{113}FeO_{11}S$	1338.68	71.78	8.51	71.49	8.63
31s	OTf	$C_{74}H_{106}F_3FeO_{11}S$	1316.56	67.51	8.11	67.34	8.43
31c[c]	CF_3CO_2	$C_{75}H_{106}F_3FeO_{10}$	1280.50	70.35	8.34	67.96	8.58
31d[c]	$C_2F_5CO_2$	$C_{76}H_{106}F_5FeO_{10}$	1330.51	68.61	8.03	67.30	8.33
31e[c]	$C_3F_7CO_2$	$C_{77}H_{106}F_7FeO_{10}$	1380.52	66.99	7.74	65.07	7.86
31f	$TCNQ^{\cdot-}$[a]	$C_{85}H_{110}FeN_4O_8$	1371.68	74.43	8.08	74.28	8.01
31g	$TCNE^{\cdot-}$[b]	$C_{79}H_{106}FeN_4O_8$	1295.59	73.24	8.25	72.72	8.38

[a] TCNQ: (N-analysis: calc.: 4.09, found: 4.26); [b] TCNE (N-analysis: calc.: 4.33, found: 3.63); [c] Elemental analysis of compounds are not correct probably due to some amount of AcOEt in the final product, as indicated by DSC measurements.

Table 7.5. *Experimental details of compounds 31(a-g)*

Syn-thesis of com-pound	*Amounts used Compound 31*		*Amounts used Oxidant*			*Yield Product*		
	mg	mmol		mg	mmol	mg	mmol	%
31a	500	0.428	AgOTs	107	0.428	420	0.316	74
31b	200	0.171	AgOTf	44	0.171	180	0.140	82
31c	200	0.171	AgO_2CCF_3	38	0.171	90	0.0735	43
31d	200	0.171	$AgO_2CC_2F_5$	46	0.171	130	0.103	60
31e	200	0.171	$AgO_2CC_3F_7$	55	0.171	120	0.089	52
31f	100	0.0856	TCNQ	17	0.0856	70	0.0522	61
31g	100	0.0856	TCNE	11	0.0856	80	0.0659	77

7.2.2.24. 4-Hydroxy-benzoic acid 4'-decyloxy-biphenyl-4-yl ester (33)

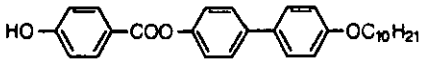

4-Hydroxy-benzoic acid 4'-decyloxy-biphenyl-4-yl ester (33) [74] is synthesised from compound 75. It is prepared using the standard experimental procedure for deprotection. Amounts used: Compound 75 3.0 g (5.58 mmol); Pd/C 30 mg; CH_2Cl_2 250 ml. Recrystallisation from hexane. Yield: 1.36 g (3.04 mmol, 52%). $R_f(CH_2Cl_2)$=0.60. **^{1}H-NMR** (200 MHz, $CDCl_3$): δ 0.89 (*s*, 3H, CH_3); 1.28 (*m*, 14H, CH_2); 1.84 (*q*, 2H, CH_2); 4.00 (*t*, 2H, CH_2); 5.57 (*s*, 1H, OH); 7.00 (*m*, 4H, arom-H); 7.29 (*d*, 2H, arom-H); 7.58 (*m*, 4H, arom-H); 8.19 (*d*, 2H, arom-H). Anal. calc. for $C_{29}H_{34}O_4$ (446.58): C 78.00 H 7.67; found: C 77.92 H 7.65.

7.2.2.25. Compound 34

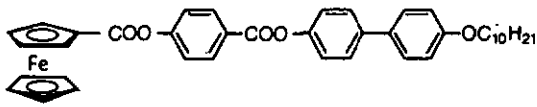

Compound 34 is synthesised from ferrocenecarboxylic acid (32) and 4-hydroxy-benzoic acid 4'-decyloxy-biphenyl-4-yl ester (33). It is prepared using the standard experimental procedure for esterification. Amounts used: Ferrocenecarboxylic acid (100 mg, 0.400 mmol); 4-hydroxy-benzoic acid 4'-decyloxy-biphenyl-4-yl ester (33) (178 mg, 0.400 mmol); DCC (82 mg, 0.400 mmol); PPy (cat. amount); CH_2Cl_2 (20 ml). Recrystallisation from EtOH-CH_2Cl_2. Yield: 190 mg (0.288 mmol, 72%). $R_f(CH_2Cl_2)$=0.88. **^{1}H-NMR** (200 MHz, $CDCl_3$): δ 0.89 (*t*, 3H, CH_3); 1.28-1.56 (*m*, 14H, CH_2); 1.81 (*q*, 2H, CH_2); 4.01 (*t*, 2H, CH_2); 4.35 (*s*, 5H, Cp-H); 4.56 (*s*, 2H, Cp-H); 5.00 (*s*, 2H, Cp-H); 6.98 (*d*, 2H, arom-H), 7.21-7.40 (*m*, 4H, arom-H); 7.51-7.67 (*m*, 4H, arom-H); 8.30 (*d*, 2H, arom-H). Anal. calc. for $C_{40}H_{42}FeO_5$ (658.61): C 72.95 H 6.43; found: C 72.90 H 6.48.

7.2.2.26. Compound 36

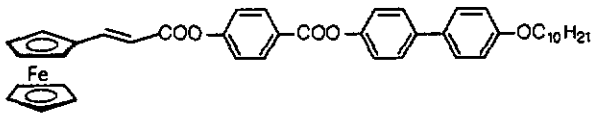

Compound **36** is synthesised from 3-ferrocenyl-2-propenoic acid (35)[81] and 4-hydroxy-benzoic acid 4'-decyloxy-biphenyl-4-yl ester (**33**). It is prepared using the standard experimental procedure for esterification. Amounts used: 3-Ferrocenyl-2-propenoic acid (**35**) (115 mg, 0.448 mmol); 4-hydroxy-benzoic acid 4'-decyloxy-biphenyl-4-yl ester (**33**) (200 mg, 0.448 mmol); DCC (92 mg, 0.448 mmol); PPy (cat. amount); CH_2Cl_2 (20 ml). Recrystallisation from EtOH-CH_2Cl_2. Yield: 155 mg (0.226 mmol,51%). $R_f(CH_2Cl_2)$=0.60. ^{1}H-NMR (200 MHz, $CDCl_3$): δ 0.89 (*t*, 3H, CH_3); 1.28-1.56 (*m*, 14H, CH_2); 1.81 (*q*, 2H, CH_2); 4.01 (*t*, 2H, CH_2); 4.24 (*s*, 5H, Cp-H); 4.52 (*s*, 2H, Cp-H); 4.59 (*s*, 2H, Cp-H); 6.22 (*d*, 1H, J^1_{trans}=15.9 Hz); 6.98 (*d*, 2H, arom-H); 7.26 (*d*, 2H, arom-H); 7.34 (*d*, 2H, arom-H); 7.52 (*d*, 2H, arom-H); 7.60 (*d*, 2H, arom-H); 7.82 (*d*, 1H, J^1_{trans}=15.9 Hz); 8.29 (*d*, 2H, arom-H). Anal. calc. for $C_{42}H_{44}FeO_5$ (684.65): C 73.68 H 6.48; found: C 73.68 H 6.36.

7.2.2.27. Compound 37

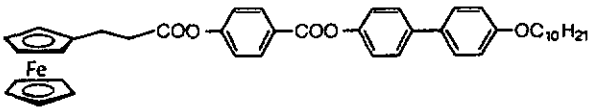

Compound **37** is synthesised from compound **36**. It is prepared using the standard experimental procedure for hydrogenation. Amounts used: **36** 100 mg (0.146 mmol); Pd/C 15 mg; CH_2Cl_2-EtOH (1:1) 16 ml. Recrystallisation from EtOH-CH_2Cl_2. Yield: 60 mg (0.087 mmol, 60%). $R_f(CH_2Cl_2)$=0.79. ^{1}H-NMR (200 MHz, $CDCl_3$): δ 0.89 (*t*, 3H, CH_3); 1.28-1.56 (*m*, 14H, CH_2); 1.81 (*q*, 2H, CH_2); 2.50-2.92 (*m*, 4H, CH2-CH2); 4.01 (*t*, 2H, CH_2); 4.15-4.55 (*m*, 9H, Cp-H); 6.98 (*d*, 2H, arom-H); 7.26 (*d*, 2H, arom-H); 7.34 (*d*, 2H, arom-H); 7.52 (*d*, 2H, arom-H); 7.60 (*d*, 2H, arom-H); 8.29 (*d*, 2H, arom-H). Anal. calc. for $C_{42}H_{46}FeO_5$ (686.68): C 73.74 H 6.75; found C 73.31 H 6.74.

7.2.2.28. Compound 38

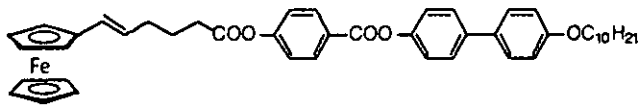

Compound **38** is synthesised from compound **17** and 4-hydroxy-benzoic acid 4'-decyloxy-biphenyl-4-yl ester (**33**). It is prepared using the standard experimental procedure for esterification. Amounts used: 6-Ferrocenyl-5-hexenoic acid (**17**) (82 mg, 0.336 mmol); 4-hydroxy-benzoic acid 4'-decyloxy-biphenyl-4-yl ester (**33**) (150 mg, 0.336 mmol); DCC (69 mg, 0.336 mmol); CH_2Cl_2 (10 ml). Recrystallisation from EtOH-CH_2Cl_2. Yield: 120 mg (0.165 mmol, 49%). $R_f(CH_2Cl_2)$=0.75. ^{1}H-NMR (200 MHz, $CDCl_3$): 0.89 (*t*, 3H, CH_3); 1.28-1.56 (*m*, 14H, CH_2); 1.81 (*q*, 2H, CH_2); 4.01 (*t*, 2H, CH_2); 4.21 (*s*, 5H, cp-H); 4.35 (*s*, 2H, cp-H); 4.47 (*s*, 2H, cp-H); 5.36-5.70 (*m*, 1H, sp^2-CH, cis+trans); 6.10 (*m*, 1H, sp^2-CH, cis+trans); 6.98 (*d*, 2H, arom-H); 7.25 (*m*, 4H, arom-H); 7.53 (*d*, 2H, arom-H); 7.58 (*d*, 2H, arom-H); 8:25 (*d*, 2H, arom-H). Elem. anal. of $C_{45}H_{50}FeO_5$ (726.73): calc.: C 74.37 H 6.93; found: C 74.25 H 6.94.

7.2.2.29. Compound 39

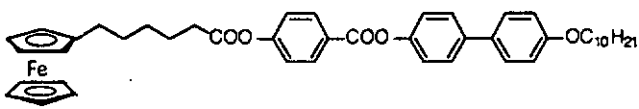

Compound **39** is synthesised from compound **38**. It is prepared using the standard experimental procedure for hydrogenation. Amounts used: **38** (100 mg, 0.138 mmol); Pd/C (20 mg); CH_2Cl_2-EtOH (1:1, 20 ml). Recrystallisation from EtOH-CH_2Cl_2. Yield: 80 mg (0.110 mmol, 80%). $R_f(CH_2Cl_2)$=0.82. ^{1}H-NMR (200 MHz, $CDCl_3$): δ 0.89 (*t*, 3H, CH_3); 1.28-1.62 (*m*, 18H, CH_2); 1.81 (*m*, 4H, CH_2); 3.00 (*m*, 2H, CH_2); 2.61 (*t*, 2H, CH_2); 4.01 (*t*, 2H, CH_2); 4.15-4.55 (*m*, 9H, Cp-H); 6.98 (*d*, 2H, arom-H); 7.26 (*d*, 2H, arom-H); 7.34 (*d*, 2H, arom-H); 7.52 (*d*, 2H, arom-H); 7.60 (*d*, 2H, arom-H); 8.29 (*d*, 2H, arom-H). Anal. calc. for $C_{45}H_{52}FeO_5$ (728.75): C 74.17 H 7.19; found: C 73.87 H 7.13.

7.2.2.30. Compound 40

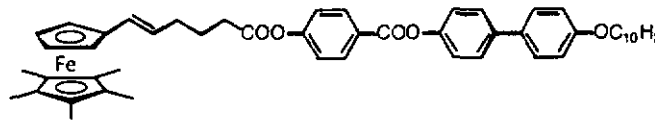

Compound **40** is synthesised from pentamethylferrocene hexenoic acid (**15**) and 4-hydroxy-benzoic acid 4'-decyloxy-biphenyl-4-yl ester (**33**). It is prepared using the standard experimental procedure for esterification. Amounts used: 6-(1,2,3,4,5-Pentamethylferrocenyl)-5-hexenoic acid (**15**) (82 mg, 0.224 mmol); 4-hydroxy-benzoic acid 4'-decyloxy-biphenyl-4-yl ester (**33**) (80 mg, 0.179 mmol); DCC (46 mg, 0.224 mmol); PPy (cat. amount), CH_2Cl_2 (8 ml). Yield: 100 mg (0.125 mmol, 56%). $R_f(CH_2Cl_2)$=0.79. **^{1}H-NMR** (200 MHz, $CDCl_3$): δ 0.89 (*t*, 3H, CH_3); 0.90-1.65 (*m*, 15H, Cp-CH_3); 1.28-1.56 (*m*, 14H, CH_2); 1.81 (*q*, 2H, CH_2); 3.65-4.25 (*m*, 4H, Cp-H); 4.01 (*t*, 2H, CH_2); 5.36-5.70 (*m*, 1H, sp^2-CH, *cis* and *trans*); 6.10 (*m*, 1H, sp^2-CH, *cis* and *trans*); 6.98 (*d*, 2H, arom-H); 7.25 (*m*, 4H, arom-H); 7.53 (*d*, 2H, arom-H); 7.58 (*d*, 2H, arom-H); 8:25 (*d*, 2H, arom-H).

7.2.2.31. Compound 41

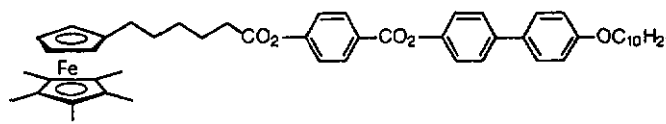

Compound **41** is synthesised from compound **40**. It is prepared using the standard experimental procedure for hydrogenation. Amounts used: **40** (85 mg, 0.107 mmol); Pd/C (20 mg); CH_2Cl_2-EtOH (1:1, 20 ml). Recrystallisation from EtOH-CH_2Cl_2. Yield: 50 mg (0.063 mmol, 59%). $R_f(CH_2Cl_2)$=0.82. **^{1}H-NMR** (200 MHz, d_6-acetone): δ 0.89 (*t*, 3H, CH_3); 1.28-1.62 (*m*, 18H, CH_2); 1.81 (*m*, 4H, CH_2); 1.87 (*s*, 15H, Cp-CH_3); 2.29 (*t*, 2H, CH_2); 2.64 (*t*, 2H, CH_2); 3.53 (*t*, 2H, Cp-H); 3.58 (*t*, 2H, Cp-H); 4.06 (*t*, 2H, CH_2); 7.04 (*d*, 2H, arom-H); 7.33 (*d*, 2H, arom-H); 7.37 (*d*, 2H, arom-H); 7.62 (*d*, 2H, arom-H); 7.70 (*d*, 2H, arom-H); 8.25 (*d*, 2H, arom-H). Anal. calc. for $C_{50}H_{62}FeO_5$ (798.89): C 75.17 H 7.82; found: C 75.39 H 7.68.

7.2.2.32. Compound 41a

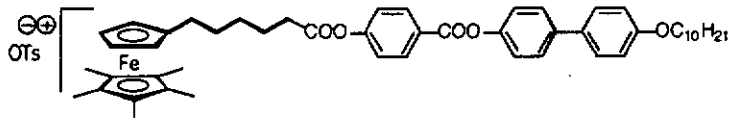

Compound 41a is synthesised from compound 41. It is prepared using the standard experimental procedure for oxidation. Amounts used: Compound 41 (100 mg, 0.125 mmol); AgOTs (32 mg, 0.113 mmol); CH_2Cl_2-acetone (1:1) (30 ml). Recrystallisation from AcOEt. Yield: 60 mg (0.0618 mmol, 55%). Anal. calc. for $C_{57}H_{69}FeO_8S$ (970.08): C 70.57 H 7.17; found: C 68.38 H 7.21. No correct microanalytical data was obtained. Furthermore, when heated, DSC measurements revealed decomposition in the liquid-crystalline state. This displays the moderate thermal stability of compound 41a and could be the reason that recrystallisation from AcOEt (bp.: 77°C) did not give an analytically pure material.

7.2.2.33. Compound 42

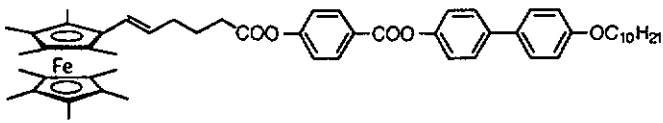

Compound 42 is synthesised from nonamethylferrocene hexenoic acid (13) and 4-hydroxy-benzoic acid 4'-decyloxy-biphenyl-4-yl ester (33). It is prepared using the standard experimental procedure for esterification. Amounts used: Nonamethylferrocene hexenoic acid (13) 1.52 g (1.778 mmol); 4-hydroxy-benzoic acid 4'-decyloxy-biphenyl-4-yl ester (33) 1.60 g (1.778 mmol); DCC 0.74 g (1.778 mmol); Ppy 53 mg (0.356 mmol, 0.2 eq.); CH_2Cl_2 60 ml. Recrystallisation from EtOH-CH_2Cl_2. Yield: 1.09 g (1.28 mmol, 72%). $R_f(CH_2Cl_2)$=0.74. ^{1}H-NMR (200 MHz, CD_2Cl_2): δ 0.89 (*t*, 3H, CH_3); 1.65 (*s*, 15H, Cp-CH_3); 1.71 (*s*, 6H, Cp-CH_3); 1.80 (*s*, 6H, Cp-CH_3); 1.92 (*quint*, 2H, CH_2); 2.28 (*quint*, 2H, CH_3); 2.68 (*t*, 2H, CH_2); 4.00 (*t*, 2H, O-CH_2); 5.69 (*dt*, 1H, sp^2-C-H, J=16.1 Hz); 6.10 (*d*, 1H, sp^2-C-H, J=16.1 Hz); 6.98 (*d*, 2H, arom-H); 7.26 (*d*, 4H, arom-H); 7.54 (*d*, 2H, arom-H); 7.62 (*d*, 2H, arom-H); 8.23 (*d*, 2H, arom-H). Anal. calc. for $C_{54}H_{72}FeO_5$ (852.97): C 76.04 H 8.04; found: C 76.09 H 8.07.

7.2.2.34. Compound 43

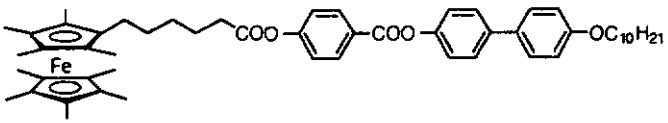

Compound **43** is synthesised from compound **42**. It is prepared using the standard experimental procedure for hydrogenation. Amounts used: **42** 1.09 g (1.28 mmol), Pd/C 100 mg; CH_2Cl_2-EtOH 120 ml. Recrystallisation from EtOH-CH_2Cl_2. Yield: 875 mg (1.02 mmol, 80%). $R_f(CH_2Cl_2)$=0.78. **^{1}H-NMR** (200 MHz, CD_2Cl_2): δ 0.98 (*m*, 30H, CH_3); 1.23 (*m*, 20H, CH_2); 1.80 (*m*, 4H, CH_2); 2.62 (*t*, 2H, OCO-CH_2); 4.00 (*t*, 2H, O-CH_2); 7.98 (*d*, 2H, arom-H); 7.26 (*d*, 4H, arom-H); 7.55 (*d*, 2H, arom-H); 7.62 (*d*, 2H, arom-H); 8.23 (*d*, 2H, arom-H). **IR** (KBr): 2924(s), 2853(s), 1761(s), 1737(s), 1500(s), 1274(s), 1206(s), 1163(s). **UV-Vis** (CH_2Cl_2): 230 (32182), 264 (27025). **FAB-MS**: 854(100), 713(9), 501(17), 338(48), 325(55). Anal. calc. for $C_{54}H_{70}FeO_5$ (854.99): C 75.86 H 8.25; found: C 75.83 H 8.18.

7.2.2.35. Compound 43a

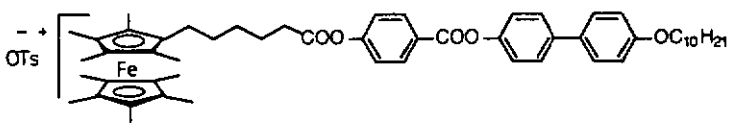

Compound **43a** is synthesised from compound **43**. It is prepared using the standard experimental procedure for oxidation. Amounts used: Compound **43** 400 mg (0.467 mmol); AgOTs 130 mg, (0.467 mmol); CH_2Cl_2-acetone (1:1) 50 ml. Recrystallisation from AcOEt. Yield: 407 mg (0.397 mmol, 85%). **UV-Vis** (CH_2Cl_2): 230(25732), 274(40707), 782(310). **FAB-MS**: 854(100), 713(11), 338(78), 325(89). Anal. calc. for $C_{61}H_{77}FeO_8S$ (1026.19): C 71.40 H 7.56; found C 71.53 H 7.52.

7.2.2.36. Compounds 45 and 46

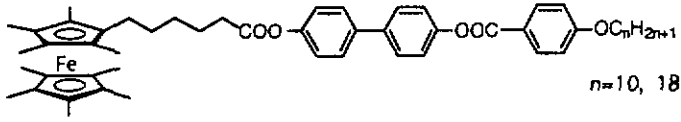

Compounds **45** and **46** are synthesised from 6-nonamethylferrocenyl-5-hexenoic acid (4-biphenyl-4'-hydroxy) ester (**22**) and corresponding 4-alkoxy benzoic acid **44**. They are prepared using the standard experimental procedure for esterification.

Amounts used: Characterisation and synthetic procedure for compound **45** (n=10): 6-Nonamethylferrocenyl-5-hexenoic acid (4-biphenyl-4'-hydroxy) ester (**22**) 180 mg (0.303 mmol); 4-decyloxy benzoic acid (**44**) 79 mg (0.303 mmol); DCC 62 mg (0.303 mmol); Ppy (cat. amount); CH_2Cl_2 20 ml. Recrystallisation from acetone. Yield: 178 mg (0.209 mmol, 69%). $R_f(CH_2Cl_2)$=0.85. **^{1}H-NMR** (200 MHz, $CDCl_3$): δ 0.89 (*t*, 3H, CH_3); 1.30 (*m*, 20H, CH_2); 1.66 (*s*, 27H, Cp-CH_3); 1.84 (*m*, 2H, CH_2); 2.18 (*m*, 2H, CH_2); 2.58 (*t*, 2H, O_2-CH_2); 4.06 (*t*, 2H, O-CH_2); 6.98 (*d*, 2H, arom-H); 7.15 (*d*, 2H, arom-H); 7.28 (*d*, 2H, arom-H); 7.59 (*d*, 2H, arom-H); 7.61 (*d*, 2H, arom-H); 8.17 (*d*, 2H, arom-H).

7.2.2.37. Compounds 45a and 46a

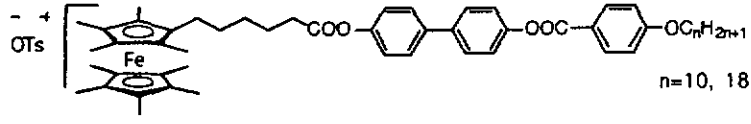

The ferrocene derivatives **45** and **46** are oxidised with silver tosylate according to the standard experimental procedure for oxidation. The oxidised products are recrystallised from AcOEt.

Table 7.6. *Elemental analyses of compounds*

compound	*n*	*anion*	*formula*	*MW*	*%C (calc.)*	*%H*	*%C (found)*	*%H*
45	10	-	$C_{54}H_{70}FeO_5$	854.99	75.86	8.25	75.81	8.25
45a	10	OTs	$C_{61}H_{77}FeO_8S$	1026.19	71.40	7.56	71.24	7.62
46	18	-	$C_{62}H_{86}FeO_5$	967.20	76.99	8.96	76.95	9.09
46a	18	OTs	$C_{69}H_{93}FeO_8S$	1138.40	72.80	8.23	72.89	8.45

Table 7.7. *Experimental details of compounds* **45a** *and* **46a**

Synthesis of compound	*Amounts used Starting ferrocene*			*Amounts used Oxidant (AgX)*			*Yield Product*		
		mg	mmol		mg	mmol	mg	mmol	%
45a	**45**	120	0.140	AgOTs	39	0.140	130	0.125	89
46a	**46**	120	0.124	AgOTs	35	0.124	110	0.100	81

7.2.2.38. Compound 49

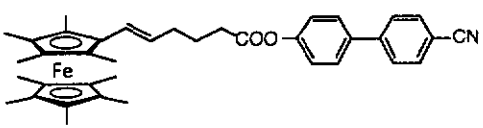

Compound **49** is synthesised from compound **13** and 4-hydroxy-4'-cyanobiphenyl (**47**). It is prepared using the standard experimental procedure for esterification. Amounts used: 6-(1',2,2',3,3'4,4',5,5'Nonamethylferrocenyl)-5-hexenoic acid (**13**) 100 mg (0.235 mmol); 4-hydroxy-4'-cyanobiphenyl (**47**) 46 mg (0.235 mmol); DCC 48 mg (0.235 mmol); Ppy (cat. amount); CH_2Cl_2 20 ml. Recrystallisation from EtOH-CH_2Cl_2. Yield: 89 mg (0.148 mmol, 63%). ^{1}H-NMR (200 MHz, $CDCl_3$): δ 1.66 (*s*, 15H, Cp-CH_3); 1.72 (*s*, 6H, Cp-CH_3); 1.82 (*s*, 6H, Cp-CH_3); 2.33 (*m*, 4H, CH_2); 2.75 (*t*, 2H, CH_2); 6.74 (*dt*, 1H, sp^2-C-H); 6.17 (*d*, 1H, sp^2-C-H); 7.27 (*d*, 2H, arom-H), 7.78 (*d*, 2H, arom-H); 7.88 (*s*, 4H, arom-H). Anal. calc. for $C_{38}H_{43}FeNO_2$ (601.61): C 75.87 H 7.20 N 2.33; found: C 75.84 H 7.22 N 2.10.

7.2.2.39. Compound 50

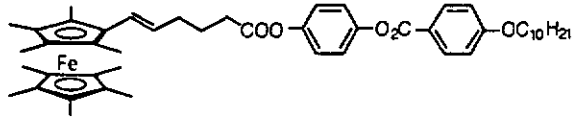

Compound **50** is synthesised from compound **13** and 4-hydroxyphenyl 4(decyloxy) benzoate (**48**). It is prepared using the standard experimental procedure for esterification. Amounts used: 6-(1',2,2',3,3'4,4',5,5'-Nonamethyl ferrocenyl)-5-hexenoic acid (**13**) 120 mg (0.283 mmol); 4-hydroxyphenyl 4(decyloxy) benzoate (**48**) 105 mg (0.283 mg); DCC 58 mg (0.283 mg); Ppy (cat. amount); CH_2Cl_2 30 ml. Recrystallisation from EtOH-CH_2Cl_2. Yield: 132 mg (0.169 mmol, 60%). ^{1}**H-NMR** (200 MHz, $CDCl_3$): δ 0.89 (*t*, 3H, CH_3); 1.29 (*m*, 16H, CH_2); 1.69 (*s*, 15H, Cp-CH_3); 1.73 (*s*, 6H, Cp-CH_3); 1.83 (*s*, 6H, Cp-CH_3); 1.91 (*m*, 2H, CH_2); 2.28 (*m*, 2H, CH_2); 2.64 (*t*, 2H, O_2C-CH_2); 4.05 (*t*, 2H, O-CH_2); 5.71 (*dt*, 1H, J=16.1Hz, sp^2-C-H); 6.10 (*d*, 1H, J=16.1Hz, sp^2-C-H); 7.02 (*d*, 2H, arom-H); 7.14 (*m*, 4H, arom-H); 8.14 (*d*, 2H, arom-H).

7.2.2.40. Compound 51

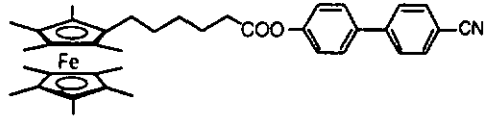

Compound **51** is synthesised from compound **49**. It is prepared using the standard experimental procedure for reduction. Amounts used: **49** 80 mg (0.133 mmol); Pd/C 10 mg; CH_2Cl_2 20 ml. Recrystallisation from EtOH-CH_2Cl_2. Yield: 63 mg (0.105 mmol, 79%). ^{1}**H-NMR** (200 MHz, $CDCl_3$): δ 1.67 (*s*, 15H, Cp-CH_3); 1.69 (*s*, 6H, Cp-CH_3); 1.72 (*s*, 6H, Cp-CH_3); 2.10 (*m*, 4H, CH_2, covered by residual solvent peak); 2.25 (*m*, 4H, CH_2); 2.60 (*t*, 2H, CO_2-CH_2); 7.24 (*d*, 2H, arom-H), 7.78 (*d*, 2H, arom-H); 7.89 (*s*, 4H, arom-H). EI-MS(70 eV): 603 (M^+, 100), 409 (9), 325 (21), 195 (71). Anal. calc. for $C_{38}H_{45}FeNO_2$ (603.33): C 75.61 H 7.51 N 2.32; found: C 75.64 H 7.57 N 2.01.

7.2.2.41. Compound 52

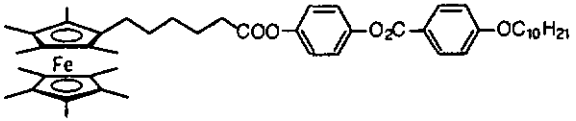

Compound 52 is synthesised from compound 50. It is prepared using the standard experimental procedure for reduction. Amounts used: 50 100 mg (0.129 mmol); Pd/C 10 mg; CH_2Cl_2 20 ml. Recrystallisation from EtOH-CH_2Cl_2. Yield: 67 mg (0.086 67%). ^{1}H-NMR (200 MHz, $CDCl_3$): δ 0.89 (*t*, 3H, CH_3); 1.29 (*m*, 16H, CH_2), 1.56 (*m*, 27H, Cp-CH_3); 1.83 (*m*, 4H, CH_2); 2.58 (*q*, 2H, CH_2); 4.05 (*t*, 2H, O-CH_2); 6.96 (*d*, 2H, arom-H); 7.20 (*m*, 4H, arom-H); 8.13 (*d*, 2H, arom-H). Anal. calc. for $C_{48}H_{66}FeO_5$ (778.99): C 74.02 H 8.54; found: C 74.01 H 8.43.

7.2.2.42. Compound 52a

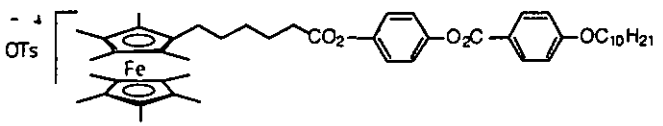

Compound 52 is oxidised with silver tosylate according to the standard experimental procedure for oxidation. Amounts used: Compound 52 100 mg (0.128 mmol); AgOTs 36 mg (0.128 mmol); CH_2Cl_2-acetone (1:1) 15 ml. Recrystallisation from acetone. Yield: 76 mg (0.083 mmol, 65%). Anal. calc. for $C_{52}H_{73}FeO_8S$ (914.03): C 68.03 H 8.05; found: C 69.30 H 7.64.

7.2.2.43. Compound 53

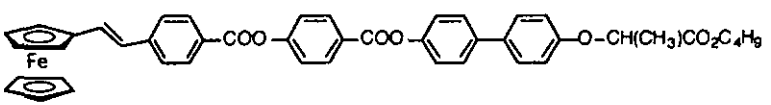

Compound 53 is synthesised from 1-ferrocenyl-2-(4'-carboxyphenyl)ethylene (18) and phenol derivative 57. It is prepared using the standard experimental procedure for esterification. Amounts used: 1-Ferrocenyl-2-(4'-carboxyphenyl) ethylene (18) 180 mg (0.542 mmol); compound 57 235 mg (0.542 mg); DCC 111

mg (0.542 mmol); Ppy (cat. amount); CH_2Cl_2 50 ml. Recrystallisation from EtOH. Yield: 267 mg (0.357 mmol, 66%). $R_f(CH_2Cl_2)$=0.74. ^{1}H-NMR (200 MHz, $CDCl_3$): δ 0.89 (*t*, 3H, CH_3); 1.30 (*quint*, 2H, CH_2); 1.65 (*m*, 2H, CH_2); 1.66 (*d*, 3H, J=6.9Hz, CH_3); 4.18 (*s*, 5H, Cp-H); 4.20 (*t*, 2H, O-CH_2); 4.37 (*t*, 2H, J=1.9Hz, Cp-H); 4.53 (*t*, 2H, J=1.9Hz, Cp-H); 4.82 (*q*, 1H, J=6.9Hz, C*-H); 6.76 (*d*, 1H, J=16.1Hz, sp^2-CH); 6.96 (*d*, 2H, arom-H); 7.10 (*d*, 1H, J=16.1Hz, sp^2-CH); 7.28 (*d*, 2H, arom-H); 7.41 (*d*, 2H, arom-H); 7.51 (*d*, 2H, arom-H); 7.56 (*d*, 2H, arom-H); 7.59 (*d*, 2H, arom-H); 8.17 (*d*, 2H, arom-H); 8.32 (*d*, 2H, arom-H). Anal. calc. for $C_{54}H_{40}FeO_7$ (748.65): C 72.19 H 5.39; found: C 72.09 H 5.40.

7.2.2.44. Compound 54

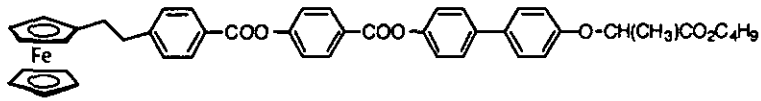

Compound 54 is synthesised from compound 53. It is prepared using the standard experimental procedure for hydrogenation. Amounts used: 53 240 mg (0.319 mmol); Pd/C 20 mg; CH_2Cl_2 40 ml. Recrystallisation from EtOH. Yield: 129 mg (0.173 mmol, 54%). $R_f(CH_2Cl_2)$=0.76. ^{1}H-NMR (200 MHz, $CDCl_3$): δ 0.89 (*t*, 3H, CH_3); 1.30 (*quint*, 2H, CH_2); 1.65 (*m*, 2H, CH_2); 1.66 (*d*, 3H, J=6.9Hz, CH_3); 2.72 (*m*, 2H, Fc-CH_2-CH_2-Ph); 2.92 (*m*, 2H, Fc-CH_2-CH_2-Ph); 4.06 (*t*, 2H, Cp-H); 4.08 (*t*, 2H, Cp-H); 4.13 (*t*, 5H, Cp-H); 4.19 (*m*, 2H, O-CH_2); 4.81 (*q*, 1H, J=6.6Hz, C*-H); 6.96 (*d*, 2H, arom-H); 7.28 (*d*, 2H, arom-H); 7.40 (*d*, 2H, arom-H); 7.51 (*d*, 2H, arom-H); 7.59 (*d*, 2H, arom-H); 8.14 (*d*, 2H, arom-H); 8.31 (*d*, 2H, arom-H). Anal. calc. for $C_{45}H_{42}FeO_7$ (750.67): C 72.00 H 5.64; found: C 71.91 H 5.74.

7.2.2.45. Compound 55

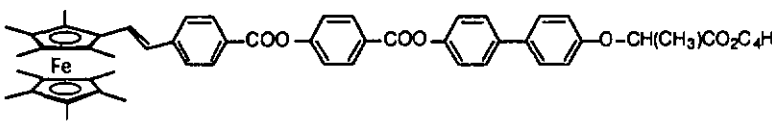

Compound 55 is synthesised from 1-nonamethylferrocenyl-2-(4'-carboxy phenyl)ethylene (19) and phenol derivative 57. It is prepared using the standard experimental procedure for esterification. Amounts used: 1-

Nonamethyl ferrocenyl-2-(4'-carboxy phenyl)ethylene (19) 275 mg (0.6 mmol); 57 250 mg (0.57 mmol); DCC 120 (0.58 mmol); Ppy 11 mg (0.07 mmol); CH_2Cl_2 20 ml. Recrystallisation from EtOH. Yield: 406 mg (0.464 mmol, 81%). mp: 146°C. $R_f(CH_2Cl_2/AcOEt\ 9:1)=0.88$. ^{1}H-NMR ($d_6$-acetone, 200 MHz): δ 0.89 (*t*, 3H, CH_2-CH_3); 1.36 (*m*, 2H, CH_2-CH_3); 1.59 (*d*, 3H, CH_3-CH, J=6.6Hz); 1.68 (*s*, 15H, Fc-CH_3); 1.80 (*s*, 6H, Fc-CH_3); 1.99 (*s*, 6H, Fc-CH_3); 4.16 (*m*, 2H, COO-CH_2); 4.16 (*m*, 2H, COO-CH_2); 4.94 (*q*, 1H, CH); 6.82 (*d*, 1H; sp^2-CH); 6.99 (*d*, 2H, arom-H); 7.18 (*d*, 1H, sp^2-CH); 7.37 (*d*, 2H, arom-H); 7.54 (*d*, 2H, arom-H); 8.14 (*d*, 2H, arom-H); 8.30 (*d*, 2H, arom-H). EI-MS: 875 (M^+, 100), 846 (18), 413 (20), 135 (36). Anal. calc. for $C_{54}H_{58}FeO_7$ (874.97): C 74.12 H 6.69; found: 74.17 H 6.75.

7.2.2.46. Compound 56

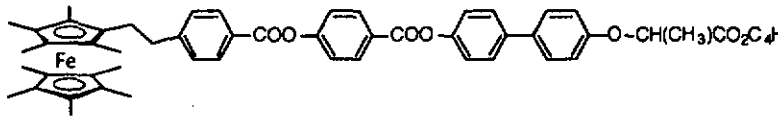

Compound 56 is synthesised from compound 55. It is prepared using the standard experimental procedure for hydrogenation. Amounts used: 55 250 mg (0.28 mmol); Pd/C 25 mg; CH_2Cl_2-EtOH (5:1) 12 ml. Recrystallisation from EtOH. Yield: 190 mg (0.217 mmol, 76%). mp: 166°C. $R_f(CH_2Cl_2/AcOEt\ 9:1)=0.88$. ^{1}H-NMR ($d_6$-acetone, 200 MHz): δ 0.89 (*t*, 3H, CH_2-CH_3); 1.36 (*m*, 2H, CH_2-CH_3); 1.59(*d*, 3H, J=6.9Hz CH_3-*CH); 1.66 (*s*, 21H, Cp-CH_3); 1.70 (*s*, 6H, CH_3); 2.59 (*t*, 2H, CH_2); 2.70 (*t*, 2H, CH_2); 4.16 (*m*, 2H, CO_2-CH_2); 4.94 (q, 1H, *CH); 6.99 (*d*, 2H, arom-H); 7.37 (*m*, 4H, arom-H); 7.53 (*m*, 6H, arom-H); 8.09 (*d*, 2H, arom-H), 8.30 (*d*, 2H, arom-H). Anal. calc. for $C_{54}H_{60}O_7Fe$ (876.99): C 73.96 H 6.90; found: C 74.09 H 6.88.

7.2.2.47. Compound 57

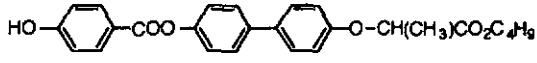

Compound 57 is synthesised from compound 76. It is prepared using the standard experimental procedure for deprotection. Amounts used: 76 1.92 g (3.6 mmol); Pd/C 190 mg; CH_2Cl_2-EtOH (4:1) 40 ml. Recrystallisation from EtOH-hexane. Yield: 1.31 g (3.0 mmol, 80%). $R_f(CH_2Cl_2$-AcOEt 2:1)=0.68. ^{1}H-NMR (200

MHz, $CDCl_3$): δ 0.90 (*t*, 3H, CH_2-CH_3); 1.35 (*m*, 2H, CH_2-CH_3); 1.65 (*d*, 3H, CH_3-*CH, J=6.9Hz), 4.19 (*m*, 2H, CO_2-CH_2); 4.80 (*q*, 1H, *CH); 6.86 (*d*, 2H, arom-H); 6.93 (*d*, 2H, arom-H); 7.20 (*d*, 2H, arom-H); 7.47 (*d*, 2H, arom-H); 7.55 (*d*, 2H, arom-H); 8.08(*d*, 2H, arom-H). **EI-MS** (70eV): 434 (M^+, 12), 314 (68), 213 (9), 185 (100), 121 (45), 93 (10). Anal. calc. for $C_{26}H_{26}O_6$ (434.52): C 71.86 H 6.04; found: C 71.83 H 5.89.

7.2.2.48. Compound 59

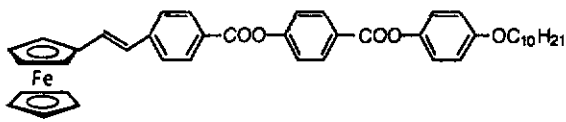

Compound 59 is synthesised from 1-ferrocenyl-2-(4'-carboxyphenyl)ethylene (18) and 58d. It is prepared using the standard experimental procedure for esterification. Amounts used: 1-Ferrocenyl-2-(4'-carboxyphenyl)ethylene (18) 200 mg (0.602 mmol); 4-(decyloxy)phenyl 4-hydroxy benzoate (58d) 224 mg (0.602 mmol); DCC 124 mg (0.602 mmol); Ppy (cat. amount); CH_2Cl_2 50 ml. Recrystallisation from EtOH-CH_2Cl_2. Yield: 228 mg (0.421 mol, 70%). R_f(CH_2Cl_2)=0.82. **^{1}H-NMR** (200 MHz, $CDCl_3$): δ 0.90 (*t*, 3H, CH_3); 1.29 (*m*, 14H, CH_2); 1.81 (*quint*, 2H, O-CH_2-CH_2); 3.97 (*t*, 2H, O-CH_2); 4.16 (*s*, 5H, Cp-H); 4.37 (*t*, 2H, J=1.8Hz, Cp-H); 4.51 (*t*, 2H, J=1.8Hz, Cp-H); 6.76 (*d*, 1H, J=16.1Hz, sp^2-CH); 6.94 (*d*, 2H, arom-H); 7.08 (*d*, 1H, J=16.1Hz, sp^2-CH); 7.14 (*d*, 2H, arom-H); 7.39 (*d*, 2H, arom-H); 7.57 (*d*, 2H, arom-H); 8.17 (*d*, 2H, arom-H); 8.30 (*d*, 2H, arom-H).

7.2.2.49. Compound 60

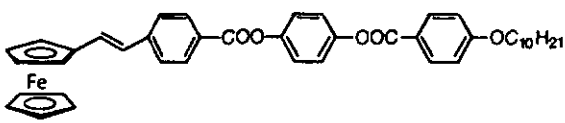

Compound 60 is synthesised from 1-ferrocenyl-2-(4'-carboxyphenyl)ethylene (18) and 48 according to the standard experimental procedure for esterification. Amounts used: 1-Ferrocenyl-2-(4'-carboxyphenyl)ethylene (18) 200 mg (0.602 mmol); 4-hydroxyphenyl (4-decyloxy) benzoate (48) 224 mg (0.602 mmol); DCC 124 mg (0.602 mmol); Ppy (cat. amount); CH_2Cl_2 50 ml. Recrystallisation from

EtOH-CH_2Cl_2. Yield: 292 mg (0.427 mmol, 71%). $R_f(CH_2Cl_2)$=0.79. ^{1}H-NMR (200 MHz, $CDCl_3$): δ 0.89 (*t*, 3H, CH_3); 1.29 (*m*, 14H, CH_2); 1.82 (*quint*, 2H, O-CH_2-CH_2); 4.01(*t*, 2H, O-CH_2); 4.17 (*s*, 5H, Cp-H); 4.36 (*t*, 2H, J=1.8Hz, Cp-H); 4.52 (*t*, 2H, J=1.8Hz, Cp-H); 6.76 (*d*, 1H, J=16.1Hz, sp^2-CH); 6.98 (*d*, 2H, arom-H); 7.08 (*d*, 1H, J=16.1Hz, sp^2-CH); 7.28 (*d*, 4H, arom-H); 7.55 (*d*, 2H, arom-H); 8.16 (*d*, 4H, arom-H).

7.2.2.50. Compound 61

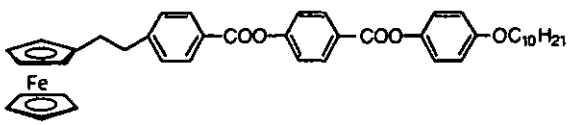

Compound 61 is synthesised from compound 59. It is prepared using the standard experimental procedure for hydrogenation. Amounts used: 59 150 mg (0.22 mmol); Pd/C 15 mg; CH_2Cl_2 20 ml. Recrystallisation from EtOH-CH_2Cl_2. Yield: 125 mg (0.183 mmol, 83%). $R_f(CH_2Cl_2)$=0.80. ^{1}H-NMR (200 MHz, $CDCl_3$): δ 0.90 (*t*, 3H, CH_3); 1.29 (*m*, 14H, CH_2); 1.80 (*quint*, 2H, O-CH_2-CH_2); 2.71 (*m*, 2H, CH_2); 2.93 (*m*, 2H, CH_2); 3.98 (*t*, 2H, O-CH_2); 4.06 (*t*, 2H, Cp-H); 4.07 (*t*, 2H, Cp-H); 4.13 (*t*, 5H, Cp-H); 6.94 (*d*, 2H, arom-H); 7.13 (*d*, 2H, arom-H); 7.33 (*d*, 2H, arom-H); 7.37 (*d*, 2H, arom-H); 8.14 (*d*, 2H, arom-H); 8.29 (*d*, 2H, arom-H).

7.2.2.51. Compound 62

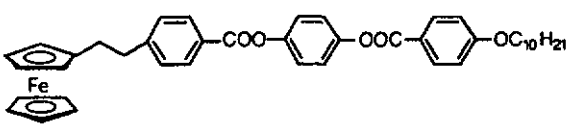

Compound 62 is synthesised from compound 60. It is prepared using the standard experimental procedure for hydrogenation. Amounts used: 60 150 mg (0.22 mmol); Pd/C 15 mg; CH_2Cl_2 20 ml. Recrystallisation from EtOH-CH_2Cl_2. Yield: 111 mg (0.163 mmol, 74%). $R_f(CH_2Cl_2)$=0.82. ^{1}H-NMR (400 MHz, $CDCl_3$): δ 0.89 (*t*, 3H, CH_3); 1.29 (*m*, 14H, CH_2); 1.80 (*quint*, 2H, O-CH_2-CH_2); 2.71 (*m*, 2H, CH_2); 2.91 (*m*, 2H, CH_2); 4.01 (*t*, 2H, O-CH_2); 4.06 (*m*, 4H, Cp-H); 4.13 (*m*, 5H, Cp-H); 6.98 (*d*, 2H, arom-H); 7.27 (*m*, 4H, arom-H); 7.31 (*d*, 2H, arom-H); 8.12 (*d*, 2H, arom-H); 8.15 (*d*, 2H, arom-H).

Table 7.8. *Elemental analyses of compounds*

compound	*formula*	*MW*	*%C (calc.)*	*%H (calc.)*	*%C (found)*	*%H (found)*
59	$C_{42}H_{44}FeO_5$	684.65	73.68	6.48	73.77	6.39
60	$C_{42}H_{44}FeO_5$	684.65	73.68	6.48	73.74	6.51
61	$C_{42}H_{46}FeO_5$	686.67	73.47	6.75	73.56	6.71
62	$C_{42}H_{46}FeO_5$	686.67	73.47	6.75	73.44	6.84

7.2.2.52. Compound 63

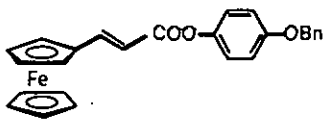

Compound 63 is synthesised from 3-ferrocenyl-2-propenoic acid [81] and hydroquinone monobenzylether. It is prepared using the standard experimental procedure for esterification. Amounts used: 3-Ferrocenyl-2-propenoic acid (2.0 g, 7.81 mmol); hydroquinone monobenzylether (1.72 g, 8.59 mmol); DCC (1.77 g, 8.59 mmol); Ppy (127 mg, 0.859 mmol). CH_2Cl_2 (140 ml). Recrystallisation from EtOH-CH_2Cl_2. Yield: 2.77 mg (6.33 mmol, 81%). mp. 122°C. $R_f(CH_2Cl_2)$=0.88. ^{1}H-NMR (200 MHz, $CDCl_3$): δ 4.21 (*s*, 5H, Cp-H); 4.47 (*s*, 2H, Cp-H); 4.56 (*s*, 2H, Cp-H); 5.07 (*s*, 2H, CH_2); 6.21 (*d*, 1H, sp^2-CH, J=15.7Hz); 7.03 (*m*, 4H, arom-H); 7.35-7.50 (*m*, 5H, arom-H); 7.75 (*d*, 1H, sp^2-CH, J=15.7Hz).

7.2.2.53. Compound 64

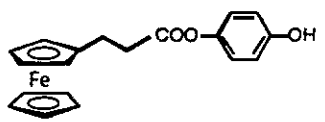

Compound 64 is synthesised from compound 63. It is prepared using the standard experimental procedure for deprotection. Amounts used: 63 (2.77 g, 6.33 mmol); Pd/C (0.3 g); CH_2Cl_2-EtOH (1:1) 300 ml. Recrystallisation from EtOH-hexane. Yield: 1.9 g (5.43 mmol, 86%). mp.: 133°C. $R_f(CH_2Cl_2)$=0.19. ^{1}H-NMR (200 MHz, $CDCl_3$): δ 2.77 (*m*, 4H, CH_2); 4.21 (*m*, 9H, Cp-H); 5.49 (*s*, 1H,

OH); 6.73 (*d*, 2H, arom-H); 6.89 (*d*, 2H, arom-H). Anal. calc. for $C_{19}H_{18}FeO_3$ (350.20): C 65.17 H 5.18; found: C 64.75 H 5.42.

7.2.2.54. Compound 65

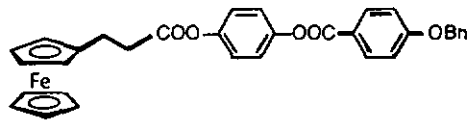

Compound 65 is synthesised from compound 64 and 4-benzoyl benzoic acid. It is prepared using the standard experimental procedure for esterification. Amounts used: 64 (1.9 g, 5.43 mmol); hydroquinone monobenzylether (1.08 g, 5.43 mmol), DCC (1.12 g, 5.43 mmol); Ppy (80 mg, 0.54 mmol); CH_2Cl_2 (100 ml). Recrystallisation from EtOH-CH_2Cl_2. Yield: 1.52 g (2.715 mmol, 50%). mp. 155°C. ^{1}H-NMR (200 MHz, $CDCl_3$): δ 2.79 (*s*, 4H, Fc-$(CH_2)_2$-Ph); 4.33 (*s*, 9H, Cp-H); 5.17 (*s*, 2H, CH_2-Bn); 7.03-7.25 (*m*, 8H, arom-H); 7.36-7.44 (*m*, 3H, arom-H); 8.15 (*d*, 2H, arom-H).

7.2.2.55. Compound 66

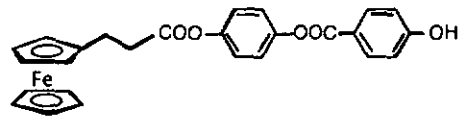

Compound 66 is synthesised from compound 65. It is prepared using the standard experimental procedure for deprotection. Amounts used: 65 (1.52 g, 2.715 mmol; Pd/C (150 mg); CH_2Cl_2 (100 ml). Recrystallisation from EtOH-hexane. Yield: 1.0 g (2.145 mmol, 79%). mp. 153°C. ^{1}H-NMR (200 MHz, $CDCl_3$): δ 2.75 (*s*, 4H, Fc-$(CH_2)_2$-Ph); 4.26 (*s*, 9H, Cp-H); 5.70 (*s*, 1H, OH); 6.85 (*d*, 2H, arom-H); 7.07 (*d*, 2H, arom-H); 7.23 (*d*, 2H, arom-H); 8.09 (*d*, 2H, arom-H).

7.2.2.56. · Compounds 67a-e

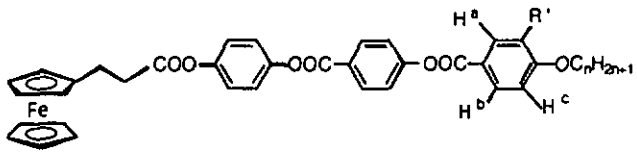

Compounds 67a-e are synthesised from compound 66 and the corresponding 4-alkoxybenzoic acid **44**. They are prepared using the standard experimental procedure for esterification.

Characterisation and synthetic procedure for compound 67c, (n=10, R'=H):
Amounts used: Compound 66 123 mg (0.262 mmol); 4-decyloxybenzoic acid (**44c**) 73 mg (0.262 mmol); DCC 54 mg (0.262 mmol); Ppy (cat. amount); CH_2Cl_2 (15 ml). Recrystallisation from EtOH-CH_2Cl_2. Yield: 115 mg (0.157 mmol, 60%). $R_f(CH_2Cl_2)$=0.52. ^{1}H-NMR (400 MHz, CD_2Cl_2): δ 0.89 (*t*, 3H, CH_3); 1.29 (*m*, 14H, CH_2); 1.83 (*q*, 2H, O-CH_2-CH_2); 2.81 (*m*, 4H, Fc-CH_2 and OCO-CH_2); 4.04-4.11 (*m*, 4H, Cp-H); 4.16 (*s*, 5H, Cp-H); 7.01 (*d*, 2H, arom-H); 7.15 (*d*, 2H, arom-H); 7.25 (*d*, 2H, arom-H); 7.39 (*d*, 2H, arom-H); 8.15 (*d*, 2H, arom-H); 8.27 (*d*, 2H, arom-H).

7.2.2.57. Compound 67f

Compound **67f** is synthesised from compound 66 and 3,4-ditetradecyloxy benzoic acid (**44f**). It is prepared using a procedure similar to that described for compound 67c.
$R_f(CH_2Cl_2)$=0.67. ^{1}H-NMR (200 MHz, $CDCl_3$): δ 0.90 (*t*, 6H, CH_3); 1.28 (*m*, 40H, CH_2); 1.84 (*m*, 4H, O-CH_2-CH_2); 2.80 (*s*, 4H, Fc-CH_2-CH_2-Ar); 4.10 (*m*, 4H, O-CH_2); 6.95 (*d*, 1H, J=8.8Hz, H^c); 7.14 (*d*, 2H, arom-H); 7.24 (*d*, 2H, arom-H); 7.37 (*d*, 2H, arom-H); 7.67 (*d*, 1H, J=2.2Hz, H^a); 7.83 (*d d*, 1H, J=8.8Hz, J=2.2Hz, H^b); 8.27 (*d*, 2H, arom-H).

Table 7.9. *Elemental analyses of compounds*

compound	*n*	*R'=*	*formula*	*MW*	*%C (calc.)*	*%H (calc.)*	*%C (found)*	*%H (found)*
67a	5	H	$C_{38}H_{36}FeO_7$	660.54	69.10	5.49	69.11	5.37
67b	7	H	$C_{40}H_{40}FeO_7$	688.60	69.77	5.85	69.82	5.58
67c	10	H	$C_{43}H_{46}FeO_7$	730.68	70.68	6.35	70.44	6.49
67d	14	H	$C_{47}H_{54}FeO_7$	686.78	71.75	6.92	71.74	6.74
67e	18	H	$C_{51}H_{62}FeO_7$	842.89	72.69	7.41	72.65	7.33
67f	14	$OC_{14}H_{29}$	$C_{61}H_{82}FeO_8$	999.16	73.33	8.27	73.29	8.30

7.2.2.58. Compounds 68a and 68b

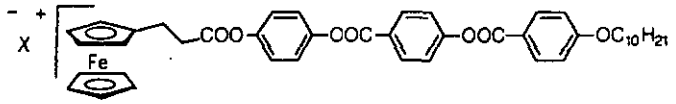

X = DDQ, I_3

Compound 68a (anion = I_3^-)

Compound 67c (100 mg, 0.137 mmol, 1 eq.) is dissolved in a mixture of benzene and hexane (8:2) and a solution of I_2 (54 mg, 0.233 mmol, 1.7 eq.) in benzene (5 ml) is added dropwise. The solution is poured onto hexane (50 ml) and the product and filtered off. The crude product is washed with hexane and recrystallised from nitromethane. Yield: 74 mg (1.102 mmol, 74%). mp. 150°C (dec.).

Compound 68b (anion=DDQ$^-$)

Compound 67c (100 mg, 0.137 mmol) is dissolved in CH_2Cl_2 (10 ml) and a solution of DDQ (31 mg, 0.137 mmol) in hexane (20 ml) is added dropwise. The solution immediately turns black. The precipitate is filtered off and washed with hexane. The crude product is recrystallised from hexane-acetone (1:1). Yield: 105 mg (0.110 mmol, 80%). mp. 134°C (dec.).

Table 7.10. *Elemental analyses of compounds*

compound	*formula*	*MW*	*%C*	*%H*	*%N*	*%C*	*%H*	*%N*
				(calc.)			*(found)*	
68a	$C_{43}H_{46}O_7FeI_3$	1111.39	46.47	4.17	-	46.36	4.04	-
68b	$C_{51}H_{46}Cl_2FeN_2O_9$	957.69	63.96	4.84	2.93	63.90	4.90	3.20

7.2.2.59. Disubstituted Ferrocenes (Compounds 72a-g)

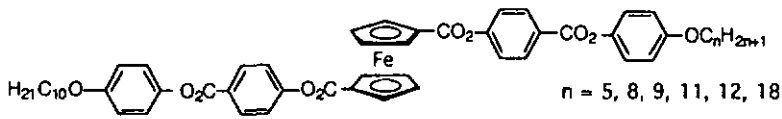

n = 5, 8, 9, 11, 12, 18

The synthetic pathways for the synthesis of compounds **69**, **58**, **70** and **71** are well established and can be depicted from the literature [50].

Characterisation and synthetic procedure for compound **52a**:
A solution of the acid chloride **71** (100 mg, 0.155 mmol), 4(pentyloxy)phenyl 4-hydroxy-benzoate (**58a**) (46 mg, 0.155 mmol) and NEt_3 (16 mg, 2 drops, 0.155 mmol) in CH_2Cl_2 (10 ml) is heated under reflux for 90 min. The solvent is evaporated and the residue is projected to column chromatography (CH_2Cl_2-AcOEt 50:1, 1x40 cm). The product is eluted and recrystallised from CH_2Cl_2-EtOH (3:4). **Yield**: 110 mg (0.121 mmol, 78%). ^{1}**H-NMR** (200 MHz, $CDCl_3$): δ 0.89-0.95 (*m*, 6H, CH_3); 1.28-1.41 (*m*, 18H, CH_2); 1.79 (*q*, 4H, O-CH_2-CH_2); 3.96 (*t*, 4H, o-CH_2); 4.68 (*t*, 4H, Cp-H); 5.11 (*t*, 4H, Cp-H); 6.91 (*d*, 4H, arom-H); 7.10 (*d*, 4H, arom-H); 7.33 (*d*, 4H, arom-H); 8.20 (*d*, 4H, arom-H).

Compounds **72b-72g** are prepared using experimental conditions similar to that described for compound **72a**.

Table 7.11. *Elemental analyses of compounds*

compound	*n*	*formula*	*MW*	*%C (calc.)*	*%H (calc.)*	*%C (found)*	*%H (found)*
72a	5	$C_{53}H_{56}FeO_{10}$	908.86	70.04	6.21	70.03	6.26
72b	8	$C_{56}H_{62}FeO_{10}$	950.94	70.73	6.57	70.56	6.65
72c	9	$C_{57}H_{64}FeO_{10}$	964.97	70.95	6.68	70.85	6.68
72e	11	$C_{59}H_{68}FeO_{10}$	993.02	71.36	6.90	71.27	6.96
72f	12	$C_{60}H_{70}FeO_{10}$	1007.05	71.56	7.00	71.11	7.12
72g	18	$C_{66}H_{82}FeO_{10}$	1091.21	72.65	7.57	72.55	7.60

7.2.2.60. 4-Hydroxy-4'-butyl-2-oxy propionate (74)

4-Benzyloxy-4'-butyl-2-oxy propionate

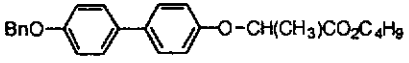

To a solution of 4-benzyloxy-4'-hydroxybiphenyl (10.4 g, 0.038 mol), triphenyl phosphine (9.97 g, 0.038 mol) and 2-hydroxy-propionic acid butyl ester (5.55 g, 0.038 mol) in anhydrous THF (40 ml) is given dropwise a solution of DEAD (40% in toluene; 16.5 g, 0.038 mol) in anhydrous THF (40 ml). The reaction mixture is stirred for 20 h at r.t. After removal of the solvent the residue is suspended in CH_2Cl_2. Insoluble triphenyl phosphine is filtered off and the filtrate is evaporated. The crude product is projected to column chromatography (CH_2Cl_2) and a colourless zone containing the product is eluted. The solvent is evaporated and the product is recrystallised form CH_2Cl_2-EtOH (1:1). Yield: 5.61 g (0.0138 mol, 36%). mp. 87°C. $R_f(CH_2Cl_2)$=0.77. ^{1}H-NMR (200 MHz, $CDCl_3$): δ 0.91 (*t*, 3H, CH_2-CH_3); 1.35 (*m*, 2H, CH_2-CH_3); 1.65 (*d*, 3H, CH_3-*CH, J=6.6Hz); 4.2 (*m*, 2H, CO_2-CH_2); 4.79 (*q*, 1H, *CH. 6.6Hz); 5.12 (*s*, 2H; Bn-CH_2); 6.92-7.07 (*m*, 4H, arom-H), 7.38-7.50 (*m*, 5H, arom-H). Anal. calc. for $C_{26}H_{28}O_4$ (404.50): C 77.20 H 6.98; found: C 77.34 H 7.11.

4-Hydroxy-4'-butyl-2-oxy propianate (74)

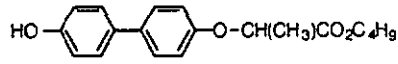

4-Hydroxy-4'-butyl-2-oxy propionate (74) is synthesised from 4-benzyloxy-4'-butyl-2-oxy propionate. It is prepared using the standard experimental procedure for deprotection. Amounts used: 4-Benzyloxy-4'-butyl-2-oxy propionate 5.61 g (0.014 mmol); Pd/C 0.6 g; CH_2Cl_2-EtOH (10:3) 130 ml. Recrystallisation from hexane. Yield: 3.04 g (9.66 mmol, 69%). mp. 108°C. $R_f(CH_2Cl_2)$=0.18. **^{1}H-NMR** (200 MHz, d_6-acetone): δ 0.88 (*t*, 3H, CH_2-CH_3); 1.23 (*m*, 2H, CH_2-CH_3); 1.59 (*d*, 3H, CH_3-*CH, J=6.6Hz); 4.15 (*m*, 2H, CO_2-CH_2); 4.88 (*q*, 1H, *CH; J=6.6Hz); 6.87-6.96 (*m*, 4H, arom-H); 7.41-7.52 (*m*, 4H, arom-H). Anal. calc. for $C_{19}H_{22}O_4$ (314.53): C 72.55 H 7.06; found: C 72.55 H 7.03.

7.2.2.61. Compound 75

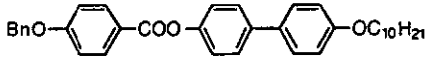

Compound 75 is synthesised from 4-benzyloxy benzoic acid and 4-decyloxy-4'-hydroxy biphenyl (73) [82]. It is prepared using the standard experimental procedure for esterification. Amounts used: 4-benzyloxy benzoic acid 1.71 g (7.49 mmol); 4-decyloxy-4'-hydroxy biphenyl (73) 2.44 (7.49 mmol); DCC 1.54 g (7.49 mmol); Ppy (cat. amount); CH_2Cl_2 60 ml. Recrystallisation from EtOH-hexane. Yield: 3.14 g (5.85 mmol, 78%). $R_f(CH_2Cl_2)$=0.85. **^{1}H-NMR** (200 MHz, $CDCl_3$): δ 0.89 (*s*, 3H, CH_3); 1.28 (*m*, 14H, CH_2); 1.84 (*q*, 2H, CH_2); 4.00 (*t*, 2H, CH_2); 5.18 (*s*, 2H, Bn-CH_2); 6.92-7.65 (*m*, 10H, arom-H); 8.19 (*d*, 2H, arom-H).

7.2.2.62. Compound 76

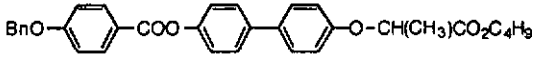

Compound 76 is synthesised from 4-benzyloxy benzoic acid and phenol derivative 74. It is prepared using the standard experimental procedure for esterification. Amounts used: 74 2.59 g (8.2 mmol); 4-benzyloxy benzoic acid 2.19 g (9.6 mmol); DCC 1.98 g (9.6 mmol); Ppy 0.18 g (1.2 mmol); CH_2Cl_2 100 ml.

Recrystallisation from EtOH. Yield: 2.44g (4.65 mmol, 58%). $R_f(CH_2Cl_2)$=0.51. ^{1}H-NMR (200 MHz, $CDCl_3$): δ 0.89 (*t*, 3H, CH_2-CH_3); 1.33 (*m*, 2H, CH_2-CH_3); 1.64 (*d*, 3H, CH_3-*CH, J=6.6Hz); 5.17 (*s*, 2H, Bn-CH_2); 6.93 (*d*, 2H, arom-H); 7.09 (*d*, 2H, arom-H); 7.27 (*d*, 2H, arom-H); 7.38-7.59 (*m*, 9H, arom-H); 8.20 (*d*, 2H, arom-H). EI-MS (70eV): 314 (M^+, 9), 211 (100), 185 (84), 91 (72). Anal. calc. for $C_{33}H_{32}O_6$ (524.65): C 75.55 H 6.15; found: C 75.50 H 6.14.

7.2.2.63. Compound 77

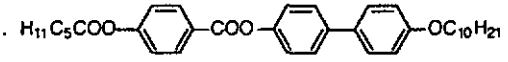

Compound *77* is synthesised from hexanoic acid and **33**. It is prepared using the standard experimental procedure for esterification. Amounts used: 4-Hydroxy-benzoic acid 4'-decyloxy-biphenyl-4-yl ester (**33**) 160 mg (0.358 mmol); hexanoic acid 41 mg (0.358 mg); DCC 74 mg (0.358 mg); Ppy (cat. amount); CH_2Cl_2 20 ml. Recrystallisation from CH_2Cl_2. Yield: 183 mg (0.336 mmol, 94%). $R_f(CH_2Cl_2)$=0.64. ^{1}H-NMR (200 MHz, $CDCl_3$): δ 0.89 (*t*, 3H, CH_3); 0.95 (*t*, 3H, CH_3); 1.29 and 1.79 (*m*, 14H, CH_2); 2.61 (*t*, 2H, O_2C-CH_2); 4.00 (*t*, 2H, O-CH_2); 6.97 (*d*, 2H, arom-H); 7.24 (*d*, 4H, arom-H); 7.49-7.62 (*m*, 4H, arom-H); 8.26 (*d*, 2H, arom-H). Anal. calc. for $C_{35}H_{44}O_5$ (544.73): C 77.17 H 8.14; found C 77.03 H 8.13.

Chapter

8

Literature

1] Deschenaux, R. and Goodby, J.W.G., Ferrocene-Containing Thermotropic Liquid Crystals in *Ferrocenes*, edited by Togni, A. and Hayashi, T.ed. VCH, Weinheim, 1995, p. 471-495

2] R. B. King and M. B. Bisnette, *J. Organomet. Chem.*, 1967, **8**, 287.

3] D. Astruc, *New J. Chem.*, 1992, **16**, 305.

4] H. Schumann, *J. Organomet. Chem.*, 1986, **304**, 341.

5] A. Wiesemann, R. Zentel and G. Lieser, *Acta Polymer.*, 1995, **46**, 25.

6] A. Wiesemann and R. Zentel, *Liquid Crystals*, 1993, **14**, 1925.

7] K. M. w Chi, J. C. Calabrese, W. M. Reiff and J. S. Miller, *Organometallics*, 1991, **10**, 688.

8] G. Wilbert, A. Wiesemann and R. Zentel, *Macromol. Chem. Phys.*, 1995, **196**, 3771.

9] L. Schwink, S. Vettel and P. Konchel, *Organometallics*, 1995, **14**, 5000.

10] H. C. L. Abbenhuis, U. Burckhardt, V. Gramlich, A. Togni, A. Albinati and B. Müller, *Organometallics*, 1994, **13**, 4481.

11] J. S. Miller and P. J. Krusic, *Mol. Cryst. Liq. Cryst.*, 1995, **120**, 27.

12] J. S. Miller, D. T. Glatzhofer, D. O'Hare, W. M. Reiff, A. Chakraborty and A. J. Epstein, *Inorg. Chem.*, 1989, **28**, 2930.

13] J. S. Miller, A. J. Epstein and W. M. Reiff, *Acc. Chem. Res.*, 1988, **21**, 114.

14] J. S. Miller, A. J. Epstein and W. M. Reiff, *Chem. Rev.*, 1988, **88**, 201.

15] J. S. Miller and A. J. Epstein, *Angew. Chem. Int. Ed.*, 1994, **33**, 383.

16] Togni, A., Ferrocene-Containing Charge-Transfer Complexes. Conducting and Magnetic Materials in *Ferrocenes*, edited by Togni, A. and Hayashi, T.ed. VCH, Weinheim, 1995, p. 433-469

17] M. E. Silva, A. J. Pombeiro, J. J. Frausto da Silva, R. Herrmann, N. Deus, T. J. Castilho and M. F. Silva, *J. Organomet. Chem.*, 1991, **421**, 75.

18] M. E. Silva, A. J. Pombeiro, J. J. Frausto da Silva, R. Herrmann, N. Deus and R. E. Bozak, *J. Organomet. Chem.*, 1994, **480**, 81.

19] U. T. Mueller-Westerhoff, T. J. Haas, G. F. Swiegers and T. K. Leipert, *J. Organomet. Chem.*, 1994, 472, 229.

20] Zanello, P., Electrochemical and X-ray Structural Aspects of Transition Metal Complexes Containing Redox-Active Ferrocene Ligands in *Ferrocenes*, edited by Togni, A. and Hayashi, T.ed. VCH, Weinheim, 1995, p. 317-430

21] C. Elschenbroich and A. Salzer. , Weinheim:VCH, 1992.

22] A. Almenningen, A. Haaland and S. Samdal, *J. Organomet. Chem.*, 1979, 173, 293.

23] S. Yu. Ketkov and G. A. Domrachev, *J. Organomet. Chem.*, 1991, 420, 67.

24] D. M. Duggan and D. N. Hendrickson, *Inorg. Chem.*, 1975, 14, 955.

25] D. Vorländer, *Ber. Dt. Chem. Ges.*, 1910, 43, 3120.

26] A. M. Giroud-Godquin and P. M. Maitlis, *Angew. Chem.*, 1991, 103, 370.

27] A. M. Giroud-Godquin and P. M. Maitlis, *Angew. Chem,Int. Ed.*, 1991, 30, 375.

28] P. Espinet, M. A. Esteruelas, L. A. Oro, J. L. Serrano and E. Sola, *Coord. Chem. Rev.*, 1992, 117, 215.

29] A. P. Polishchuk and T. V. Timofeeva, *Russ. Chem. Rev.*, 1993, 62, 291.

30] S. A. Hudson and P. M. Maitlis, *Chem. Rev.*, 1993, 93, 861.

31] F. Neve, *Adv. Mater.*, 1996, 8, 277.

32] H. Tanaka and T. Hongo, *Macromol. Rapid Commun.*, 1996, 17, 91.

33] M. J. Cook, G. Cooke and A. Jafari-Fini, *J. Chem. Soc. ,Chem. Commun.*, 1995, 1715.

34] J. Malthête and J. Billard, *Mol Cryst. Liq. Cryst.*, 1976, 34, 117.

35] R. Deschenaux, M. Rama and J. Santiago, *Tetrahedron Lett.*, 1993, 34, 3293.

36] R. Deschenaux and J. Santiago, *Tetrahedron Lett.*, 1994, 35, 2169.

37] R. Deschenaux, J. Santiago, D. Guillon and B. Heinrich, *J. Mater. Chem.*, 1994, 4, 679.

38] D. Navarro-Rodriguez, Y. Frere, P. Gramain, D. Guillon and A. Skoulios, *Liquid Crystals*, 1991, **9**, 321.

39] E. Bravo-Grimaldo, D. Navarro-Rodriguez, A. Skoulios and D. Guillon, *Liquid Crystals*, 1996, **20**, 393.

40] J. G. Jegal and A. Blumstein, *J. Polym. Sci. ,Polym. Chem. ,Part A*, 1995, **33**, 2673.

41] D. W. Bruce, S. Estdale, D. Guillon and B. Heinrich, *Liquid Crystals*, 1995, **19**, 301.

42] M. Tabrizian, A. Soldera, M. Couturier and C. G. Bazuin, *Liquid Crystals*, 1995, **18**, 475.

43] J. J. H. Nusselder, J. B. F. N. Engberts and H. A. van Doren, *Liquid Crystals*, 1993, **13**, 213.

44] E. J. R. Suedhoelter, J. B. F. N. Engberts and W. H. de Jeu, *J. Phys. Chem.*, 1982, **86**, 1908.

45] C. J. Bowlas, D. W. Bruce and K. R. Seddon, *J. Chem. Soc. ,Chem. Commun.*, 1996, 1625.

46] C. G. Bazuin, D. Guillon, A. Skoulios and J. F. Nicoud, *Liquid Crystals*, 1986, **1**, 181.

47] P. Cheng, A. Blumstein and S. Subramanyam, *Mol. Cryst. Liq. Cryst.*, 1995, **269**, 1.

48] D. W. Bruce, S. C. Davis, D. A. Dunmur, S. A. Hudson, P. M. Maitlis and P. S. Styring, *Mol. Cryst. Liq. Cryst.*, 1992, **215**, 1.

49] D. W. Bruce, D. A. Dunmur, E. Lalinde and P. M. Maitlis, *Nature*, 1986, **323**, 791.

50] R. Deschenaux, J. L. Marendaz and J. Santiago, *Helv. Chim. Acta*, 1993, **76**, 865.

51] R. Deschenaux, I. Kosztics, J. L. Marendaz and H. Stoeckli-Evans, *Chimia*, 1993, **47**, 206.

52] N. J. Thompson, J. W. Goodby and K. J. Toyne, *Liquid Crystals*, 1993, **13**, 381.

53] C. Loubser, C. Imrie and P. H. Rooyen, *Adv. Mater.*, 1993, **5**, 45.

54] C. Imrie and C. Loubser, *J. Chem. Soc. ,Chem. Commun.*, 1994, 2159.

55] K. L. Cunningham and D. R. Mcmillin, *Polyhedron*, 1996, 15, 1673.

56] U. Siemeling, *Chem. Ber.*, 1995, **128**, 1135.

57] E. E. Bunel, L. Valle and J. M. Manriquez, *Organometallics*, 1985, 4, 1680.

58] G. G. A. Balavoine, G. Doisneau and T. Fillebeen-Khan, *J. Organomet. Chem.*, 1991, **412**, 381.

59] R. A. Paciello, J. M. Manriquez and J. E. Bercaw, *Organometallics*, 1990, 9, 260.

60] G. E. Herberich, U. Englert, F. Marken and P. Hofmann, *Organometallics*, 1993, **12**, 4039.

61] P. G. Gassmann, J. W. Mickelson and J. R. Sowa, *J. Am. Chem. Soc.*, 1992, **114**, 6942.

62] R. B. King, W. M. Douglas and A. Efraty, *J. Organomet. Chem.*, 1974, 69, 131.

63] U. Kölle, B. Fuss, F. Khouzami and J. Gersdorf, *J. Organomet. Chem.*, 1985, 290, 77.

64] J. W. Fitch and J. J. Lagowski, *Inorg. Chem.*, 1965, 910.

65] J. C. Smart and C. J. Curtis, *Inorg. Chem.*, 1977, 16, 1788.

66] E. W. Neuse and M. S. Loonat, *J. Organomet. Chem.*, 1985, 286, 329.

67] T. Y. Dong and S. H. Lee, *J. Organomet. Chem.*, 1995, **487**, 77.

68] M. I. Rybinskaya, A. Z. Kreindlin, P. V. Petrovskii, R. M. Minyaev and R. Hoffmann, *Organometallics*, 1994, 13, 3903.

69] A. Z. Kreindlin, E. I. Fedin, P. V. Petrovskii, M. I. Rybinskaya, R. M. Minyaev and R. Hoffmann, *Organometallics*, 1991, 10, 1206.

70] A. Z. Kreindlin, P. V. Petrovskii, M. I. Rybinskaya, A. I. Yanovskii and Yu. T. Struchkov, *J. Organomet. Chem.*, 1987, 319, 229.

71] A. Z. Kreindlin, S. S. Fadeeva and M. I. Rybinskaya, *Izv. Akad. Nauk SSSR, Ser. Khim.*, 1984, 403.

72] A. Z. Kreindlin and M. I. Rybinskaya, *Izv. Akad. Nauk SSSR, Ser. Khim.*, 1982, 174.

73] R. Broos, D. Tavernier and M. Anteunis, *j. Chem. Educ.*, 1978, 55, 813.

74] I. G. Shenouda, Y. Shi and M. E. Neubert, *Mol. Cryst. Liq. Cryst. Sci. Technol. Sect. A*, 1994, 257, 209.

75] A. Hassner and V. Alexanian, *Tetrahedron Lett.*, 1978, 4475.

76] D. Demus, H. Demus and H. Zaschke. *Flüssige Kristalle in Tabellen*, Leipzig:VEB Deutscher Verlag für Grundstoffindustrie, 1974.

77] D. Demus and H. Zaschke. *Flüssige Kristalle in Tabellen II*, Leipzig:VEB Deutscher Verlag für Grundstoffindustrie, 1984.

78] T. A. Kizner, M. A. Mikhaleva and E. S. Serebryakova, *Chem. Heterocycl. Comp. (Engl. Trans.)*, 1991, 27, 313.

79] Y. Sakurai, A. Tamatami, K. Teshima, S. Kusabayshi and S. Takenaka, *Mol. Cryst. Liq. Cryst. Sci. Technol. Sect. A*, 1992, 213, 163.

80] P. Keller, *Mol. Cryst. Liq. Cryst.*, 1985, 123, 247.

81] C. R. Hauser and J. K. Lindsay, *J. Org. Chem.*, 1957, 22, 906.

82] G. Scherowsky and M. Sefkov, *Mol. Cryst. Liq. Cryst.*, 1991, 202, 207.

83] D. W. Bruce, D. A. Dunmur, E. Lalinde, P. M. Maitlis and P. S. Styring, *Liquid Crystals*, 1988, 3, 385.

84] W. E. Broderick, D. M. Eichhorn, X. Liu, P. J. Toscano, S. M. Owens and B. M. Hoffman, *J. Am. Chem. Soc.*, 1995, 117, 3641.

85] N. F. Bolm, E. W. Neuse and H. G. Thomas, *Transition Met. Chem.*, 1987, 12, 301.

86] R. Deschenaux, J. L. Marendaz and J. Santiago, *Helv. Chim. Acta*, 1995, 78, 1215.

87] R. Deschenaux, I. Kosztics, U. Scholten, D. Guillon and M. Ibn-Elhaj, *J. Mater. Chem.*, 1994, 4, 1351.

88] M. I. Rybinskaya, A. Z. Kreindlin and S. S. Fadeeva, *J. Organomet. Chem.*, 1988, 358, 363.